Dissertation

submitted to the Combined Faculties for the Natural Sciences and for Mathematics of the
Ruperto-Carola University of Heidelberg, Germany
for the degree of
Doctor of Natural Sciences

presented by
Master of Science – Chemical Engineering Michael Lang
born in Mulhouse (France)

Oral-examination: ……

Identification and characterization of interaction partners of Heat Shock Transcription Factor 1 during the cellular heat shock response

Referees: Prof. Dr. Matthias Mayer

Prof. Dr. Georg Stoecklin

Table of Contents

Abstract

The heat shock transcription factor 1 is the main regulator of the mammalian heat shock response. The synthesis of molecular chaperones, required for proper folding, refolding and disaggregation of proteins is dependent on the activation of HSF1 from an inactive monomer into a DNA-bound trimer. The mechanism of trimerization of HSF1 was extensively studied, and recent progress led to speculate over a model in which the trimerization is dependent on temperature and concentration. Also, the existence of an equilibrium between active and inactive HSF1 under non-stress conditions was proposed, explaining the expression of target genes of HSF1 in the absence of cellular stress. The attenuation phase of the heat shock response was proposed to be regulated through a negative feed-back mechanism in which the molecular chaperone complex Hsp70/Hsp40 represses the transcription activity of trimeric HSF1. The mechanism of this attenuation as well as the nature of the cochaperones interacting with HSF1 during that phase of the heat shock response are still unknown.

The aim of this work was to identify new interaction partners of HSF1 during the attenuation phase, to characterize these interactors, and to establish their role in the heat shock cycle. The identification part was performed by generating a stable human cell line constitutively in a state close to the attenuation phase. This was achieved by overexpressing a tagged version of HSF1 in these cells, significantly increasing its concentration in the cytoplasm, leading to a concentration-dependent trimerization in the absence of stress. Moreover, this cell line was shown to be resistant to mild heat shock, indicating that these cells have an increased pool of molecular chaperones. Immunoprecipitation and shotgun proteomics identified Hsp70, Hsc70, Bag2 and Bag4 as main interaction partners of HSF1. The two first proteins of the list have been known for decades to interact with the transcription factor during the attenuation phase, but the Hsp70 nucleotide exchange factor Bag2 and Bag4 were interesting new potential partners, as these interactions were confirmed to be direct, and not only through the Hsp70 chaperone.

Full-length Bag2 and the Bag domain of Bag4 were purified, and their activity as nucleotide exchange factor was investigated. Surprisingly, the Bag domain of Bag4 proved to be much more efficient than the full length Bag2, and both proteins were able to stimulate the ADP-release of Hsc70 better than of Hsp70. Both purified proteins were also able to support refolding of heat-denaturated luciferase in the presence of Hsc70 and the J-domain protein Hdj1. In this experiment, differences between Bag2 and the Bag domain of Bag4 were small.

Finally, the roles of these two nucleotide exchange factors were investigated *in vivo*. The overexpression of both full-length Bag2 and Bag 4 proteins in U2-OS cells led to a strong activation of heat shock gene transcription, even in the absence of cellular stress. The repression of HSF1 by the Hsp70/Hsp40 complex is most probably short-lived, as the overexpression of the two Bag proteins stimulates the release of trimeric HSF1, hence allowing the transcription of heat shock genes and the subsequent production of molecular chaperones to continue. Fragments of Bag2 and Bag4, when overexpressed, could not stimulate the heat shock response, hinting at the fact that both Bag domain and N-terminal fragment are necessary for this effect. Taken together, these results are an additional indication of the existence of an equilibrium between active and inactive HSF1, equilibrium which is displaced towards active trimeric HSF1 in the case of cellular stress.

Zusammenfassung

Der Hitzeschocktranskriptionsfaktor 1 (HSF1) ist der Hauptregulator der Hitzeschockantwort bei Säugentieren. Die Herstellung von molekularen Chaperonen, die für eine korrekte Faltung, Rückfaltung und Disaggregation benötigt werden, ist abhängig von der Aktivierung von HSF1, vom inaktiven Monomer zum DNA-gebundenen Trimer. Der Mechanismus der Trimerisierung von HSF1 wurde weitreichend untersucht und neuste wissentschaftliche Fortschritte führen zu Schlussfolgerungen über ein Modell, in dem die Trimerisierung temperatur- und konzentrationsabhängig ist. Auch wurde vorgeschlagen, dass Hsf1 immer im Gleichgewicht zwischen aktivem und inaktivem Zustand vorliegt, wodurch die Expression von Zielgenen von HSF1 in Abwesenheit von Zellstress erklärt wird. Für die Attenuation der Hitzeschockantwort wurde ein negativer Rückkopplungsmechanismus vorgeschlagen, bei dem der molekulare Chaperonkomplex Hsp70/Hsp40 die Transkriptionsaktivität von trimerem HSF1 unterdrückt. Der Mechanismus dieser Attenuation sowie die Natur der Co-chaperonen, die mit HSF1 während dieser Phase der Hitzeschockantwort interagieren, sind noch unbekannt.

Das Ziel dieser Arbeit war es, neue Interaktionspartner von HSF1 in der Attenuationsphase zu identifizieren und zu charakterisieren, und ihre Rolle im Hitzeshockzyklus zu bestimmen. Der Identifikationsteil wurde durch Erzeugen einer stabilen menschlichen Zelllinie, die konstitutiv in einem Zustand nahe der Attenuationsphase ist, durchgeführt. Dies wurde erreicht, indem eine markierte Version von HSF1 in diesen Zellen überexprimiert wurde. Eine deutliche Erhöhung der Konzentration von HSF1 im Cytoplasma in Abwensenheit von Zellstress führte zu einer konzentrationsabhängigen Trimerisierung von HSF1. Darüber hinaus wurde gezeigt, dass diese Zellinie gegenüber einem leichten Hitzeschock resistent ist, was beweist, dass sie eine erhöhte Menge an molekularen Chaperonen aufweist. Durch Immunopräzipitation und Shotgun Proteomics wurden Hsp70, Hsc70, Bag2 und Bag4 als Haupt-Interaktionspartner von HSF1 identifiziert. Von den beiden ersten Proteinen der Liste ist seit mehreren Jahren bekannt, dass sie mit dem Transkriptionsfaktor während der Attenuationsphase interagieren. Die Hsp70-Nukleotid-Austauschfaktoren Bag2 und Bag4 waren als Interaktionspartner noch unbekannt und waren daher interessante potentielle Partner, insbesondere da gezeigt werden konnte, dass diese Interaktionen direkt und nicht Hsp70 vermittelt stattfindet.

Das Bag2 Protein und die Bag-Domäne von Bag4 wurden gereinigt und ihre Aktivität als Nukleotid-Austauschfaktoren untersucht. Überraschenderweise erwies sich die Bag-Domäne von Bag4 als viel effizienterer Austauschfaktor als Bag2, und beide Proteine konnten die ADP-Dissoziation von Hsc70 besser stimulieren als von Hsp70. Beide gereinigten Proteine waren auch in der Lage, die Rückfaltung

von hitzedenaturierter Luziferase in Gegenwart von Hsc70 und dem J-Domänenprotein Hdj1 zu unterstützen. In diesem Experiment wurden keinen signifikanten Unterschiede zwischen Bag2 und der Bag-Domäne von Bag4 beobachtet.

Schließlich wurden die Rollen dieser beiden Nukleotid-Austauschfaktoren *in vivo* untersucht. Die Überexpression beider volllängen Bag-Proteine in U2OS-Zellen führte zu einer starken Aktivierung von HSF1, auch ohne Zellstress. Die Repression von HSF1 durch den Hsp70/Hsp40-Komplex ist höchstwahrscheinlich dadurch reduziert, dass die Überexpression der beiden Bag-Proteine die Dissoziation von trimerischem HSF1 stimuliert und somit die Transkription von Hitzeschock-Genen und die anschließende Produktion von molekularen Chaperonen fördert. Fragmente von Bag2 und Bag4 konnten die Hitzeschockantwort nicht stimulieren, was darauf hinweist, dass sowohl Bag-Domäne als auch N-terminales Fragment für diesen Effekt notwendig sind. Zusammengefasst sind diese Ergebnisse ein zusätzlicher Hinweis für die Existenz eines Gleichgewichts zwischen aktivem und inaktivem HSF1. Dieser Gleichgewicht wird bei zellulärer Belastung zum aktiven trimerischen HSF1 verschoben.

Chapter 1. Introduction

1.1 Chaperone proteins

Proteins must adopt a specific tridimensional structure to fulfil their respective roles. This tridimensional structure is obtained through a specific folding. Disruption in the folding process can lead to non-active misfolded proteins which, in turn, can form aggregates. In the middle of the XXth century, "the thermodynamic hypothesis" speculated that the structure of a protein was solely determined by its amino acid sequence (Anfinsen 1973). In this theory, the native state of a protein would be its thermodynamically most stable state, with the lowest Gibbs free energy. However, Anfinsen was able to fold and refold proteins at low temperature and low concentration. These conditions are not respected in living cells, where in addition many more proteins are expressed simultaneously.

Newly synthetized proteins as well as already misfolded proteins require the help of a whole class of proteins, called molecular chaperones, in order to go from a linear chain of amino-acids into a well-folded functional protein. Most of the time, this would require energy in the form of ATP. Cellular stresses, such as temperature increase, or change of pH can lead to an increase of protein denaturation which can result in non-functional proteins, or even in cytotoxic aggregates (Morimoto 1998; Richter et al. 2010), and therefore to cellular death. Molecular chaperones are able to prevent the excessive accumulation of denaturated proteins, and hence the formation of toxic protein aggregates (Frydman 2001).

Chaperones have been reported to prevent aggregation, to fold newly synthetized and refold misfolded proteins, and also to dissolve protein aggregates. Prevention of aggregation is believed to happen through binding of the chaperone to exposed hydrophobic regions of the misfolded protein. Hence, these regions will not stabilize themselves by interacting with other exposed hydrophobic regions of other proteins (Haslbeck et al. 2005). Folding, unfolding and refolding of proteins implies however the need of ATP hydrolysis to accompany a succession of binding and release of the substrate, each cycle bringing it closer to its native state. Chaperone disaggregase activity requires the cooperation of several chaperones (Goloubinoff et al. 1999; Sousa 2014).

Many chaperones are heat shock proteins (Hsp). This name describes the fact that the expression of these chaperones is highly up-regulated upon elevated temperature, or other stresses.

1.2 The Heat Shock response

As mentioned earlier, the nature of cellular stresses can vary: oxidative stress, change of temperature, pH or osmolarity, reactive oxygen species, presence of heavy metals, or other types of physical and chemical changes of the environment. These stresses can lead to chemical changes in contact between amino-acid residues, and therefore to changes in the tridimensional structure of the protein they form. These changes can lead to the loss of function of the protein, and to formation of protein aggregates that can be harmful for the cell. To counter this, cells evolve a highly sophisticated mechanism to increase the amount of chaperone proteins in the cell. This mechanism is called the Heat Shock response (HSR).

In the 1960's, geneticists accidentally observed chromosomal puffs in drosophila larvae when these were exposed to higher temperature, resulting in the idea of the transient up-regulation of the transcription of certain genes upon temperature stress (Ritossa 1962). Today, it is known that the Heat Shock response is characterized by significant decrease in total gene transcription, while a specific set of genes known as heat shock genes and coding for heat shock proteins are heavily over-expressed (Heikkila et al. 1982; Ashburner & Bonnert 1979; Hightower 1980). The function of these heat shock proteins is to attenuate the effect of the proteotoxic stress, by facilitating the folding of unfolded and misfolded proteins (Diamant et al. 2001; Pinto et al. 1991; Martin et al. 1992). In summary, the Heat Shock response is the phenomenon in which global protein expression decreases, but the synthesis of heat shock proteins increases (Anckar & Sistonen 2011).

In prokaryotes, a transcription factor called σ^{32} directs the core bacterial RNA polymerase to the promoters of heat shock protein. Under normal condition, σ^{32} is an unstable protein and is targeted for degradation by the DnaK chaperone, but its stability and transcriptional efficiency increases during heat shock, hence its concentration (Straus et al. 1990).

It was established in the 1990s that the regulator of the Heat Shock response in eukaryotic cells is a transcription factor called Heat Shock Factor 1 or HSF1(Wu 1995). In metazoan, HSF1 is inactive as a monomer, but acquires its DNA-binding capacity by forming a trimer. HSF1 binds to extended repeats of the sequence nGAAn, called Heat Shock Elements (hereafter called HSE), which are abundantly present in the promoters of heat shock genes (Littlefield & Nelson 1999; Xiao & Lis 1987; Amin et al. 1988).

In yeast, a single heat shock factor exists. It is constitutively trimeric, and is bound to HSE even in the absence of stress. Post-translational modifications such as phosphorylation, and release of interaction partners trigger its transcriptional activity (Sorger & Pelham 1987; Westwoodt & Wu 1993; Santoro et al. 1998).

In mammals, five HSF were identified so far (HSF1, HSF2, HSF3, HSF X and HSF Y), but only HSF1 has an irreplaceable role in the Heat Shock response (Mcmillan et al. 1998) . HSF2 and HSF3 were shown to interact with HSF1 during the HSR , in order to modulate the transcription of Heat Shock proteins (Sandqvist et al. 2009; Jaeger et al. 2016), but their major role seems to be linked with development (Åkerfelt et al. 2007; Östling et al. 2007). HSF2 was also suggested to bind promoters of heat shock proteins during mitosis, so that HSF1-mediated transcription can start directly after the end of cell-division (Xing et al. 2005). HSF Y was reported to play a role in spermatogenesis (Shinka et al. 2004) and the function of HSF X is still unknown.

1.3 Heat Shock transcription Factor 1

1.3.1 The different domains of HSF1

Most probably due to HSF1's flexibility, only partial structural information is available on HSF1. Different domains were identified, but their lack of defined structure proved to be challenging in obtaining significant insight on a global structure of the protein.

Figure 1: Domain structure of human HSF1. The DNA-binding domain (DBD, orange) is located at the N-terminus of the protein. It is the most conserved domain of HSF1. The amphiphilic heptad repeats HR-A and HR-B (magenta) are involved in the formation of trimers with other molecules of HSF1. The regulatory domain (RD, green) is subject to many post-translational modification and modulates the transcriptional activity of HSF1 by acting on its transactivation domain (TAD, blue), located at the C-terminus. Between RD and TAD, the heptad repeat HR-C interacts with HR-A/B and prevents trimerization.

In fact, the only domain tridimensional structure of HSF1 is the one of its DNA-binding domain (DBD). HSF1's DBD is, as many other DBD of transcription factors, of a looped helix-turn-helix type. However, unlike other DBD of this type, the loop does not make direct contact with DNA, but was proposed to stabilize the trimer, by interacting with a DBD of another HSF1 (Vuister et al. 1994; Littlefield & Nelson 1999). It was then suggested that the loop is required for full activity, and its deletion would lead to a weakened DNA-binding (Cicero et al. 2001). More recently, a structure of the trimeric human DBD bound to DNA, along with parts of the HR-A/B was proposed (Neudegger et al. 2016). In this structure, as well as in some previously published studies, each DBD of a HSF1 trimer recognizes a single nGAAn

repeat in the major groove of the DNA helix and binds to it (Littlefield & Nelson 1999; Amin et al. 1988; Xiao & Lis 1987).

The oligomerization domain of HSF1 is located at the C-terminus of the DBD, and includes both HR-A and HR-B. In the trimeric form of HSF1, circular dichroism studies and X-ray crystallography proved this domain to be made of a triple α-helix coiled-coil, formed by the hydrophobic heptad repeat HR-A and HR-B (Peteranderl & Nelson 1992; Neudegger et al. 2016). In the absence of any stress, it has been shown that spontaneous oligomerization is prevented by the amphiphilic heptad repeat HR-C, interacting with HR-A/B through an intramolecular leucine zipper (Rabindran et al. 1993; Hentze et al. 2016). This was confirmed by mutational analysis, where mutants lacking some hydrophobic residues in the HR-C heptad repeat would be constitutively trimeric (Rabindran et al. 1993; Zuo et al. 1994). Consequently, the transition from monomer to trimer goes from an intramolecular coiled-coil to an intermolecular coiled-coil.

The region framed by HR-A/B and HR-C is known as the regulatory domain (RD). Upon stress, the RD undergoes a great number of posttranslational modification : 19 phosphorylation sites were identified, as well as some acetylation sites, and one phosphorylation dependent sumoylation site (Kline & Morimoto 1997; Hietakangas et al. 2003; Guettouche et al. 2005; Hietakangas et al. 2006). Phosphorylation were shown to either repress the transactivation activity of HSF1 (serine 303 and serine 307), or, in the case of Phosphoserines 320 and 326, to play a critical role in the induction of HSF1 (Holmberg et al. 2001; Guettouche et al. 2005). The sumoylation of lysine 298 was shown to be dependent on the phosphorylation of serine 303, and was able to repress transcriptional activity of HSF1. Desumoylation was interestingly shown to be temperature dependent: mild heat shock leads to a slow removal of the SUMO protein from K298, whereas acute temperature stress was accompanied by rapid desumoylation, hence contributing to a strong heat shock response (Anckar et al. 2006). The mechanism by which SUMO delayed the HSR is still unclear. Acting as a regulator of HSF1 stability, conformation or localization has to be considered (Geiss-friedlander & Melchior 2007).

The very C-terminal part of HSF1 is called the transactivation domain (TAD). Its role is to regulate the magnitude of HSF1 activation, and altogether to facilitate the transcription to target genes. Despite being globally unfolded, it contains a small α-helical hydrophobic motif which interacts *in vitro* with the basal transcription component TAF-9 (Choi 2000). Mutations of hydrophobic residues contained in this motif reduces HSF1 trans-activation capacity (Newton et al. 1996). The TAD is rich in hydrophobic and acidic residues, but also rich in proline, which attests for a global absence of α-helices. An interaction between some hydrophobic residues and BRG1, the ATPase subunit of the chromatin

remodeler SWI/SNF, was also reported (Sullivan et al. 2001). The SWI/SNF complex is required for heat-inducible chromatin remodeling of heat-shock genes (Corey et al. 2003).

1.3.2 Localization of HSF1

HSF1 was detected both in the cytoplasm and the nucleus, but its concentration in the nucleus increases after cellular stress (Sarge et al. 1993; Brown & Rush 1999; Mercier et al. 1999; Stacchiotti et al. 1999). In addition, it was shown that the import of HSF1 from the cytoplasm to the nucleus was under the control of the relatively potent importin-α/β, and that this import was more efficient than the export from the nucleus pathway, which is not under the control of the classical exportin-1 system (Vujanac et al. 2005). More recently, it was shown that HSF1 co-translocated from the cytosol to the nucleus with Bag3, a co-chaperone of the Hsp70 family, and that the shuttling of HSF1 is hindered with lower levels of Bag3 (Jin et al. 2015). Moreover, a simultaneous translocation to the nucleus of HSF1 with the E3- ubiquitin ligase CHIP has also been reported (Dai et al. 2003), but in that case, CHIP was promoting HSF1 trimerization, and it was unclear whether the transport of HSF1 was really CHIP-dependent. In this study, CHIP (-/-) mice were temperature-sensitive, and unable to mount a heat shock response (Dai et al. 2003).

1.3.3 HSF1-mediated transactivation of heat shock genes

It is established that HSF1 is the main player in the cellular stress response. The rapid expression of heat shock genes following temperature stress has served as model for transcriptional response studies. Indeed, the expression of HSP70 upon protein-damaging stress is one of the best-understood models for the activation of transcription. In D. melanogaster, the HSP70 promoter is constitutively primed for activation by a complex formed by the GAGA factor, the transcription factor IID, and a paused RNA polymerase II (Rougvie & Lis 1988; Rasmussen & Lis 1993). Moreover, it was suggested that the presence of this paused complex is critical for HSF1 binding *in vivo* (Shopland et al. 1995). Upon cellular stress, HSF rapidly accumulates at the promoter, recruiting the mediator complex and the transcription elongation factor p-TEFb (Lis et al. 2000). To facilitate transcription elongation, topoisomerase I relieves DNA coiling (Gilmour et al. 1988), and the FACT complex removes nucleosomes (Andrulis et al. 2000). Similar mechanisms can be found in mammals, such as the HSF1-dependent release of RNA Pol II, and the removal of nucleosomes downstream of the polymerase

(Brown et al. 1996). More recently, HSF1 has been shown to interact with replication factor A (RPA) and with FACT to maintain the HSP70 promotor highly accessible for HSF1 (Fujimoto et al. 2012).

1.3.4 Regulation of the HSF1 activation-attenuation cycle

1.3.3.1 Activation of HSF1

Since the discovery of its role, the mechanism of activation of HSF1 has been extensively studied in models ranging from cell culture assays to the level of full-organism in nematodes, mice or rats. In general, monomeric HSF1 trimerizes upon stress and leads to the synthesis of heat shock proteins, and, after some time, the stress response decreases in intensity. Some heat shock proteins are molecular chaperones, and hence protect the cell from proteotoxic damages and help in maintaining protein homeostasis. In time, when the concentration of molecular chaperones had increased to levels more adapted to the needs of the cells, an attenuation of HSF1 transcriptional activity happens most likely through a negative feedback loop. The chaperones were proposed to interact with the hydrophobic and unstructured transactivation domain of HSF1 (Abravaya et al. 1991a; Shi et al. 1998a). HSF1 activation is not completely understood, and several theories describing mechanisms of activation were proposed so far.

The first model thought came out of observations that monomeric HSF1 can trimerize and acquire its DNA-binding capacity *in vitro* when exposed to higher temperatures (Mosser et al. 1990; Goodson & Sarge 1995; Farkas et al. 1998). This observation lead to the development of the “intrinsic response” activation model, in which HSF1 is able to “sense” temperature changes, and undergoes conformational changes leading to trimerization. Advocates of this model identified the α-helical amphiphilic heptad repeats HR-A/B and HR-C, which were believed to interact with each other in the inactive form (Rabindran et al. 1993), hence preventing HSF1 to trimerize. Mutations in these heptads repeats disrupted these interactions, and HSF1 was found to be constitutively trimeric. More recently, Hydrogen Exchange Mass Spectrometry measurements could confirm the interaction between HR-C and HR-A/B in monomeric HSF1. This interaction was however not visible when measuring trimeric HSF1, hence confirming the validity of this model (Hentze et al. 2016). Moreover, it was shown that the disruption of the Leucine zipper interaction between HR-A/B and HR-C was not only temperature-dependent, but also concentration-dependent. In fact, the temperature of activation of HSF1, would be reduced in higher concentration of purified HSF1 (Hentze et al. 2016).

The second model, called “chaperone titration” is based on the fact that HSF1 was shown to interact with heat shock proteins (Shi et al. 1998a; Zou et al. 1998; Neef et al. 2014). This model was established when HSF1’s activity was shown to be repressed by a multi-chaperone complex containing Hsp90, and depletion of Hsp90 lead to immediate HSF1 activation (Zou et al. 1998; Ali et al. 1998; Guo et al. 2001). In addition, it was shown that elevated levels of Hsp70 and Hsp90 were able to prevent trimerization of HSF1 (Shi et al. 1998b). Also, Hsp90 inhibitors could trigger HSF1 stress response pathway in mice (Lee et al. 2013). According to this model, the accumulation of misfolded proteins would titrate heat shock proteins away from HSF1, hence allowing it to trimerize. However, other evidences suggested that rather than maintaining it inactive or inhibiting its DNA binding, Hsp90 broadens HSF1 activation temperature window (Hentze et al. 2016). Other data mentioned the interaction between Hsp90 and HSF1, but only after DSP-crosslinking, suggesting a very transient interaction. In addition, the same study reveals an interaction between inactive HSF1 and the cytosolic chaperonin TRiC/CCT. This interaction could be disrupted by the small molecule HSF1A, a chemical activator of the heat shock response (Neef et al. 2014). More recently, it was suggested that Hsp70 and Hsp40, a J-domain protein, prevents transactivation of HSF1 in yeast, and that the growth defect caused by HSF1 overexpression could be partially suppressed by overexpressing Hsp70 and Hsp40 (Zheng et al. 2016). This chaperone titration theory was modelized in mammalian organism by Sivéry and colleagues (Sivéry et al. 2016).

Another model of HSF1 activation is based on the existence of a ribonucleoprotein complex consisting of the translation elongation factor eEF1A and a constitutively expressed non-coding RNA called heat shock RNA-1 (HSR-1) (Shamovsky et al. 2006). In this model, the non-coding RNA directly acts as a thermosensor, and undergoes changes in secondary structures upon stress (Kugel & Goodrich 2006). It can then interact with eEF1A, which became available due to the global shut-down of protein synthesis, and in turn with HSF1, promoting its trimerization (Shamovsky & Nudler 2008).

The last activation model concerns whole organisms. It is based on the discovery of thermosensory neurons (called AFDs) in *C. elegans* (Clark et al. 2007), and on the fact that activation of HSF1 may depend on these neurons (Prahlad et al. 2008). Living nematodes with disrupted AFDs were shown not to display a cellular heat shock response in the tissue where the heat shock was applied, but also in remote parts of the organism (Prahlad & Morimoto 2009). More recently, it was shown that excitation of AFDs was not enough to trigger the HSR in remote cells, but that this activation of HSF1 needed the release of neuronal serotonin in the specific tissue. Serotonin was shown to be released following AFD excitation, even in the absence of temperature increase (Tatum et al. 2015).

These four models are not necessarily mutually exclusive, and could happen simultaneously in vivo, hence leading to a very fast setting up of the heat shock response.

1.3.3.2 Attenuation of the heat shock response

It is commonly accepted that the heat shock response undergoes an attenuation phase, when the synthesis of more heat shock proteins is not needed anymore. Two distinct pathways were proposed so far: the negative feed-back loop and the acetylation of HSF1.

The negative feed-back loop relies on the idea that an excess of molecular chaperones that was synthetized during the heat shock response interacts with trimers of HSF1, hence repressing its transcriptional activity (Mosser et al. 1988). Evidences of a protein-protein interaction between HSF1 and the Hsp70/Hsp40 complex were shown at the late stages of the heat shock response (Mosser et al. 1988; Abravaya et al. 1991b; Baler et al. 1992; Shi et al. 1998b), and a possible recruitment of the transcriptional repressor CoREST through Hsp70/Hsp40 was suggested, as down-regulation of CoREST rendered Hsp70 incapable of repressing HSF1-dependent transcription (Gómez et al. 2008). However, the interaction of HSF1 with Hsp70 does not suppress the DNA-binding activity of the trimer of HSF1, suggesting another mechanism at play (Rabindran et al. 1994; Shi et al. 1998b). Hsp90 was also reported to interact with the Regulatory Domain of trimeric HSF1 in heat-shocked cells, but only as a complex with FKBP52 and p23 (Ali et al. 1998; Bharadwaj et al. 1999; Guo et al. 2001). Disruption of this complex lead to a delayed attenuation phase, suggesting that it could also play a role in HSF1's attenuation.

The acetylation pathway has been shown to be responsible for the disruption of the interaction between HSE-containing DNA and trimeric HSF1. In heat-shocked cells, HSF1's acetylation gradually increases, and inhibition of sirtuins, a family of deacetylase, lead to increase the levels of acetylation, and reduced amount of Hsp70 produced after heat shock *in vivo*. On the contrary, overexpression of the deacetylase SIRT1 significant reduced HSF1 acetylation, and heat shock genes promoter occupancy (Westerheide et al. 2009). Among the nine lysines that were stated to be acetylation site of HSF1, Lys80 was reported to be the one whose acetylation by the acetyl-transferase p300-CBP (CREB-binding protein) would lead to a decrease in DNA-bound HSF1. In addition, the acetylation of Lys80 was reported to have a role to play in HSF1 degradation by the proteasome system, hence contributing even more to the attenuation of the heat shock response (Westerheide et al. 2009; Raychaudhuri et al. 2014).

The most recent model of HSF1 activation/attenuation cycle is presented in figure 2.

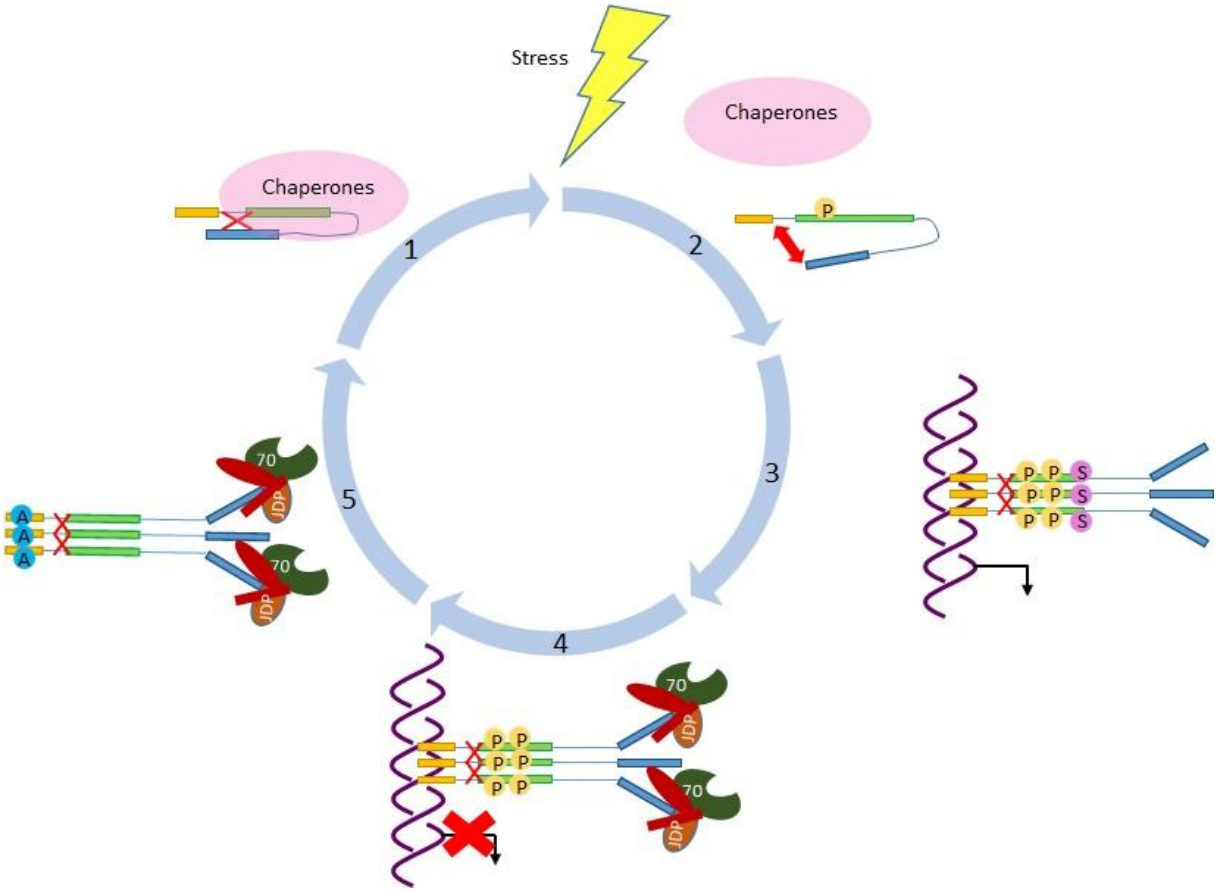

Figure 2: The Heat-Shock response. In the absence of stress (1), HSF1 is monomeric and inactive. Upon stress, the "chaperone cage" is titrated away, and disruption of the intra-molecular leucine-zipper occurs (2). HSF1 then undergoes several post-translational modifications such as phosphorylation and sumoylation, trimerizes, and acquires its DNA-binding capacity. The trimer binds to HSE in the promoter of heat shock genes, and drives the transcription of heat shock genes (3). Attenuation of the heat-shock response starts as a negative feed-back regulation, when Hsp70 and JDP bind to the TAD, and represses the transcription of heat shock genes (4). Trimeric HSF1 is undocked from the DNA after acetylation of Lys80 located in the DBD, and according to some studies, HSF1 is then targeted for degradation (5).

1.3.5 Other roles of HSF1

HSF1 is involved in cellular pathway other than the heat shock response. Several studies report an implication of HSF1 in the absence of stress in other cellular mechanisms such as development regulation, disease or insulin signaling.

Although not required for survival in adulthood in mammals, HSF1 deficient mice exhibit prenatal lethality, growth retardation, and abnormally regulated cytokine production (Xiao et al. 1999; Christians et al. 2000; Inouye et al. 2004). Evidence was provided that HSF1 fulfils its developmental functions through an activation mechanism different from- the one that applies to stressed cells (Åkerfelt et al. 2010; Fujimoto et al. 2004; Masson et al. 2011). The regulation of HSF1's activity was

also shown to be critical in the case of its developmental role, as *Hsf1 -/-* mice have a spermatogenesis defect (Salmand et al. 2008), and constitutively active HSF1 renders mice infertile (Nakai et al. 2000). HSF1 was also shown to be involved in processes critical for the survival of malignant cells. Indeed, Dai and colleagues showed that *Hsf1 -/-* mice were highly resistant to treatment leading normally to tumorigenesis. In addition, in cell culture, HSF1 modulates pathways needed for cancer cell survival, such as Protein Kinase A activation, or glucose metabolism (Dai et al. 2007). This link between HSF1 and cancer can be easily explained by the fact that cancer cells are dependent on higher amounts of molecular chaperones for survival, and therefore on a stronger activation of HSF1 (Whitesell & Lindquist 2009). Another model is built on evidences that HSF1 and the transcription factor FOXO are both silenced by insulin signaling (Cohen et al. 2006; Hsu et al. 2003), hence suggesting a role of HSF1 in expanding lifespan in *C. elegans* (Morley & Morimoto 2004).

1.4 Overview of Hsp70's role and mechanism of action

According to the broadly accepted model of activation and attenuation of the heat shock response, molecular chaperones interact with HSF1 at many points during the cycle. Hsp90, the chaperonin complex TRiC/CCT or Hsp70 were all reported to maintain HSF1 inactive (Zou et al. 1998; Guo et al. 2001; Neef et al. 2014; Shi et al. 1998b). During the attenuation phase, it is mainly established that Hsf1 is a substrate of the Hsp70/Hsp40 machinery. Hsp70 thereby has a central role in the heat shock response, but also in HSF1's regulation.

1.4.1 Hsp70s' functions in the cell

The 70 kDa heat shock protein is one of the most studied molecular chaperones. It performs many functions under stress conditions, but also in optimal growth conditions (Richter et al. 2010). Interacting with the polypeptide nascent chain directly at its exit from the ribosome tunnels (Deuerling et al. 1999; Teter et al. 1999), chaperones from the Hsp70 family bind to solvent accessible hydrophobic zones rich in positively charged residues of their substrate proteins. The binding in an ATP-dependent manner of Hsp70 at these hydrophobic clusters therefore prevents protein-protein aggregation, and assists in protein folding. Later in the process, if it is needed, Hsp70 hands these partially folded substrates to the Hsp60 (TRiC/CCT in mammals) or Hsp90 machinery (Young et al. 2004; Li et al. 2012).

As mentioned earlier, Hsp70s are overexpressed during cellular stress, when proteins are likely to be misfolded and to aggregate. In collaboration with molecular chaperones of the Hsp100s family, Hsp70s are able to dissolve protein aggregate, and subsequently refold their substrate to their native form (Chiti & Dobson 2006; Mayer & Bukau 2005). In that case, Hsp70s extricate a fragment of the aggregated protein, hands it to Hsp100 for disaggregation, and then promotes its refolding (Glover & Lindquist 1998; Goloubinoff et al. 1999; Liberek et al. 2008; Weibezahn et al. 2004), hence preventing the accumulation of proteotoxic aggregates, lethal to the cell.

Hsp70s are also involved in protein translocation into organelles. Indeed, it was proposed that cytoplasmic Hsp70 prevents aggregation of protein before translocation, maybe by keeping the transit peptide soluble. Hsp70 may keep the protein in a partially-folded state, which is appropriate for membrane transport. Meanwhile the mitochondrial Hsp70 binds the substrate when it emerges from the translocation pore, and assists the process until complete translocation (Neupert & Brunner 2002; Wiedemann et al. 2004).

In addition to its protein folding and refolding roles, it was shown that Hsp70s can play a critical role in targeting protein for degradation. The interaction of heat shock cognate 70, the constitutively expressed Hsp70 in the cytosol, with the ubiquitin E3 ligase CHIP is well established (Connell et al. 2001; Meacham et al. 2001; Höhfeld et al. 2001), and it was suggested that CHIP polyubiquitinylates substrates of Hsc70 which underwent too many association dissociation cycles. Substrates that are only associate for a short time with Hsc70 (i.e. which are folded/refolded quickly to their native state) are therefore less likely to be targeted for degradation (Stankiewicz et al. 2010).

Through their protective roles, Hsp70s are known to allow the survival of cancer cells (Nylandsted et al. 2000; Shin et al. 2003), and inhibition of Hsp70s is a long-thought strategy to treat cancer patients (Mckeon et al. 2016). On the contrary, it has been shown that overexpression of Hsp70 mildens symptoms of neurodegenerative diseases such as Alzheimer's disease, or Parkinson's disease (Klucken et al. 2004; Auluck et al. 2002; Bonini 2002). In a similar manner, induction of Hsp70 through chemical-activation of HSF1 was shown to reduce α-synuclein aggregation in cells (Kilpatrick et al. 2013). The connection between HSF1 and Hsp70 is therefore in the center of pathways involved in oncogenesis and neurodegeneration, hence accentuating the necessity of understanding the molecular mechanisms that regulate Hsp70.

1.4.2 Mechanism of action of Hsp70

Hsp70 is evolutionary highly conserved. From the bacterial DnaK to the human Hsp70, all homologs of Hsp70 consist of a 45kDa N-terminal nucleotide binding domain (NBD), and a 25 kDa C-terminal substrate binding domain (SBD), which is in turn composed of a β-sandwich sub-domain that contains a hydrophobic cleft for client binding, and a helical lid sub-domain that controls access to the cleft (Pellecchia et al. 2000). Both domains are connected by a hydrophobic linker. Hsp70 functions in cooperation with a J-domain protein (JDP), and with a nucleotide exchange factor. The ATPase cycle of Hsp70 (see figure 3) is a succession of an ATP-bound state characterized by low affinity for its substrate, and an ADP-bound state with high substrate-affinity (Schmid et al. 1994; Mayer, Schröder, et al. 2000).

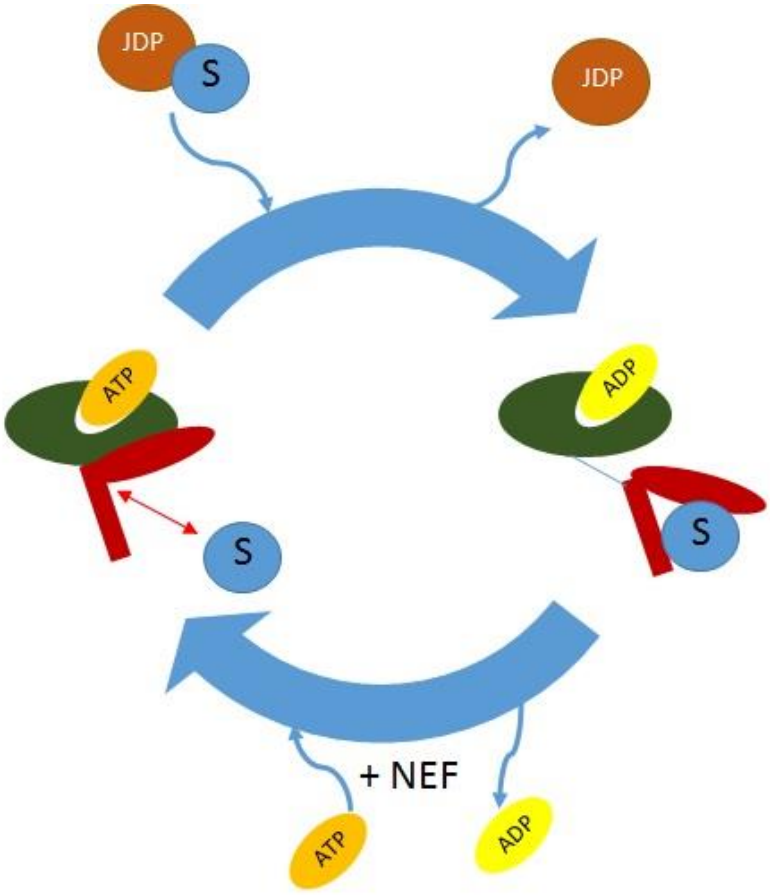

Figure 3: Hsc70 cycle. Hsp70 cycles between the ATP-bound state and the ADP-bound state. The first one has low affinity and high exchange for its substrate, whereas the latter one is characterized by low exchange rates and high affinity for its substrate (S, in blue). ATP or ADP binds to the nucleotide binding domain (NBD, in green), and the substrate binds to the substrate binding domain (SBD, in red). The cycle is controlled by internal allostery and these conformation changes are catalyzed by co-chaperones. The J-domain protein (JDP, in brown) provides the substrate to the SBD and stimulates ATP hydrolysis, resulting in strong binding of the substrate. Nucleotide exchange factors (NEF) facilitate ADP release, hence allowing the binding of a new molecule of ATP, and subsequently the release of the substrate.

At the beginning of the cycle, the JDP provides the substrate to the SBD of Hsp70, and stimulates ATP hydrolysis by the NBD (Gamer et al. 1996; Karzai & Mcmacken 1996; Kampinga & Craig 2010). ATP hydrolysis increases the affinity of the SBD for its substrate, hence leading to its entrapment. The release of the substrate is highly stimulated through the binding of a new molecule of ATP, hence through the release of ADP. This rate-limiting step is highly stimulated by nucleotide exchange factors (NEF).

Two alternatives models have been proposed to explain the mechanism of action of Hsp70. The first one, called "kinetic partitioning", is based on the fact that protein aggregation is a concentration dependent process. The model proposes that Hsp70 binds misfolded proteins, hence reducing the concentration of misfolded protein available for aggregation and allowing more time to fold correctly. This model assumes that Hsp70 undergoes no active change in conformation, which is unlikely. In the second model, Hsp70 locally unfolds some misfolded proteins, allowing them to refold, this time correctly (Ben-zvi & Goloubinoff 2001; Pierpaoli et al. 1997; Mayer, Rüdiger, et al. 2000; Slepenkov & Witt 2002).

1.4.3 J-domains proteins and nucleotide exchange factors

In order for the Hsp70 cycle to function at an efficient pace, co-chaperones such as J –domain proteins or NEF are needed. J-domain proteins (JDP), are proposed to bind substrates, before delivering them to Hsp70, while stimulating its ATPase activity. Many different JDPs exist, and they differ in their function, as well as in their domain composition (Kelley 1998). For instance, six JDPs exist in *E. coli*, and so far 44 (not counting splice variants) have been identified in human cells. All three classes of JDP have the J-domain in common, through which a JDP interacts with Hsp70 (Wall et al. 1994; Genevaux et al. 2002).

In the presence of JDP, the release of ADP is a rate-limiting step. It is however stimulated by the action of nucleotide exchange factors (Liberek et al. 1991; Gässler et al. 2001; Brehmer et al. 2001). In bacteria, only one NEF is present, called GrpE, and its homologs are conserved in mitochondria and chloroplasts of eukaryotic cells. In the cytoplasm and the endoplasmic reticulum of eukaryotes however, three divergent families of NEF have been identified: the Hsp110/Grp170 family (four different proteins), the HspBP1/Sil1 family (two members), and the Bag-domain protein family (Bag1 to Bag6) (Hohfeld & Jentsch 1998; Kabani, Beckerich, et al. 2002; Kabani, McLellan, et al. 2002; Steel et al. 2004; Dragovic et al. 2006; Raviol et al. 2006). This diversity of NEF was suggested to contribute to the appropriate allocation of Hsp70 folding capacity within the proteostasis network (Bracher & Verghese 2015). Even though the NEFs from the three different families are structurally different, they

all seem to target the IIb sub-domain of the nucleotide binding domain of Hsp70 hence stabilizing the NBD into its open conformation (Sondermann et al. 2001; Polier et al. 2008; Shomura et al. 2005). Both Hsp110 and Bag proteins possess a 3 helix bundle (3HBD for Hsp110/Bag domain for Bag proteins). In Bag proteins, the three-helix bundle binds IIb and Ib and thereby pries open the nucleotide binding cleft. In Hsp110s, the 3HBD binds to the outside of IIb, and the NBD of HSP110 is interacting with the NBD of Hsp70 to open the nucleotide binding cleft. In the case of the human HspBP1, four Armadillo repeats capped at each end with a α-helix pair wrap the IIb sub-domain. This leads to displacement of the Ib sub-domain of Hsp70s' NBD, and local unfolding of the complex (Shomura et al. 2005). The six Bag proteins all possess this C-terminal α-helix bundle called the Bag domain. However, the Bag domains of Bag3, Bag4 and Bag5 form shorter three-helix bundles than Bag1, the first Bag protein to be characterized (Briknarová et al. 2002; Brockmann et al. 2004; Arakawa et al. 2010). Bag2 bag domain, on the other hand, possesses three α-helices, and two of them were reported to be able to form homodimers with two helices of the Bag domain of another Bag2 molecule. This Bag domain was dubbed Brand New Bag domain, or BNB (Xu et al. 2008).

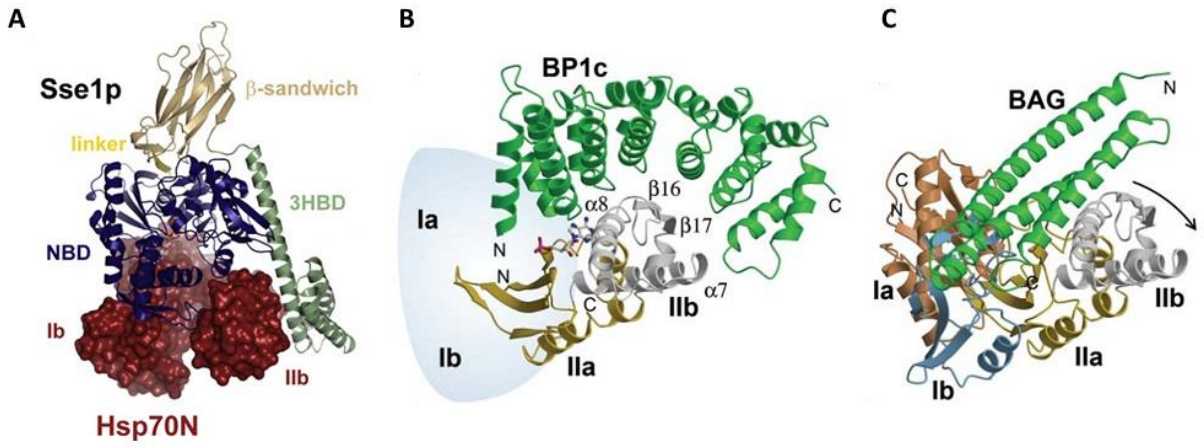

Figure 4: Structure of nucleotide exchange factors bound to Hsp70 (adapted from Polier et al (2008) and Shomura et al (2005)). (A) Frontal view of the crystal structure of Sse1p.ATP-Hsp70 NBD complex. Sse1 is the yeast Hsp110. The triple helix bundle domain (3HBD) interacts with the IIb sub-domain of Hsp70s' NBD, while the NBD of Hsp110 lead to an opening of the cleft between Ib and IIb of 21°. (B) Top view of the crystal structure of human HspBP1 core domain (BP1c) in complex with Hsp70s' NBD. The concave face of the four Armadillo repeats wraps around the IIb sub-domain. (C) Top view of the crystal structure of human Bag1 Bag domain (BAG) in complex with Hsc70's NBD. As for Sse1, the sub-domain IIb rotates away from Ib (14°C).

The diversity of NEFs in eukaryotic cells might allow fine-tuning of the Hsp70 cycling rate which might be needed for different substrates. Rauch and colleagues showed that certain Hsp70/JDP/NEF are more or less efficient in refolding thermally denaturated firefly luciferase (Rauch & Gestwicki 2014). It is however not known how specific combinations made of Hsp70, JDP and NEF are able to select suitable clients.

Chapter 2. Aim of the thesis

Since the beginning of the 1980s, HSF1 has been extensively studied. Its crucial role in the cellular stress response mechanism, alongside its complex mechanism of activation from inactive monomer to transcriptionally active homotrimer were solid reasons for researchers to investigate the role of this protein. In the late 90s, HSF1 even became a model protein in studies in the field of transcriptional response. At the same time however, the instability of the protein when recombinantly expressed and purified and the lack of methods to obtain structural insights on such a flexible protein lead to a loss of interest in the molecular characterization of its mechanisms of action. In the last years, progress made in methods such as mass-spectrometry or X-Ray crystallography lead to a renewal in the field. Unfortunately, so far, mostly HSF1s' mechanism of activation, through the intrinsic response, the chaperone titration model, or in the whole organism, through the action of thermosensory neurons were given much thought. How the attenuation phase is regulated however, stays unknown.

It has been known for decades that the Hsp70/Hsp40 machinery interacts with trimeric HSF1 in the late phase of the heat shock response, shutting its transactivational capacity down, in a negative feedback manner. However, reproducing this *in vitro* has proven to be challenging, suggesting that some parameters, or co-chaperones involved are still unknown to us.

In this study, the identification of new interaction partners of HSF1 during the attenuation phase of the heat shock response was intended. The relatively low amount of native HSF1, combined with the absence of competent immunoprecipitation antibody targeted against this protein, lead us to generate a stably transfected cell line overexpressing a tagged version of HSF1. The identification of interaction partners co-immunoprecipitated with HSF1 was performed using dimethyl labelling combined with shotgun proteomics.

Furthermore, the biochemical and biophysical characterization of the interaction partners identified alongside the impact of these novel interaction partners on the attenuation phase were investigated.

Taken together, our findings pave the way to more investigations of these interactions, which would lead to a broadened understanding of the attenuation phase of the heat shock response.

Chapter 3. Results

3.1 Establishment of a HSF1 overexpressing cell line

U2-OS cells were transfected with pIRES-GFP II-CtermHA-HsHSF1, and successful transfects were selected with G418. Due to cell stability issues that could arise regarding to the genomic insertion locus of the transcription plasmid, it was decided not to generate a single clone cell line, but rather a heterogeneous population of different HSF1-overexpressing clones where any unexpected behavior ensuing from the stable transfection would be averaged out. These clones would, alongside a C-terminus HA-tagged HSF1, express the green fluorescent protein (GFP), which would allow an enrichment of positive clones in the population using Fluorescent assisted cell sorting (FACS). Three successive sorts were performed. As control cells, U2-OS cells were transfected with pIRES-GFP II-HA, and selected according to the same procedure. These cells are called mock cells.

It was established around this time that the activation of HSF1 could be concentration-dependent, i.e., that higher concentration of HSF1 could lead to spontaneous trimerization, in the absence of any cellular stress (Hentze et al. 2016). In the case of the U2-OS pIRES-GFP II-CtermHA-HsHSF1 cell line, the overexpression of HSF1 being under the control of a strong CMV promoter, it is possible that the increased concentration of HSF1 in these cells lead to the activation of HSF1. In order to verify this, the levels of mRNA of HSPA1A (coding for Hsp70), and of the constitutively expressed HSPA8 (coding for Hsc70), were assayed in the absence of heat-shock using RT-qPCR, with HPRT1 as a housekeeping gene for normalization (Figure 5).

The fold increases, relative to the wild type cells, observed for both mRNAs in both cells lines suggest that despite a higher concentration of HSF1, which would *in vitro* lead to spontaneous activation, the transcription of the HSPA1A gene does not seem to be up-regulated. The variations observed in the levels of HSPA8 mRNA are actually more important than the ones observed in the levels of HSPA1A mRNA, even if the expression of Hsc70 is said to be independent from HSF1, hence proving that the amount of mRNA coding for Hsp70 in the stably transfected HSF1 overexpressing cells are similar to the ones in the wild type cells.

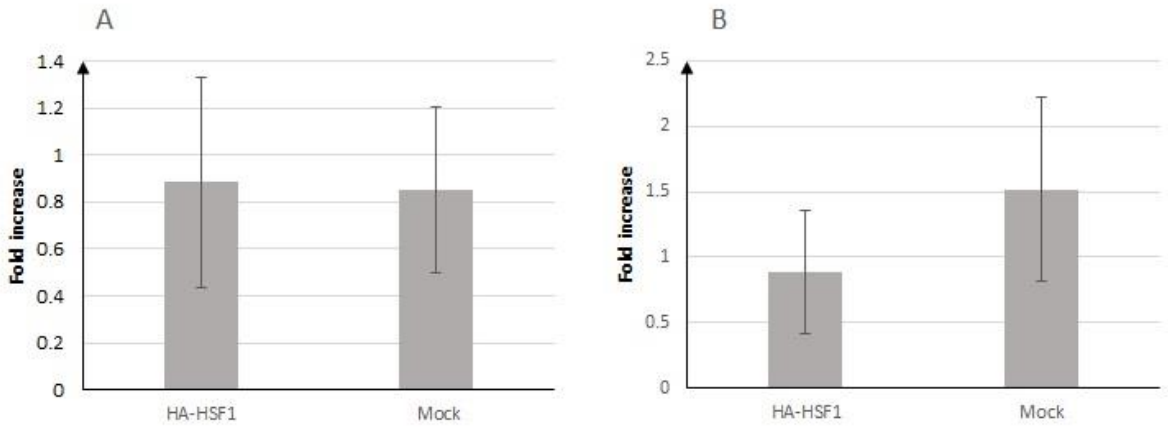

Figure 5: Relative levels of mRNA of HSPA1A (A) and HSPA8 (B). Real time qPCR was performed on cDNA produced from total RNA extract originated from non-stressed U2-OS WT, U2-OS HA-HSF1 and U2OS mock cells. The values presented represent the fold increase of the mRNA of HSPA1A (A) and HSPA8 (B), relative to the WT cells. HPRT1 was used as a housekeeping gene for normalization. The error bars represent the standard error of the mean of three replicates.

Next, the amount of Hsp70 in WT and HA-HSF1 cells at 37°C and at different time points after temperature upshift to 42°C was determined using through immunoblotting (Figure 6).

Consistent with the literature, Hsp70 was hardly detectable in the absence of stress in U2-OS wild type (WT) cells. In contract, Hsp70 was clearly detectable at 37°C in HA-HSF1 overexpressing cells. These cells seemed however able to resist short temperature increases, and a significant effect was only seen after 4 hours of heat-shock. This experiment was repeated three times with similar results, and the average of the band intensity for each cell line and each time interval at 42°C is presented in Figure 6C. This result could be explained by the fact that a larger pool of chaperone proteins could be present in the HA-HSF1 cells, due to concentration-dependent HSF1 trimerization, and that this larger amount of chaperone would be available to buffer the harmful effect of the temperature increase, up to a certain point. This is similar to induced thermotolerance by a short pre-heat shock.

These two experiments show no effect of HSF1 overexpression at the mRNA level, but a clear effect at the protein level. In order to conclude, HA-HSF1 and WT cells were transiently transfected with a reporter system in which the gene for the Firefly luciferase is under the control of the promoter to the mitochondrial Hsp70 (mtHsp70), containing heat shock elements (HSE). 48 hours after transfection, cells were submitted to heat shock at 39°C and 42°C for one hour, and allowed one hour to recover before being harvested. This one hour recovery has the purpose of allowing the cell to translate produced mRNA, and to refold the already produced Firefly luciferase, which is rendered inactive at 42°C. Upon HSF1 activation, a HSF1 trimer should bind to the promoter upstream of the gene of the

luciferase, hence driving its transcription. Figure 7A shows that after one hour of heat shock at 42°C, WT cells display a significant expression of Firefly luciferase, indicating an activation of HSF1.

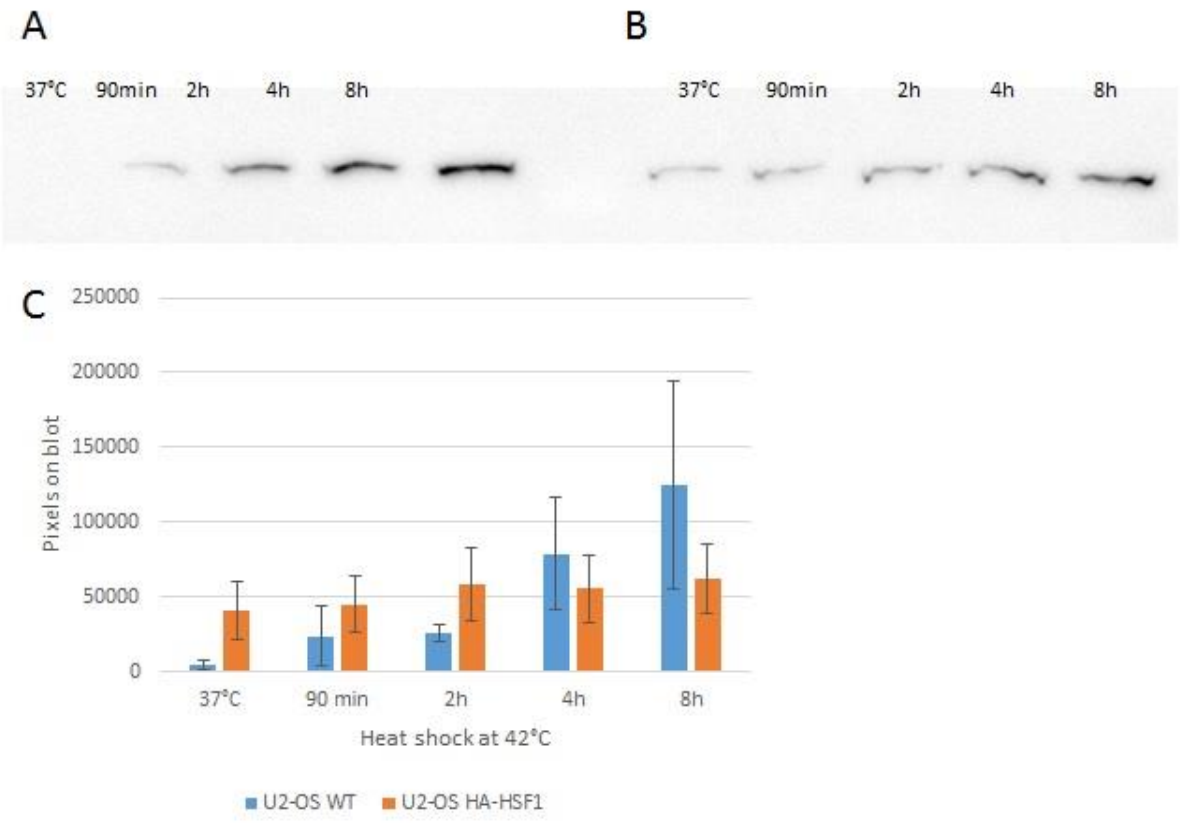

Figure 6: Anti-Hsp70 Western Blot against heat-shocked cells. U2-OS wild type (A) and U2-OS pIRES-GFP II-CtermHA-HsHSF1 cells were submitted to a 42°C heat shock for 90 minutes, 2, 4 and 8 hours, and total protein extract were blotted against an anti-Hsp70 antibody. C) This experiment was repeated three times with similar results. An average of the intensity of the bands is shown for each time interval at 42°C. The error bars represent the standard error of the mean.

HA-HSF1 cells however already show a basal activation of HSF1 in the absence of cellular stress, and do not show any further response to the two different heat shocks applied to them. In this assay again, HA-HSF1 cells seem to display a permanent HSF1 activation and are resistant to further heat shocks. It also appears that one hour heat shock at 39°C is not sufficient to trigger the heat shock response on U2-OS WT cells. Applying a 42°C heat shock for different time intervals on the two cell lines confirms the observation made in Figure 6: whereas WT cells respond as expected to a temperature increase, HSF1 overexpressing cells seem to be resistant to heat-shocks, and only more aggressive stresses can trigger a small increase in their basal HSF1 activation (Figure 7B/C).

Higher luciferase activity is the result of a higher basal activity of HSF1, which lead to a higher concentration of chaperone proteins in the cell. This is consistent to the higher concentration of Hsp70

observed in the absence of temperature stress in Figure 6B. It is also this larger pool of chaperones that might prevent the cells to react as WT cells do in the case of short-length temperature increase: enough chaperones are present in the cytoplasm so that HSF1 can be maintained inactive, and the cells can be protected from proteotoxic effects. Upon very long heat shock, more heat shock proteins might be needed to cope with misfolded proteins, hence the increase in the signal observed in Figure 7C. The fact that, at 37°C, no increase in HSPA1A mRNA levels but elevated levels of luciferase activity were noted, suggests that HSF1 might still be active for the newly brought HSE-containing promoter, but that something prevents bound HSF1 on the promoter of heat shock genes to start transcription. Altogether, these results imply that the U2-OS pIRES-GFP II-CtermHA-hsHSF1 is constitutively in the attenuation phase.

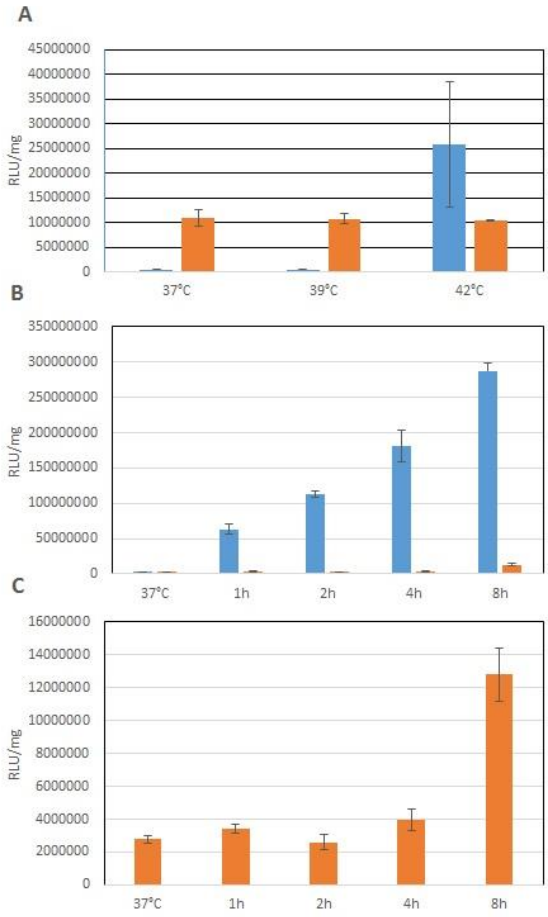

Figure 7: Luciferase assay on U2-OS WT and U2-OS HA-HSF1 cells. HA-HSF1 (orange) and WT (blue) cells were heat-shocked for different length of time at different temperatures, and allowed to recover for one hour. The cells were then harvested, lysed, and the luminescence generated by the Firefly luciferase in the presence of luciferin was measured. The values are normalized with the concentration of total protein in lysate. A) Cells were heat-shocked at different temperatures for one hour (plus one hour recovery at 37°C). Two biological replicates showed a similar trend. The error bars represent the standard error of the mean of three technical replicates. B) and C) Cells were heat-shocked at 42°C for several length of time, and allowed to recover for one hour. The error bars represent the standard error of the mean of three technical replicates.

3.2 Identification of HSF1-binding proteins

In order to identify binding partners of HSF1 during the attenuation phase of the heat shock cycle, anti-HA immunoprecipitations were performed on U2-OS HA-HSF1 and on U2-OS mock cells, using anti-HA agarose beads. Elution from the beads was performed by incubating the beads three times with 0,2 mg/mL HA-peptide (Figure 8).

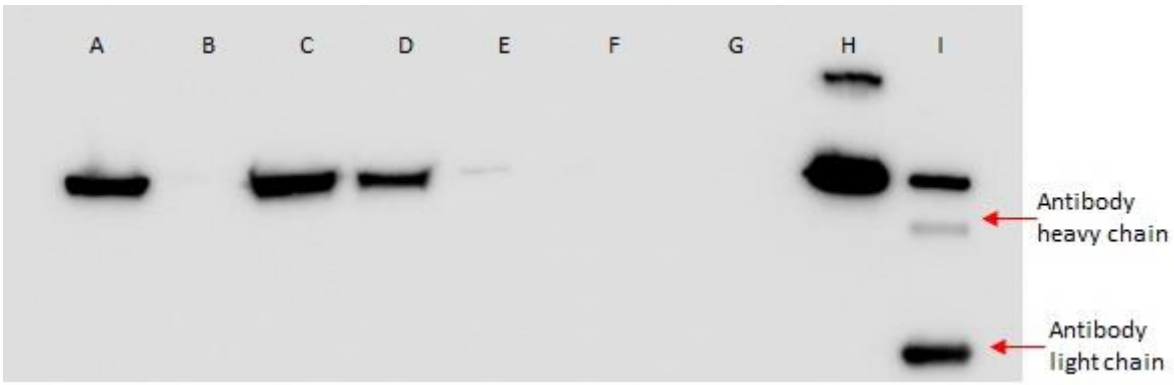

Figure 8: Balance anti-HA western-blot for the anti-HA immunoprecipitation. A: Crude cell extract, B: Resuspended pellet, C: Clarified lysate, D: unbound fraction, E F and G: Washes, H: Peptide elution, I: Cooked beads. 1/1000 of the total crude cell extract, pellet, lysate, unbound fraction and washes, 1/50 of the peptide elution, and 1/5 of the cooked beads were loaded.

The presence of a protein carrying a HA-tag in the crude extract confirms the expression of HA-HSF1 in these cells. The binding of HA-HSF1 was however not complete, as some HA-tagged protein remained in the flow- through (Figure 8, lane D), proving the anti-HA beads were completely saturated with HA-HSF1. Surprisingly, two bands are seen in the peptide elution lane. This is not expected, as any oligomers of HSF1 (which could eventually spontaneously form through higher concentration of HSF1) should not be present in a SDS-PAGE gel. This could eventually be explained by the age of the Sample buffer used: an old sample buffer might contain non-active DTT, allowing some HSF1 to remain trimeric. Then peptide elution was however not complete, as some protein remained bound to the beads, and could only be released by cooking the beads in 2X Laemmli buffer.

After parallel immunoprecipitation on the lysates of the two cell lines were performed, co-immunoprecipitated were labeled with dimethyl for three replicates (peptides issued from U2-OS HA-HSF1 cells, and peptides issued from mock cells were labeled with medium-weight dimethyl and light-weight dimethyl respectively), and one replicate was obtained after having grown the cells in SILAC (Stable Isotope Labelled Aminoacid Cell culture) growth-medium for control. The medium containing

the heavier amino-acid was given to the cells overexpressing HSF1. In contrast to regular SILAC procedure, cell lysates were not mixed together before immunoprecipitation, but at a 1:1 total protein concentration after elution from the beads, to have similar conditions than for the dimethyl-labelling replicates. This SILAC pull-down was meant to control whether the same hits are found using a different method. In order to only select strong candidates, only potential hits with a medium/light ratio above two in at least two of the four replicates were considered.

Table 1 recapitulates the identified interaction partners fulfilling these criteria.

Table 1: Identification of interaction partners of HSF1[1].

Category	Gene Name	Protein	M/L Ratio (DML 1)	M/L ratio (DML 2)	M/L Ratio (DML 3)	M/L Ratio (SILAC)
Chaperones	HSPA8	Hsc70	61,4	10,2	194,2	16,4
	HSPA1A	Hsp70	62,8	8,3	382	13,2
	HSPA9	mtHsp70	10,8	74,9	24,3	9,5
	HSPA5	Endoplasmic reticulum Hsp70	4,2	0,7	11,2	4,4
Co-chaperones	BAG2	Bag2	3,1	15,9	44,5	12,5
	BAG4	Bag4	3,7	9,1	3,6	9,9
Carcinogenesis	DMBT1	Deleted in Malignant Brain Tumor Protein 1	2,0	1,9	0,8	2,6
Transcription elongation	HTATSF1	HIV-TAT Specific Factor 1	-	3,0	2,4	2,3
Chromatin remodeling	SMARCD2	SWI/SNF-related matrix-associated actin-dependent regulator of chromatin subfamily D member 2	2,6	2,1	Not quantified	-

The identification of molecular chaperones of the Hsp70 family is not surprising. It has been shown in several studies that the Hsp70/Hsp40 complex represses the transactivational capacity of HSF1, attenuating the heat shock response. No protein of the Hsp40 family was identified, but this could be due to the fact that the interaction between the J-domain protein and its substrate is transient, weak, and therefore that no Hsp40 was co-immunoprecipitated. The presence of the mitochondrial and of the endoplasmic reticulum Hsp70s are not expected, as HSF1 is not supposed to be present in those organelles. It is hence most likely that those protein/protein interactions happened after cell lysis, during the two and a half hour incubation with the anti-HA beads used for immunoprecipitation.

[1] DML 1, 2 and 3 represent the three independent replicates analyzed with dimethyl labelling shotgun proteomics.

Besides Hsp70s, the Hsp70 co-chaperones Bag2 and Bag4 were identified in the four replicates with high Medium over Light ratios. Bag proteins are nucleotide exchange factors of the Hsp70 family, and finding them in such a screening is interesting, as co-chaperones of Hsp70 during the attenuation phase of the heat shock cycle are still unknown. It is however possible that Bag2 and Bag4 do not interact directly with HSF1, but rather through Hsp70.

None of the other potential interaction partners identified is present in the four replicates, and their ratios are much lower than the ones of the hits already mentioned. The Deleted in Malignant Brain Tumor Protein 1 (DMBT1) was never reported to interact with HSF1, but HSF1s' involvement in cancer cells metabolism has been established in many studies. The presence of proteins involved in transcription and chromatin remodeling is consistent with the fact that HSF1 is a transcription factor. Indeed, HIV-Tat Specific Factor 1 is a transcription elongation factor which also plays a role in cells that are not infected with HIV as well are in tissues originated from seropositive patients (Li & Green 1998), and the SWI/SNF-related matrix-associated actin-dependent regulator of chromatin subfamily D member 2, also known as BAF60B, is a member of the SWI/SNF complex, which is known to be a nucleosome remodeling complex (Lorès et al. 2010).

The high medium/light ratios, combined with the fact that the interactions of Bag proteins with Hsc70 or Hsp70 through their Bag domain are already studied (Gässler et al. 2001; Xu et al. 2008; Rauch & Gestwicki 2014) lead us to investigate this interaction further.

3.3 Bag2 and Bag4 interact directly with HSF1

To confirm the interaction (direct or indirect) of Bag2 and Bag4 with HSF1, U2-OS HA-HSF1 cells are transiently transfected with plasmids encoding 3xMYC tagged Bag2, Bag4, or fragments of these two proteins, alongside an empty vector as control, and immunoprecipitation against MYC and against HA were performed. (Figure 9).

As the interaction between Bag proteins and Hsp70/Hsc70 is thought to happen through their C-terminal Bag domain, the Bag domains of Bag2 and Bag4 (respectively Bag2_BD and Bag4_BD) are also overexpressed. Curiously, the Bag domain of Bag4 is a one third shorter triple-helix bundle than the Bag domain of other Bag proteins. It should however still be functional (Briknarová et al. 2002).

The sequences of these two proteins outside of the Bag domain are not characterized. In fact, apart from a predicted coiled-coil domain close to the N-terminus of Bag2, no domain structure exists for the N-terminal parts of Bag2 and Bag4 (respectively 108 and 374 amino-acids). Hence the whole N-

terminal parts of the two nucleotide exchange factors are also overexpressed. From now on, these polypeptides will be called Bag2_NTD and Bag4_NTD.

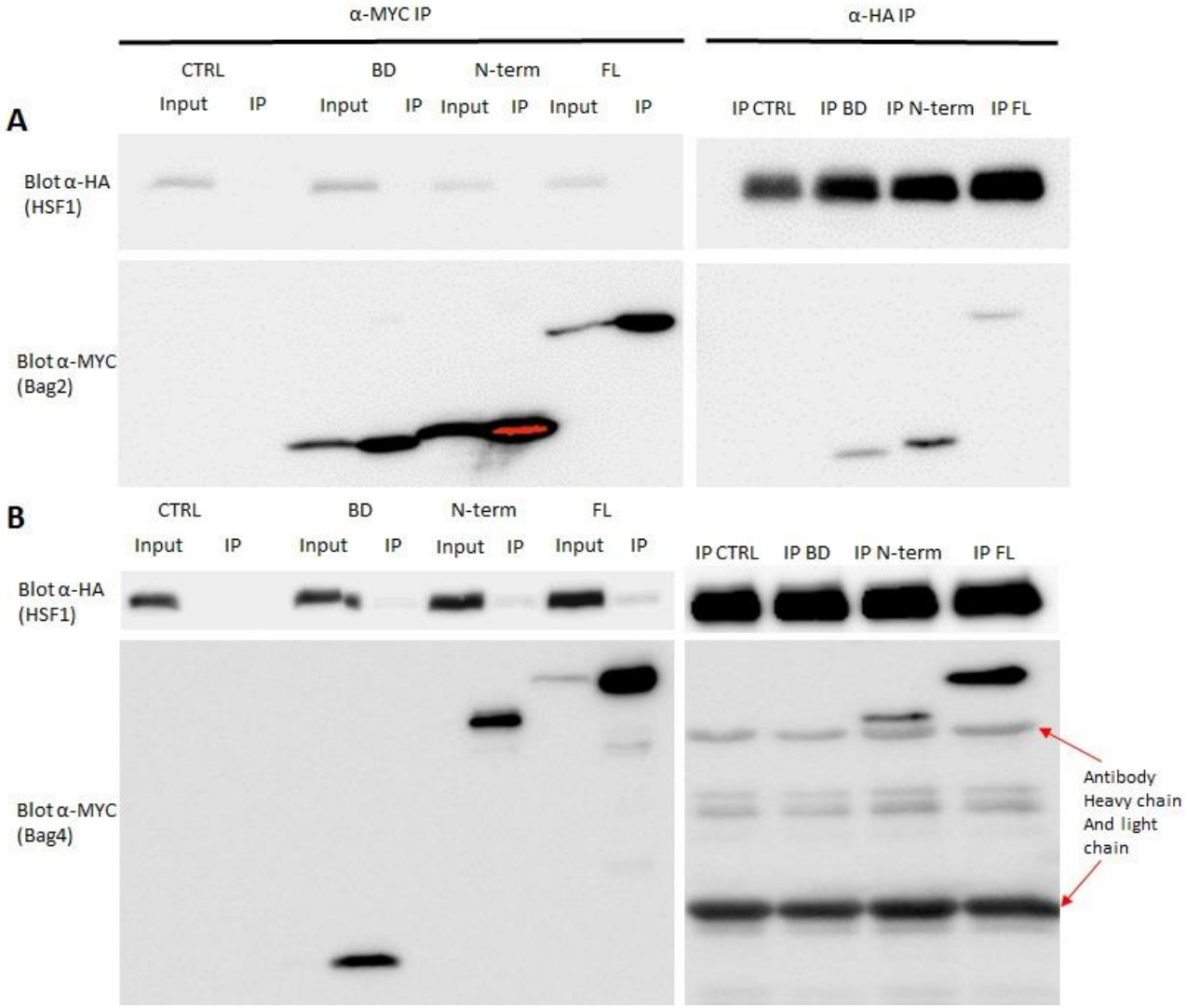

Figure 9: Co-Immunoprecipitation on U2-OS HA-HSF1 cells transiently transfected with 3xMYC-Bag2 or 3xMYC-Bag4. 3xMYC-Bag2 (A) and 3xMYC-Bag4 (B) were transfected, and cells were harvested 48 hours after transfection. The cell lysates were used for parallel anti-MYC and anti-HA immunoprecipitation. Input and precipitates (IP) were blotted against HA, to visualize HSF1, or against MYC, to visualize the Bag proteins. Both immunoprecipitation were repeated three times, and results were identical.

In Figure 9A, the immunoprecipitations of Bag2 and its fragments were successful (left panel). All three constructs seem to interact with HSF1, as they are all co-immunoprecipitated with the latter protein (Figure 9A, right panel). This is actually surprising, but reveals that the Bag domain of Bag2 might be structurally different than the Bag domain of other Bag proteins, as suggested by Xu and colleagues (Xu et al. 2008). Pulling down 3xMYC-Bag2 or fractions of it, it was in our hands not possible to detect co-immunoprecipitated HSF1. This can be due to the fact that Bag2 was reported to be non-client

specific, and therefore interacting with many clients of Hsc70 (Taipale et al. 2014), hence with a lesser fraction of HSF1. It could also be due to different antibody-sensitivity between the anti-HA and the anti-MYC antibodies. In Figure 9B, it appears that Bag4_BD and Bag4_NTD are not well expressed. However, the immunoprecipitations were successful, and these polypeptides could be concentrated in the precipitates. Pulling on HSF1 through its HA tag, it is clear that HSF1 interacts with full length Bag4, but also with its "N-terminal domain". There is however no band visible for the Bag domain of Bag4, suggesting that HSF1 does not (or only weakly) interact with the Bag domain of Bag4 (Figure 9B). In the reverse pull-down (MYC-IP) HSF1 co-immunoprecipitates with Bag4 full length, with Bag4_NTD and eventually with Bag4_BD. This last interaction is however not clear, and could be unspecific, even if the band seen is above background. The amount of MYC-tagged proteins seen in the input in Figure 9A is much lower than the amount of MYC-tagged proteins detected in Figure 9B. Comparing the intensity of the bands corresponding to the Bag proteins pulled-down in these two experiments, it is likely that much more proteins should have been loaded in order to see HSF1 co-immunoprecipitated with ——————————ag2.

The interactions between HSF1 and Bag2 or Bag4 were here confirmed *in vivo*. It is however possible that these interactions are indirect and happens through Hsp70/Hsc70. In order to control this, U2-OS HA-HSF1 cells are transiently transfected with the same constructs as previously, and anti-HA and anti-MYC immunoprecipitations followed by a western blot against both Hsc70 and Hsp70 are performed (Figure 10).

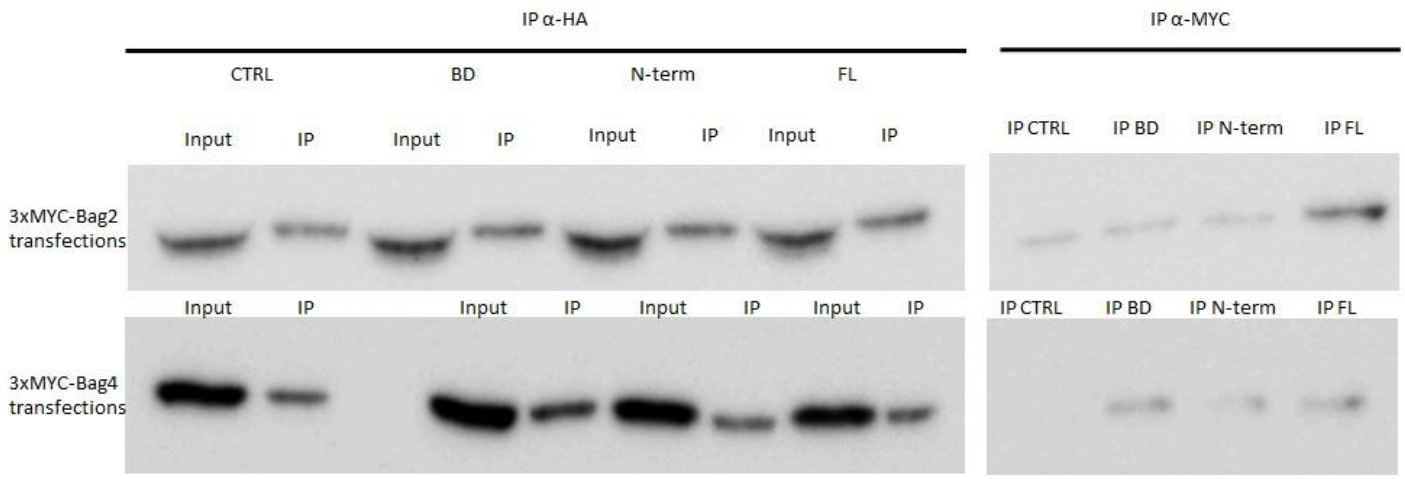

Figure 10: Anti-Hsc70/Hsp70 western blot on immunoprecipitated U2-OS HA-HSF1 cells lysates. Hsc70 and Hsp70 are co-immunoprecipitated with HSF1 (through anti-HA western blot) and with Bag2 and Bag4 (through anti-MYC western blot).

Hsc70/Hsp70 is pulled-down alongside HSF1, confirming the interaction seen with shotgun proteomics. Both Bag2 and Bag4 interact as full length protein with Hsc70/Hsp70. Bag2_BD and Bag2_NTD alone do not seem to interact with a molecular chaperone of the Hsp70 family, as the intensity of the band seen is similar to the unspecific band detected in the control, when an empty vector is being transfected. Hence, to interact properly with Hsc70 or Hsp70, the Bag domain of Bag2 appears not to be sufficient. On the other hand, Bag4 precipitates with Hsc70/Hsp70 as a full length protein, and it seems that its Bag domain alone is able to interact with the chaperone as well. Bag4_NTD seems to slightly interact with Hsc70 or Hsp70 as well. This could however be due to the fact that Bag4_NTD is rather unstructured and might therefore be a considered by the chaperone as a substrate. It is consequently here possible to emit the hypothesis that Bag4 interact with Hsp70 through its Bag domain, and through HSF1 through the N-terminal part of the protein. For Bag2, it would be tempting to conclude the same, but our data show otherwise: Both Bag domain and N-terminal domain are able to interact with HSF1, and it seems that only the full length protein is able to interact with Hsp70 *in vivo*. This could be explained by the structural differences between the Bag domains of Bag2 and Bag4.

Next, in order to confirm these direct interactions *in vitro*, expressions a N-terminal Glutathione-S-transferase (GST) fusion of Bag2, Bag2_NTD Bag2_BD, Bag4, Bag4_NTD and Bag4_BD in MC-1061 *E. coli* were made, and GST pull-down using Glutathione agarose, in the presence or the absence of 2 µM of purified HSF1 were subsequently performed. GST alone was expressed as a control. The N-terminal domains of both nucleotide exchange factors were cloned as well, but their expression in MC-1061 could not be detected. This is most probably due to the unstructured nature of those polypeptides, making them susceptible to protease degradation. The GST-fusion proteins were eluted from the Glutathione agarose using a glutathione solution, and SDS-PAGE followed by anti-HSF1 and anti-GST immune-blotting were subsequently performed (Figure 11).

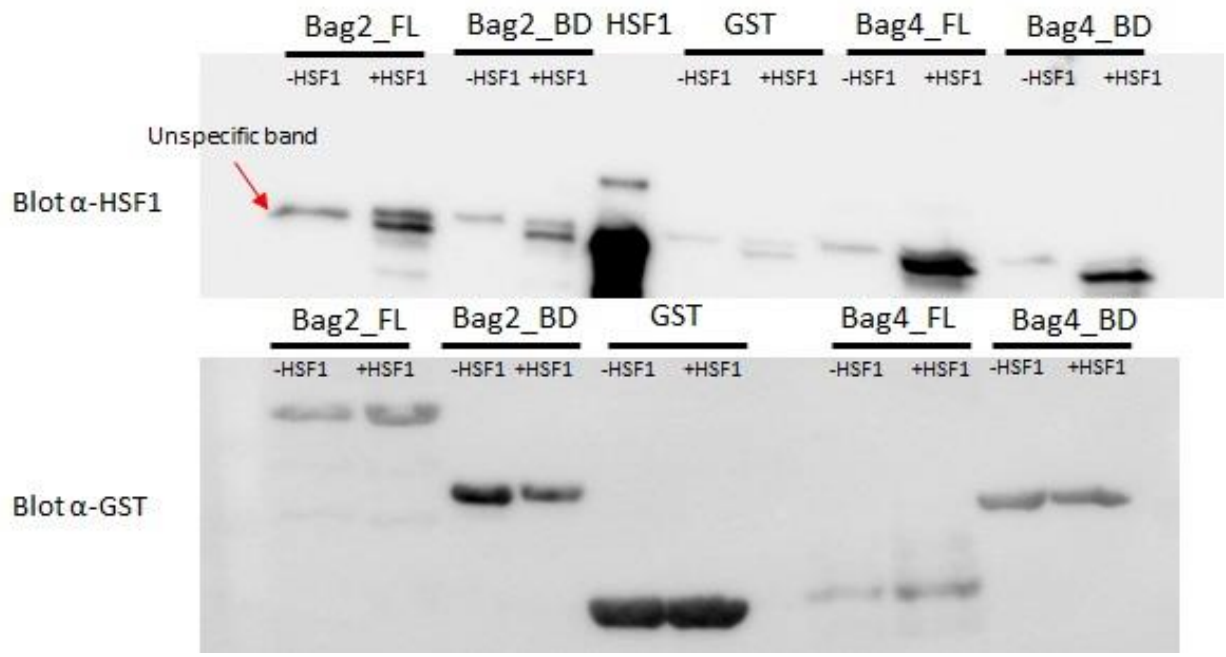

Figure 11: In vitro GST pull-downs of Bag2_FL, Bag2_BD, GST, Bag4_FL and Bag4_BD. Purified HSF1 was loaded in the middle of the gel as a control. MC 1061 bacterial lysates were incubated with 20 µL of Glutathione agarose 4B, and, when indicated, with 2 µM of purified HSF1. This experiment was repeated twice with similar results.

In this experiment, the interactions seen can only be direct interactions, as Hsp70 is missing in the cytoplasm of *E. coli*. It appears that both Bag2_FL and Bag4_FL interact as GST fusion with HSF1. When GST was expressed alone, a slight HSF1 band can be seen. This is most probably negligible, as GST was strongly expressed compared to the GST fusion of Bag2 and Bag4, and the co-precipitated HSF1 observed much more abundant. It is hence safe to suppose that the HSF1 band seen in the "GST +HSF1" lane is the result of not properly washed beads. Therefore, Bag2 and Bag4 directly interact with HSF1, and not through a chaperone of the Hsp70 family. For both proteins, it seems that the Bag domains are also able to interact with HSF1. This was already seen *in vivo* for Bag2, but not in the case of Bag4. This could be explained by the fact that in presence of Hsc70/Hsp70, Bag4_BD would preferably interact with the molecular chaperone. In the absence of the latter, the Bag domain of Bag4 could then interact with HSF1 in a similar manner than Bag2_BD.

The full-length version of Bag4 was not well expressed and partly degraded, as the GST-fusion detected through immuno-blotting was much lighter than it should have been. In fact, it is barely bigger than GST alone. Nevertheless, it seemed that this shortened version of Bag4 was still able to interact strongly with HSF1, confirming the interaction of Bag4's NTD with HSF1.

Bag2's role as a nucleotide exchange factor of Hsp70 is established, though not quantitatively (Dai et al. 2005; Xu et al. 2008; Rauch & Gestwicki 2014), but Bag4 was left out of many studies on the nucleotide exchange activity of members of the Bag protein family.

3.4 In vitro characterization of Bag2 and Bag4

3.4.1 Purification of Bag2, Bag4 and Hsc70.

Bag2 full length, Bag2 Bag domain, Bag4_BD and Hsc70 were expressed as N-terminal 6xHis-SUMO-fusion in BL21(DE3) Rosetta™ *E. coli* and purified as described in chapter 5. The purification of Bag4 full length was attempted, but obtaining the full length protein was not met with success, as the suspected unstructured N-terminus of the protein was protease sensitive. Figure 12 presents the purification balance for each protein purified.

The challenge encountered in purifying Bag2_FL was the fact that even a His-tag depleted Bag2 was still able to interact with the Nickel beads. To overcome that issue, Nickel resin was saturated with Ulp1 SUMO-protease beforehand, and the digestion was performed on column, for 2 hours. This way, Bag2 could not interact with the nickel ions, and a mixture containing Bag2 and the free SUMO was generated. Gel filtration using a Superdex 75 gel filtration column was performed as a last step, allowing the separate Bag2 from the free SUMO, and additional impurities that were bound to the Nickel column in an unspecific manner.

The Bag domain of Bag2 was purified according to Xu and colleagues (Xu et al. 2008), and a Superdex Peptide 10/300 GL was used instead of the Superdex 75 they used. The initial steps were almost identical as for Bag2_FL, with Nickel affinity purification, and cleavage of the SUMO tag using the Ulp1 protease.

The purification of the Bag domain of Bag4 did not required any additional step after SUMO cleavage, besides two extra Nickel affinity purification, in order to bind Ulp1, and free SUMO. As a matter of fact, the removal of Ulp1 and free SUMO proved unsuccessful after the second Nickel affinity purification, and a third one was necessary.

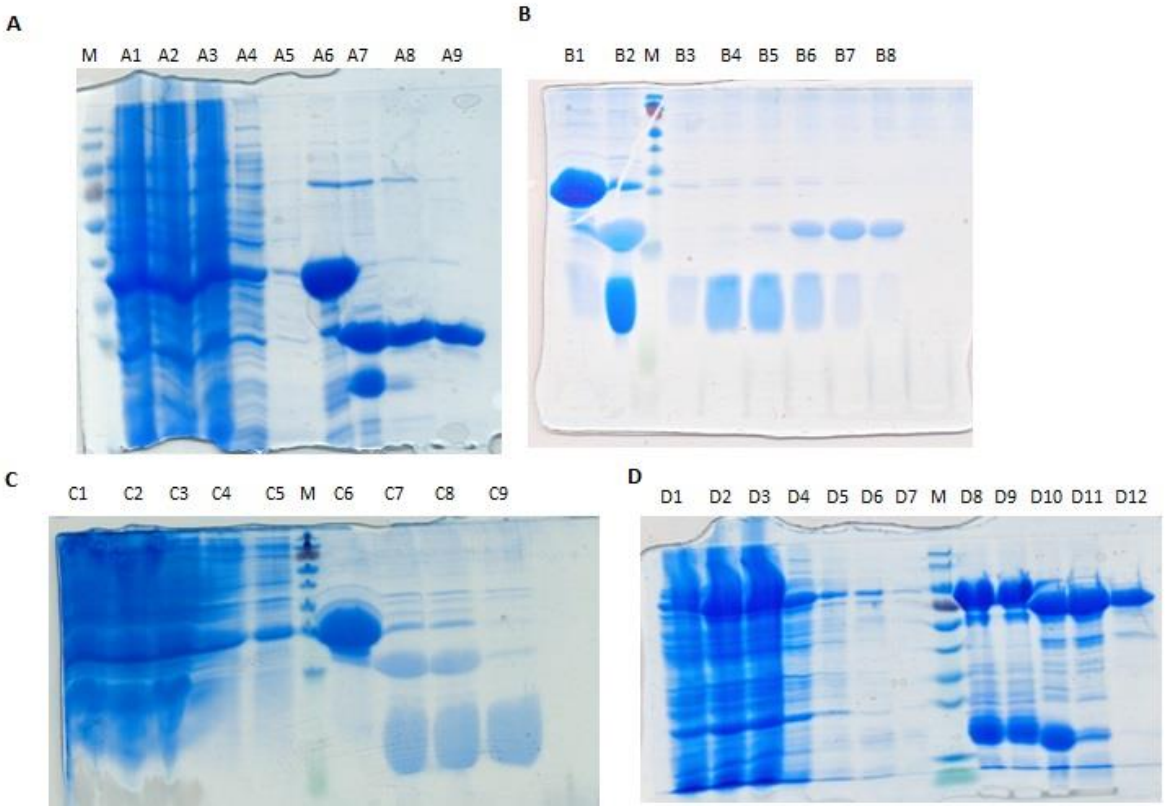

Figure 12: Purification of recombinant Bag2_FL (A), Bag2_BD (B), Bag4_BD (C) and Hsc70 (D).

M: Molecular weight marker (from top to bottom: 170 kDa, 130 kDa, 100 kDa, 70 kDa, 55 kDa, 40 kDa, 35 kDa, 25 kDa, 15 kDa, 10 kDa), A1: Crude lysate, A2: Clarified lysate, A3: Flow-through Nickel beads, A4: Wash with lysis buffer, A5: Wash with high-salt buffer, A6: Imidazole elution from the Nickel beads, A7: After on column Ulp1 digestion, A8: fractions 25 and 26 of S75 gel filtration, A9: Fraction 27 of S75 gel filtration; B1: Imidazole elution from Nickel beads, B2: After overnight Ulp1 digestion, B3 to B8: fractions 16 to 21 after Superdex Peptide 10/300 GL gel filtration; C1: Crude lysate, C2: clarified lysate, C3: Flow-through Nickel beads, C4: Wash with lysis buffer, C5: Wash with high-salt buffer, C6: Imidazole elution from the Nickel beads, C7: After overnight Ulp1 digestion, C8: After second Nickel affinity purification, C9: After third Nickel affinity purification; D1: Crude lysate, D2: clarified lysate, D3: Flow-through Nickel beads, D4: Wash with lysis buffer, D5: Wash with high-salt buffer, D6: ATP wash, D7: Wash with lysis buffer, D8: Imidazole elution from the Nickel beads, D9: After buffer exchange, D10: After overnight Ulp1 digestion, D11: After second Nickel affinity purification, D12: After Res Q anion exchange chromatography.

The first steps of the purification of Hsc70 differed from the three other purifications described in this work, as an ATP-wash was performed in order to induce substrate release of substrate that could have been bound by Hsc70. After additional wash, elution was performed with an Imidazole containing buffer, as previously. Moreover, anion exchange chromatography was performed at the very end of the purification.

3.4.2 Secondary structure analysis of Bag2 and Bag4

Before using the proteins previously purified in *in vitro* biochemical assays, it was necessary to make sure that they were well-folded. As the Bag domains of both Bag2 and Bag4 were reported to be α-helical, the secondary structures of Bag2 and Bag4_BD are obtained through far-UV circular dichroism (CD) spectroscopy. This method is based on the interactions between polarized light and chiral molecules and is one of the best method to determine alpha helicity. Proteins, mostly through the carbon atom of the peptidic bond, are chiral macro-molecules. It is therefore possible to obtain an idea of the α-helical, β-sheet, or random coil composition of a protein. The CD spectra of Bag2, Bag4_BD, and Bag2_BD are displayed in Figure 13.

With maxima at 195 nm, and two minima at respectively 208 and 222 nm, both Bag2_FL and Bag4_BD are mostly α-helical. This is to be expected for the latter protein, as it was reported than a canonical Bag domain is made of a triple α-helix bundle. It is therefore possible to assume than Bag4_BD is properly folded, and hence that it should be active for *in vitro* assays. The Bag domain of Bag2 makes up almost half of the full length protein, and was also reported to be made of three α-helixes. The remaining 12.3 kDa of the protein contain a short predicted coiled-coil domain which is also made of α-helixes.

The Bag domain of Bag2 is, according to Xu and colleagues, made of three α-helix (Xu et al. 2008). Hence, the first CD spectrum, obtained directly after purification, was not surprising, displaying a well-defined α-helical pattern (Figure 13C, right panel). However, snap-freezing the protein and thawing it for subsequent experiments revealed a different spectrum (Figure 13C, right panel), as the 195 nm peak, characteristic of α-helixes became a rather flat-line. Since random coil spectra exhibit a minimum at 195 nm, it is possible that the flat line with a θ value roughly equal to 0 $deg.cm^2.dmol^{-1}$ is actually an average of α-helical maximum and random-coil minimum. Moreover, the 208 nm minimum was lost, and replaced by a 215 nm minimum, characteristic of β-sheets, implying an eventual aggregation of the protein after thawing. This allow us to conclude that Bag2_BD cannot be frozen and still maintain its activity when thawed.

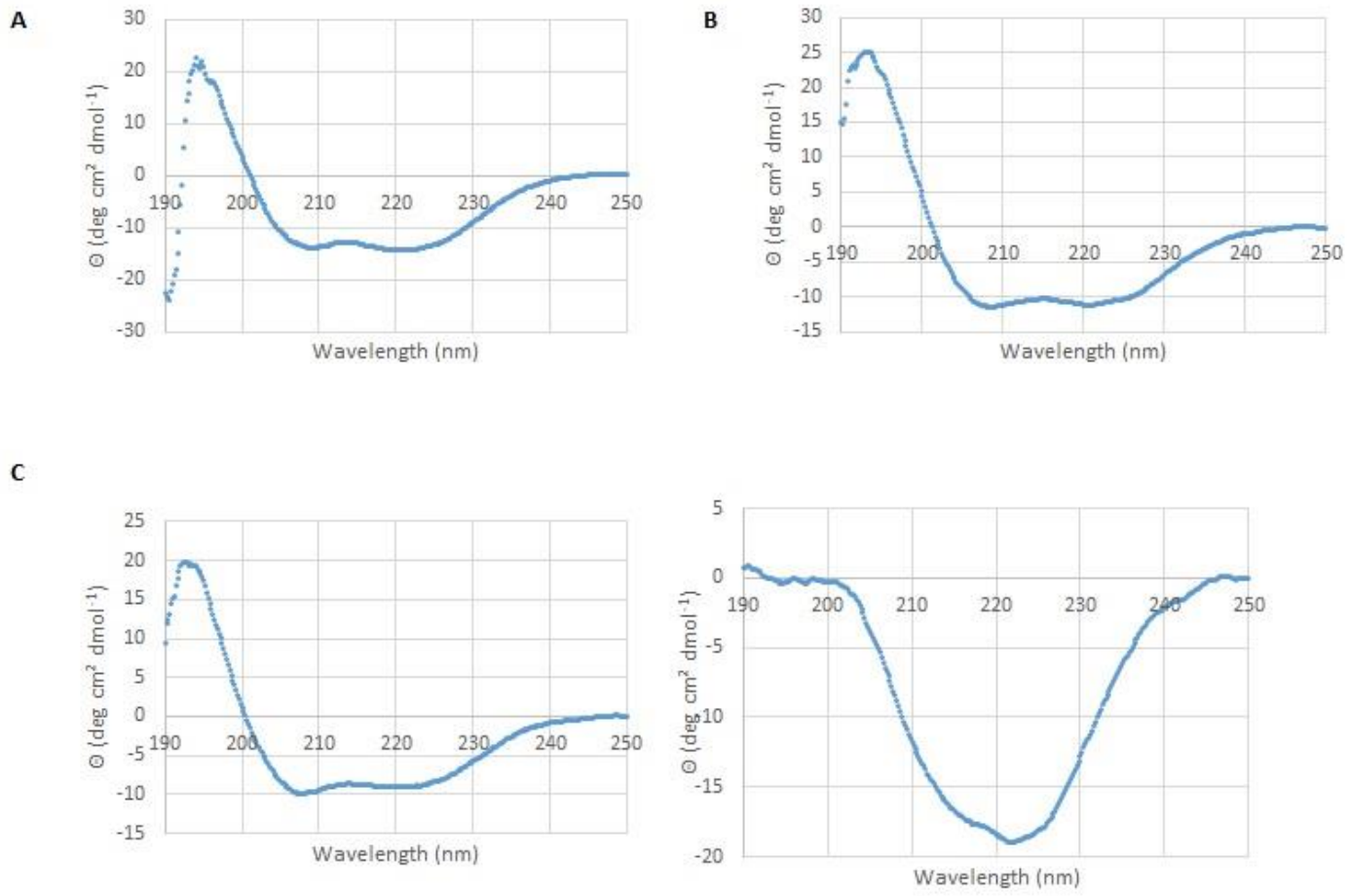

Figure 13: Circular dichroism spectra of Bag2_FL (A), Bag4_BD (B) and Bag2_BD (C). In C, the left panel represents the CD spectrum of Bag2_BD directly after purification. The right panel is the CD spectrum of the same protein, after one freeze-thaw cycle.

3.4.3 Thermal stability of Bag2 and Bag4

In order to establish how these proteins can be handled for *in vitro* experiments, their thermal stability was assayed. Thermal stability can be assayed using CD by following the changes in CD-value while increasing temperature. The single wavelength of 222 nm was chosen, and the signal at that wavelength is recorded at each temperature. A gradient of 20°C/hour, ranging from 10°C to 90°C was performed on each of the three Bag proteins purified (Bag2_FL, Bag2_BD, and Bag4_BD).

The denaturation curves are presented on Figure 14. From these results, it is clear that Bag2 full length is folded and stable until 40°C, temperature after which it starts to unfold. The process seems to be in two steps: one sharp increase in CD values happening between 50 and 60 °C, and a shallower, linear increase from 60°C to 90°C (Figure 14 A). The denaturation of the Bag domain of Bag4 appears to follow a sigmoidal pattern, with shallow signal change from 10°C to 50°C, indicating non-cooperative

unfolding. This is followed by a steeper increase in CD values up to 75°C. Slower increase in the CD signal up to 90°C finishes the recording. Bag4_BD hence seems to start unfold already at low temperature, hinting that this protein would not be completely stable. It is however not the complete protein, and a stabilization of the Bag domain by parts of its N-terminal sequence could be considered (Figure 14 B). Bag2_BD, which was assumed to be aggregated after thawing displays an almost linear denaturation curve, confirming the idea that this protein is unfolded, aggregated, and might therefore not be active (Figure 14 C).

The sharp increase in CD value observed in Figure 14 A suggests high cooperativity in the unfolding mechanisms. According to Xu and colleagues, Bag2 forms homodimers that can *in vivo* interact with

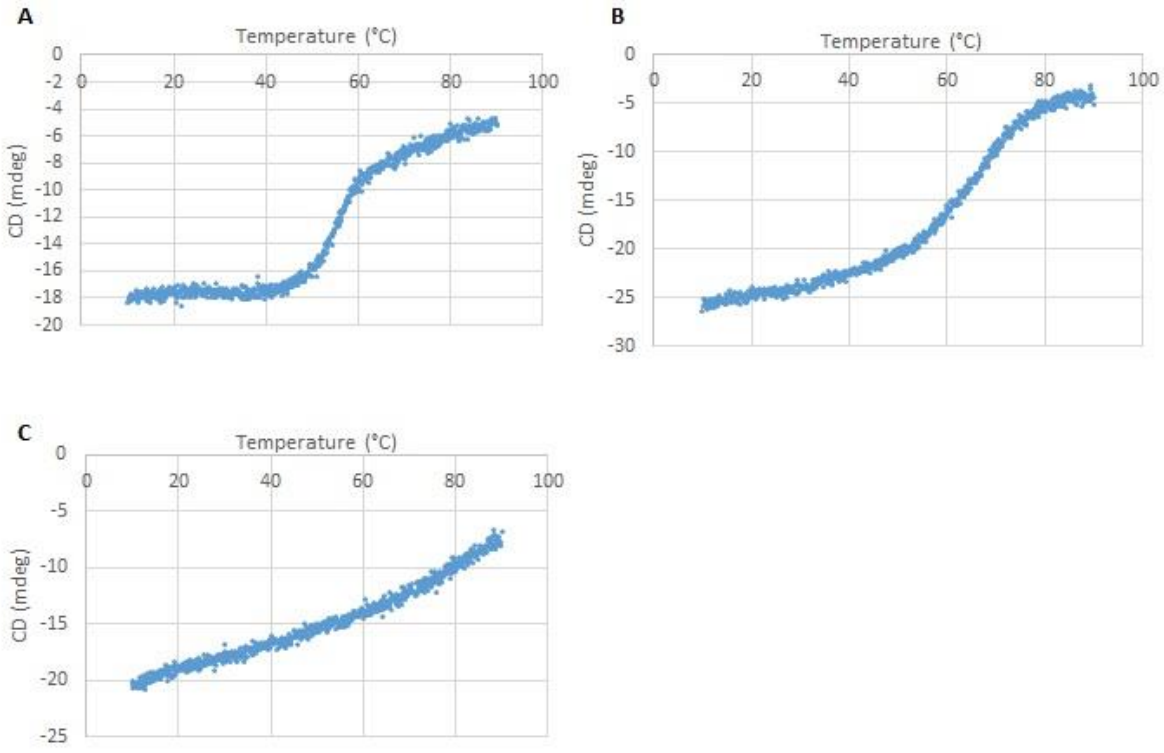

Figure 14: Temperature denaturation of Bag2_FL (A), Bag4_BD (B) and Bag2_BD (C). The curves display the CD value at 222 nm for each temperature of the scan. The curve for Bag2_BD was obtained from a frozen aliquot.

several Hsp70s close to each other (Xu et al. 2008). If one admits this hypothesis, it could very well be that homodimers of Bag2 are present in the sample measured here, and that the steep CD values increase actually represents some unfolding leading to monomerization of the protein. From there, the denaturation appears to be linear, as it is the case for the Bag domain of Bag2, which is most

probably already misfolded. It is however unknown to us whether Bag2 forms homodimers, the structure published by Xu and colleagues being of its Bag domain only.

Taken together, these data tell us that *in vitro* assays involving Bag2_FL can be performed at physiological temperature, and lower. The Bag domain of Bag4 becomes less stable at temperatures above 30°C. Therefore, no *in vitro* assays can be performed at a temperature above 30°C. Finally, purified Bag2_BD starts to unfold at 10°C, indicating that it is not stable under in vitro conditions.

3.4.4 Bag2 and Bag4 act as nucleotide exchange factors of Hsp70

As mentioned earlier, Bag2 is not well characterized. For example, no rates of nucleotide exchange dependent on the concentration of Bag2 have been determined. In addition, Bag4 was always left out comparison studies between the different proteins of the Bag family. As no full length Bag4 was available, its Bag domain will be used, and compared to Bag2.

In order to investigate the influence of the Bag proteins on nucleotide exchange capacity of Hsc70 and Hsp70, ADP release stimulations by Bag2 and Bag4_BD are measured with stopped-flow instrumentation. The reaction will be followed by using the synthetic ADP analog MABA-ADP, which was shown to have similar kinetic property as its natural counterpart in the case of Bag1 (Gässler et al. 2001), and of the *E. coli* Hsp70-like chaperone DnaK (Theyssen et al. 1996). Since fluorescence intensity of MABA-ADP at 420 nm is strongly increased when it is bound to Hsp70, its release can then be followed by a decrease in fluorescence (Figure 15 A).

This decrease in fluorescence (Figure 15 A) was fitted using a single exponential decay function, and the MABA-ADP.Hsp70/Hsc70 complex dissociation coefficient (k_{off}) was plotted against the concentration of nucleotide exchange factor (Figure 15 B).

The Bag domain of Bag2 did not stimulate the release of MABA-ADP, as increasing concentration of Bag2_BD did not have any effect on the value of k_{off}. This observation indicates that the Bag domain of Bag2 was inactive, consistent with the conclusions drawn from the CD spectra. Bag2 full length however does have an effect on the dissociation of the complex between MABA-ADP and Hsp70/Hsc70. In addition, it appears that Bag2's stimulation of nucleotide exchange is much stronger on Hsc70 than on Hsp70. This is interesting, as it was shown by Gässler and colleagues that Bag1-M stimulated both Hsp70 and Hsc70 to a similar degree, with a slightly stronger stimulation of Hsp70 (Gässler et al. 2001). The Bag domain of Bag4 turned out to be a much more efficient nucleotide

exchange factor than Bag2, but similar to Bag2, it stimulates nucleotide exchange more efficiently in Hsc70 than in Hsp70. This weaker effect of Bag2 could be due to the different nature of its Bag

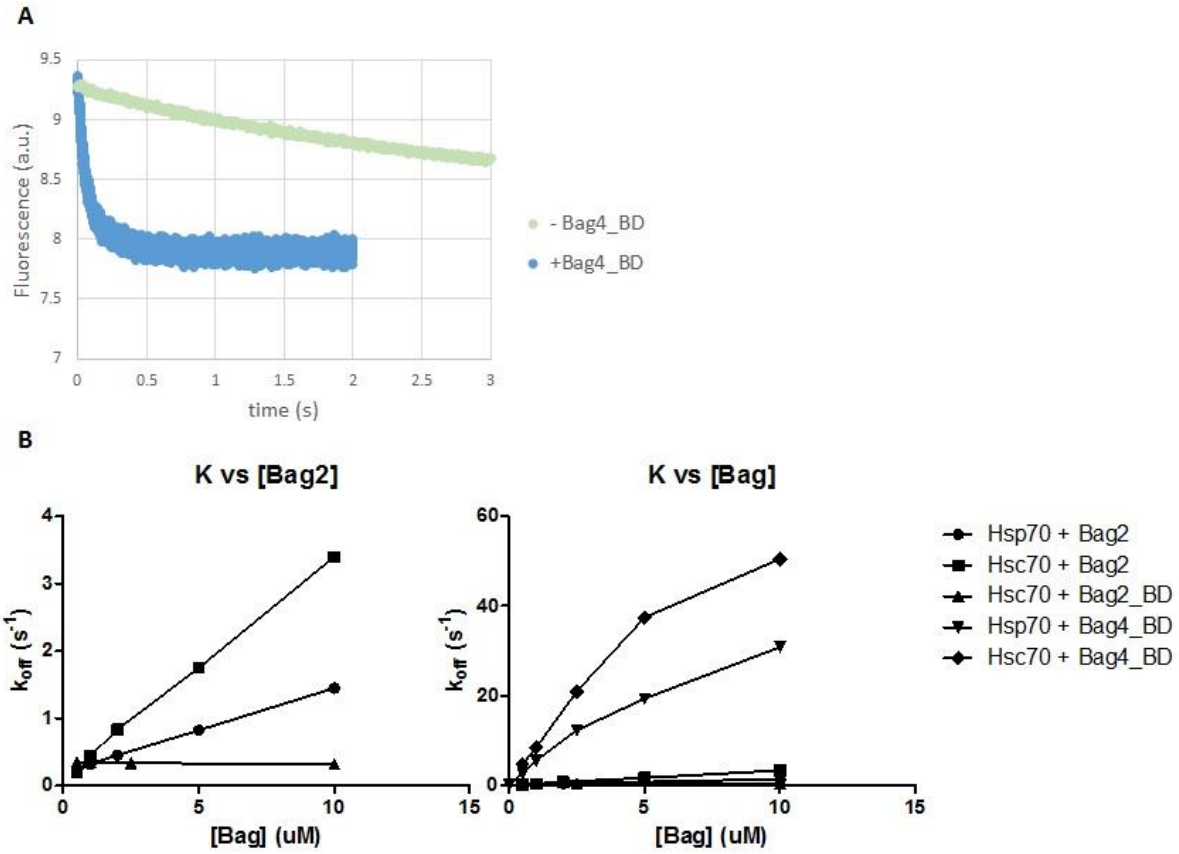

Figure 15: Stimulation of ADP release from Hsp70/Hsc70 by Bag2 and Bag4_BD. Hsp70 and Hsc70 were both incubated with MABA-ADP for 30 minutes at 30°C, to allow saturating binding of the nucleotide analog to the chaperone before the nucleotide exchange factor is injected with the stopped-flow device. A) Dissociation of the MABA-ADP.Hsc70 complex after addition of an excess of unlabeled ATP in the absence (green) and presence (blue) of Bag4_BD (2.5 µM). B) k_{off} values for MABA-ADP complexes with Hsp70 and Hsc70 as indicated in the presence of increasing concentration of Bag protein.

domain, not being the canonical triple helix bundle. It is however hard to draw any conclusion regarding to the stronger stimulation of Bag4 in relation to Bag2, as only the Bag domain of Bag4 was used, and not the full length protein. Moreover, it was shown that the Bag domain of Bag1-M is a more active nucleotide exchange factor than its full length version (Gässler et al. 2001).

To conclude, purified Bag2 and Bag4_BD clearly are nucleotide exchange factor of Hsp70. Unfortunately, the concentration obtained after purification of the two proteins did not allow to titrate the Bag proteins to higher concentrations to reach saturation of the dissociation rate.

3.4.5 Bag2 and Bag4 increase luciferase refolding rates

Nucleotide exchange factors increase the rates of ADP release. In the theoretical work cycle of Hsp70s, the release of ADP allows the binding of a new molecule of ATP, which in turn decreases the affinity of Hsp70 for its substrate. Hence, release of ADP leads to substrate release. Up to a certain concentration, the presence of a nucleotide exchange factor should therefore accelerate the rates of refolding of Hsp70s' substrate. Passed a certain concentration of NEF, the effect could be negative on substrate refolding, as the latter one would be released before having attained a conformation that refolds efficiently.

To verify the cooperation of the purified Bag proteins with an Hsp70-family chaperone in a classical chaperone function, the model protein Firefly luciferase was used. Firefly luciferase unfolds at 42°C, but can be refolded in the presence of Hsp70 and a J-domain protein co-chaperone. The addition of a nucleotide exchange factor up to a certain concentration should enhance the reaction. Since Hsc70 was more stimulated than Hsp70 by both nucleotide exchange factors tested, this chaperone will be used for refolding heat-denaturated Firefly luciferase. As Bag2 and Bag4_BD were not very temperature-stable *in* vitro, Firefly luciferase was first denaturated for 10 minutes at 42°C in the presence of Hsc70 and the J-domain protein Hdj1. The Bag proteins were added after return at 30°C for the refolding reaction. At regular time intervals, the activity of luciferase was assayed. The influence of Bag2 and of Bag4_BD on luciferase refolding by Hsc70 is presented in Figure 16.

At all concentrations tested, Bag4_BD (Figure 16 A) and Bag2 (Figure 16 B) are positively affecting the kinetics of refolding, as it can be observed when compared with the refolding kinetics in the absence of nucleotide exchange factor (Hsc70 + Hdj1, black dots). The kinetics were also measured in the presence of Bag2_BD (Figure 16 C), but luciferase refolding was actually slower in the presence of the nucleotide exchange factor (for the concentration tested) as in its absence. This is an additional evidence that the purified Bag2_BD is not active. Being misfolded, it could actually act as a substrate of Hsc70, competing with Luciferase for binding to Hsc70. During the time in which the chaperone might be trying to refold Bag2_BD, luciferase might aggregate, hence preventing any further refolding.

At 4 µM of Bag2_BD, it is possible that most of the NEF is aggregated, hence allowing the refolding of luciferase to be comparable to the one observed in the absence of nucleotide exchange factor. Comparing the refolding after an incubation time of 60 minutes, for the different concentrations of Bag protein tested, no significant difference between Bag2 and Bag4_BD are noticeable (Figure 16 D). The same is observed when comparing the initial rates of refolding (Figure 16 E). This is interesting, as Bag4_BD appeared to be much more efficient at stimulating ADP-release than Bag2. However, it is

possible that a too fast ADP-release would lead to a premature substrate release, hence prolonging the number of Hsp70 cycles needed for efficient luciferase refolding. The curves representing the refolding after 60 minutes as a function of the concentration of Bag protein (Figure 16 D), and the curves representing the initial rates of refolding against the concentration of Bag protein (Figure 16 E)

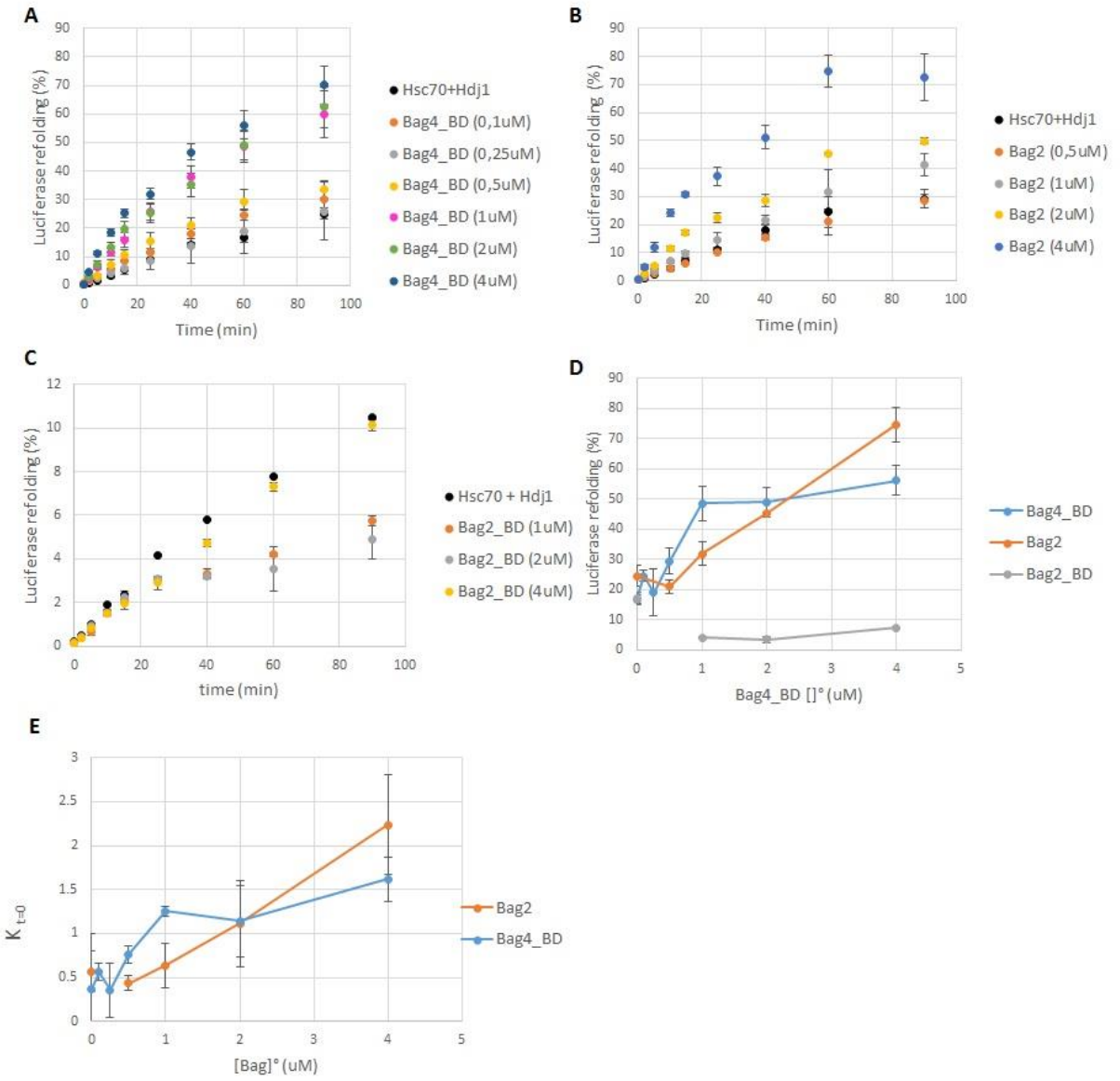

Figure 16: Refolding of heat-denaturated luciferase by Hsc70, Hdj1 and either Bag2 or Bag4_BD. A) B) and C), refolding kinetics for different concentrations of Bag4_BD (A), Bag2 (B) and Bag2_BD (C). D) Percentage of refolded luciferase after 60 min of refolding at 30°C in the presence of increasing amounts of nucleotide exchange factor. The refolding were normalized to the activity of luciferase before denaturation. E) Initial refolding rates for increasing concentrations of Bag protein. The error bars represent the standard error. The "Hsc70 + Hdj1" kinetics were always measure anew, in parallel to each nucleotide exchange factor: the values might therefore differ.

curiously follow very similar trends, this implying that the levels of refolding after one hours are dependent on the initial rate of reaction, which in turn depends of the concentration of nucleotide exchange factor.

Bag2 and the Bag domain of Bag4 are both able to act as a nucleotide exchange factor, and, through this role, can have a positive role on the rates of luciferase refolding. It is therefore safe to postulate that the full length Bag4 would have similar effects on both ADP-release and luciferase refolding, even if the numerical values obtained are certainly different. The role that both proteins play while interacting with HSF1 can be independent from this role as nucleotide exchange factor, but the fact the Bag2 and Bag4 were found interacting with HSF1 alongside Hsp70 and Hsc70 could be a hint on their role during the attenuation phase of the heat shock response.

3.5 Bag2 and Bag4 are positive regulators of the heat shock response

Bag 2 and Bag4 are both able to accelerate the rate of luciferase refolding *in vitro* by facilitating the release of ADP, leading to binding of ATP and, through the subsequent conformation changes, to the release of Hsp70s' substrate. Earlier in this work, it was shown that both Bag2 and Bag4 interact *in vivo* with HSF1, most probably during the attenuation phase of the heat shock cycle. Transposing what is known about nucleotide exchange factors of Hsp70, it would be logical to think that Bag2 and Bag4 stimulate the release of HSF1 from Hsp70, or its constitutively expressed family member Hsc70. In analogy to yeast HSF1 which is constitutively trimeric, and repressed by binding of Hsp70, stimulation of the dissociation of Hsp70 from HSF1 should stimulate the heat shock response.

To verify whether this hypothesis describes the *in vivo* reality, Bag2, Bag4, both of their N-terminal domains, alongside the Bag domain of Bag4 were cloned into a mammalian expression vector, and transiently transfected into U2-OS WT cells. Due to its inactivity *in vitro*, the Bag domain of Bag2 was not included in this experiment. An empty vector was transfected as a control.

In addition to the Bag expressing vector, a dual luciferase reporter gene vector was simultaneously co-transfected. This vector would express Renilla luciferase, which gene is under the control of a constitutively activated promoter, and Firefly luciferase, under the control of the promoter of the mitochondrial Hsp70, hence which expression is dependent on the activation of HSF1. Renilla luciferase and Firefly luciferase has a different substrates, respectively called coelenterazine and luciferin. Firefly luciferase was measured first, followed by injecting coelenterazine in a Firefly Luciferase quenching buffer and subsequent Renilla luciferase measurement. This prevented any

background luminescence of the first luciferase when measuring the activity of the second. In this experiment, the luminescence generated by Renilla would be used to normalize the Firefly signal, which can be dependent on the transfection efficiency, and the amount of cells lysed.

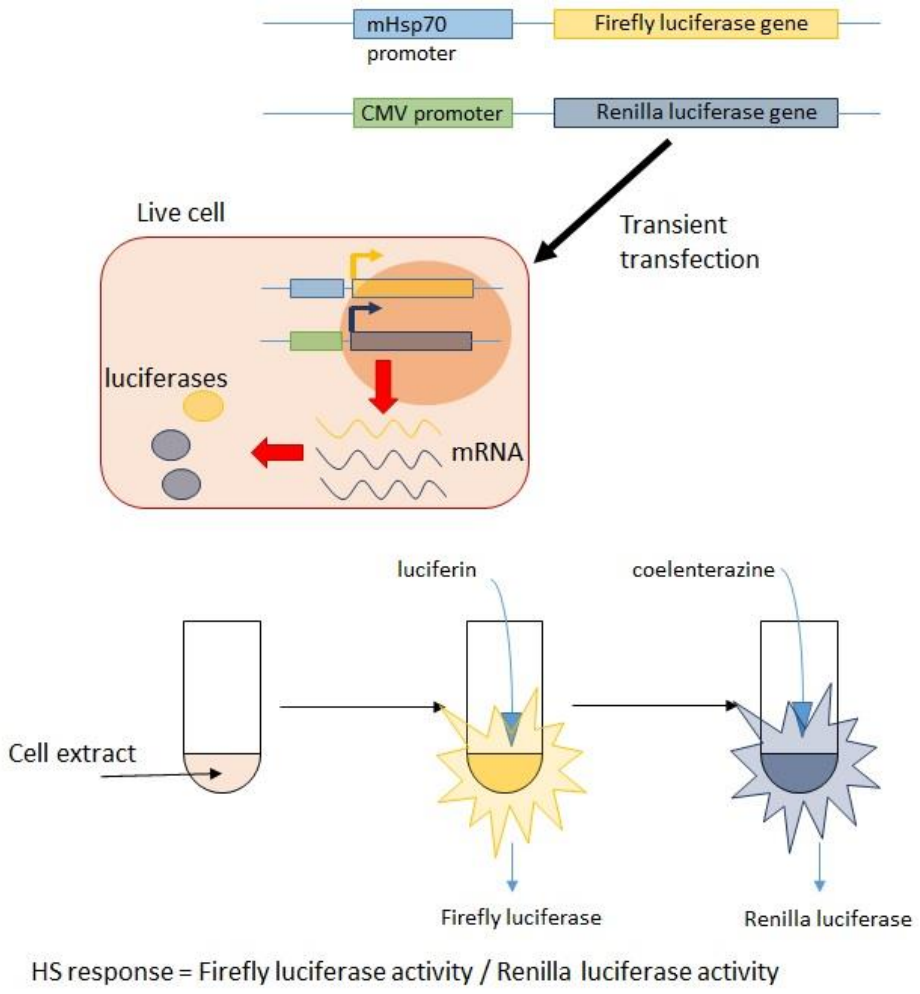

Figure 17: The dual-luciferase assay. U2-OS cells were transfected with a single vector containing the genes of both luciferases. Renilla luciferase is constitutively express, whereas Firefly luciferase is only expressed through binding of trimeric HSF1 to its promoter. The cells were lysed using Passive Lysis Buffer (Promega), and Firefly luciferase activity was measured first, by adding luciferin dissolved in the F. luciferase appropriate buffer. Its activity was then quenched by adding the R. luciferase assay buffer (containing colenterazine), in which F. luciferase is not active.

Each batch of dual-transfected cells were split into six different groups 24 hours after transfection, and cells were heat-shocked at 42°C for several time intervals. After each heat shock, the cells were allowed to recover for one hour, so that the heat-denaturated luciferase could be refolded into its native state. The cells were then lysed, and the luminescence generated by both luciferases was measured. Figure

18 displays the heat shock response level for each Bag construct transfected, and each duration of heat shock.

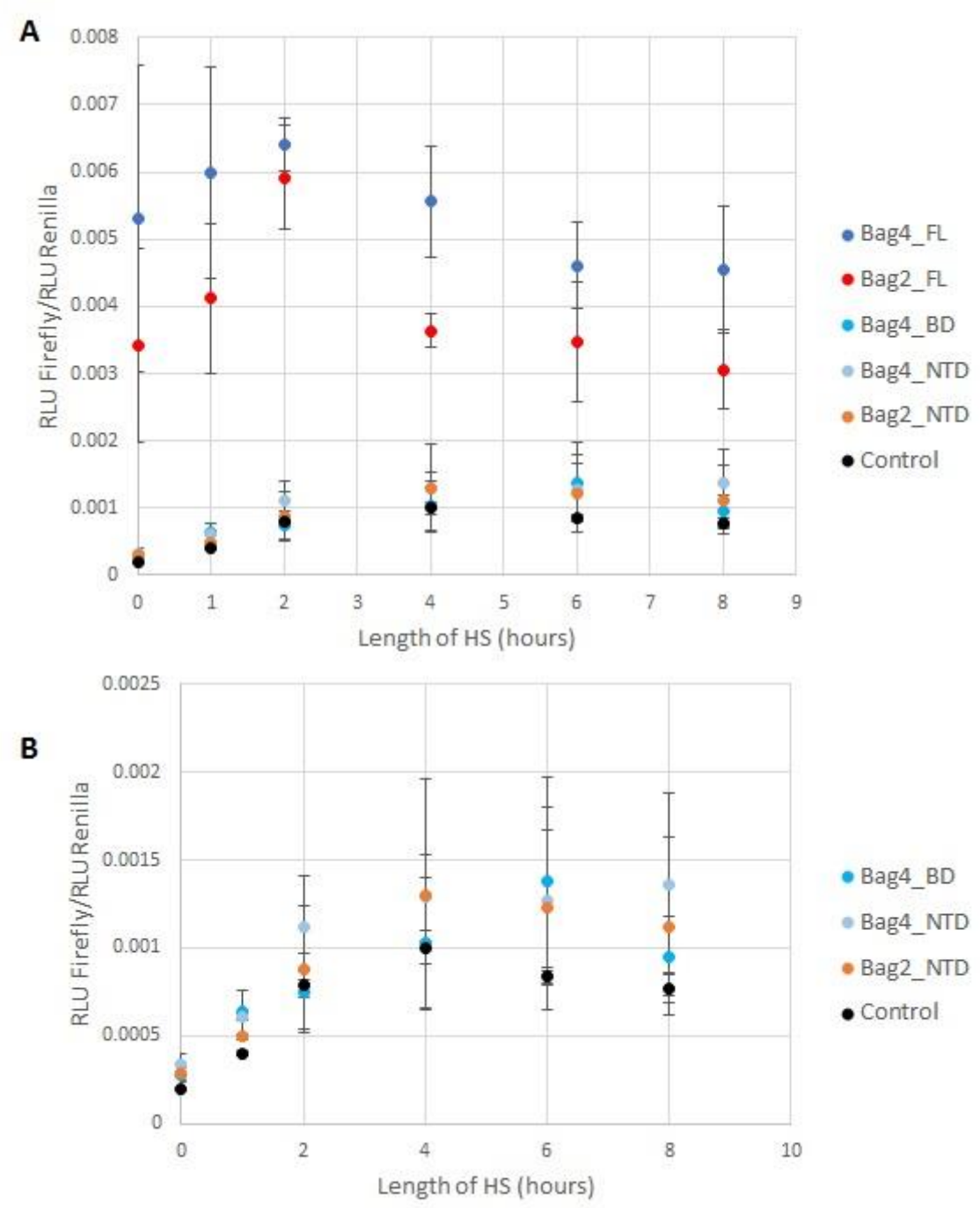

Figure 18: In vivo effect of Bag2 and Bag4 overexpression in U2-OS cells during heat shock at 42°C. A) Bag2 and Bag4 (full-length proteins and fragments) are transiently overexpressed in U2-OS cells, which are in turn heat shocked at 42°C for several length of time. On the y-axis, the ratio between the luminescent signals emitted by the Firefly luciferase and Renilla Luciferase are displayed. The x-axis represents the duration of the different heat shocks to which the different batches of transfected cells were submitted. B) Zoom in on the fragments of the fragments of Bag2 and Bag4. The value displayed are the average of three independent biological replicates. The error bars represent the standard error of the mean.

The behavior of control cells, which were transfected with an empty vector is quite expected: the ratio between the signals of the two luciferases goes up, meaning an increase in the amount of Firefly luciferase synthetized in the cells. This is due to the activation of the heat shock response, due to the heat-induced trimerization of HSF1. After four hours, the ratio starts to decrease, reflecting the attenuation phase. Indeed, enough molecular chaperones were produced during the first hours of heat shock to cope with proteotoxic damage, and the negative feedback regulation happens.

When Bag2 and Bag4 are overexpressed, the ratios of the two signals are much stronger, even before the cells were submitted to heat shock. Upon heat shock, the ratios increases, as HSF1 trimerizes and binds to the promoter upstream of the gene coding for the Firefly luciferase, hence boosting its cellular concentration. The concentration of Renilla luciferase is expected to stay constant. After reaching a maximum at two hours of heat shock, both ratios decrease to come back to values similar to their levels prior to stress. This shows that the overexpression of these two nucleotide exchange factors are positive regulators of the heat shock response. Curiously, it appears that Bag4 have a stronger effect on the heat shock than Bag2. Its Bag domain was also more performant at stimulating the ADP-release than the full length Bag2. Maybe Bag4 is altogether a better nucleotide exchange factor of Hsp70 than Bag2.

Earlier in this work, it was shown that it was the N-terminal domain of Bag4 that was interacting with HSF1 *in vivo*, and that both Bag domain and N-terminal fragment of Bag2 were able to interact with HSF1. It was also shown that the Bag domain of Bag4 could act as a nucleotide exchange factor of Hsp70 when purified on its own. Interestingly, when cells where fragments of both Bag2 and Bag4 are overexpressed show similar behavior between each other during heat shock (taking in account the standard error) Furthermore, the values of the dual luciferase ratios obtained when transfecting fragments of Bag proteins (Figure 18B) are barely higher than the ratios obtained for the control cells, suggesting that fragments of these two nucleotide exchange factors are incapable to influence the heat shock response on their own through stimulation of HSF1 release from Hsp70. The slight increase observed (when compared to control cells) might be caused by aggregation of the overexpressed proteins which can be misfolded. These aggregates could be titrating Hsp70 away from trimeric HSF1, thereby leading to a small increase in F. luciferase synthesis. It is hence possible to postulate that in order to stimulate the release of HSF1 from Hsp70/Hsc70, Bag proteins need both their Bag domain and their N-terminal domain, implying a specificity of these two proteins in this role.

A shift in the maximal intensity ratios for the cells transfected with the two full-length proteins was observed when compared to control cells, reflecting an earlier entry into attenuation phase. This can easily be explained by the fact that stronger heat shock response (visualized by a relatively stronger Firefly luciferase-generated luminescence) would issue in more molecular chaperones synthetized in

a shorter time, and therefore a faster and more efficient protection from and repair of cell damage. Hsp70 and Hsc70 would then be earlier available for interacting with HSF1, hence decreasing its transcription capacity.

Finally, the fact that the heat shock response is already activated before the start of the cellular stress implies the existence of trimeric HSF1 in the absence of any stress. It is already known that HSF1 have roles other than triggering the heat shock response, and it was suggested that human HSF1 might constantly be activated, attenuated by Hsp70 and then monomerized, thus maintaining the transcription of genes with HSE-containing promoters at a low level (Hentze et al. 2016). In the case of Bag2 and Bag4 overexpression, the release of trimeric HSF1 by Hsp70 would displace this equilibrium between inactive and active HSF1 towards DNA-bound trimer, with the consequence of a constitutive heat shock response.

Chapter 4. Discussion

The aim of the current work was to identify and to characterize new interaction partners of HSF1 during the attenuation phase of the heat shock response. Several studies in the late 1980's and the early 1990's identified Hsp70 as negative regulator of the transcriptional capacity of HSF1 (Mosser et al. 1988; Abravaya et al. 1991a; Baler et al. 1992). It was naturally postulated that Hsp70 represses HSF1 in concert with a co-chaperone of the Hsp40 family, which one is unknown, as more than 40 J-domain proteins have been identified in human cells. It is also disputed whether other chaperones or co-chaperones play a role in HSF1 attenuation.

In this work, a human cell line supposedly constitutively in the attenuation phase of the heat shock cycle was established, by stably overexpressing HSF1. This cell line was characterized by a slightly elevated basal pool of heat shock proteins, and by a certain resistance to further heat shocks applied to them. These cells were used to perform a screening for proteins interacting with HSF1, and the two molecular chaperones Hsp70 and Hsc70 were identified, alongside with Bag2 and Bag4, two nucleotide exchange factors of Hsp70/Hsc70. The interactions between HSF1, Bag2 and Bag4 were confirmed *in vivo*, and *in vitro*, and evidence that this interaction is direct was provided. Moreover, it was shown that in the case of Bag4, the interaction was taking place through the N-terminal domain of the protein, its Bag domain interacting with Hsp70 or Hsc70. In the case of Bag2, it was less clear, as it appeared that both Bag domain and N-terminal fragment can interact on their own with HSF1.

Bag2, and the Bag domain of Bag4 were then purified, and circular dichroism measurement showed that these two polypeptides mostly have a α-helical secondary structure, as Bag domain are known to be. Both proteins could stimulate ADP-release by Hsp70 and Hsc70, and increase the refolding rates of heat-denaturated luciferase. Finally, overexpressed in human cells, Bag2 and Bag4 could increase dramatically the heat shock gene transcription in the absence and presence of thermal stress, most probably by leading Hsp70 to release trimeric HSF1. Although the Bag domain of Bag4 was active *in vitro*, clear evidences were provided in this work that only the full length Bag2 and Bag4 are able to tune up the heat shock response.

4.1 Implications of the eventual interaction partners identified

The ten hits that were detected above the threshold chosen for the screening could be seen as a relatively small group of potential interactors of HSF1, even during the sole attenuation phase of the

heat shock response. It has however to be taken in account that the criteria chosen were very restrictive, as the medium/light ratios had to be over 2 in at least two of the four replicates. Hence, some unspecific partners were ruled out from the beginning. It was also surprising that many proteins that were previously reported to interact with HSF1 were not found in this screening. Hsp90 was reported to inhibit the transactivation of HSF1 in Xenopus oocytes (Ali et al. 1998) and Guo and colleagues suggested that Hsp90 forms a complex with FKBP52 and p23 to suppress the transcriptional activity of trimeric HSF1 in HeLa cells (Guo et al. 2001). The latter interaction was however only seen after DSP-crosslinking, hinting its transient nature. During the immunoprecipitation performed in this work, the incubation times with the anti-HA antibody were more than twice as long as in the pull-downs performed by Guo and colleagues. Moreover, in this work, it is highly possible that the stringent washes dissociated some of the weaker interactions.

An interaction between HSF1 and Replication protein A (RPA) was shown to facilitate the access of trimetric HSF1 to the promoter of HSPA1A by recruiting the histone chaperone FACT (Fujimoto et al. 2012). In this study, neither RPA nor FACT were found interacting with HSF1. However, in the U2-OS HA-HSF1 cell line, it would be expected that the promoters of heat shock are already fully accessible, as the transfection of the pIRES vector was stable, and HSF1 had been overexpressed for several months by the time of the immunoprecipitation. SMARCD2, a member of the SWI/SNF complex, responsible for nucleosome remodeling was however identified interacting with HSF1 in this study. The SWI/SNF complex was suggested to cooperate with HSF1 to un-pause the RNA polymerase II at the promoter of HSPA1A (Brown et al. 1996; Brown et al. 1998). According to Brown et al, the RNA pol II would be paused on the promoter of Hsp70, this pause being due to the nucleosome density around that gene. A combination of trimeric HSF1, a transcription elongation factor, and the SWI/SNF complex would then disrupt the nucleosome organization and relieves the RNA polymerase (Brown et al. 1998; Sullivan et al. 2001; Corey et al. 2003). In the present work, a transcription elongation factor, HIV-Tat-Specific Factor 1 was also identified as a potential interactor of HSF1, though only in three of the four replicates. Therefore, SMARCD2 and HIV-Tat-SF1 could be involved in chromatin rearrangement at the promoter of heat shock genes.

The putative interactors of HSF1 Bag2 and Bag4 identified in the screening performed in this work were already identified by Taipale and colleagues in a LUMIER screening involving the Hsp70 and Hsp90 chaperones (Taipale et al. 2014). Indeed, this study reports strong interactions between HSF1 and Bag1, Bag3, Bag5, and weaker interactions with Bag2 and Bag4. Another work reported Bag3 interacting directly with HSF1 in stressed and non-stressed cells, and affecting the shuttling of HSF1 out of the nucleus (Jin et al. 2015). Overexpression of Bag3 was shown to decrease the concentration of nuclear HSF1, in accordance to the fact that among all the Bag proteins, Bag3 is the only one which

expression is HSF1-dependent (Pagliuca et al. 2003; Franceschelli et al. 2008; Rosati et al. 2009). An up-regulation of Bag3 would then participate in the reduction of the intensity of the heat shock response, by reducing the amount of HSF1 present in the nucleus, hence decreasing the chance of re-binding to DNA. Neither Bag2 nor Bag4 were reported so far to play a role in the heat shock response, as Bag2 was reported to be a general non-client-specific cofactor of Hsp70, and Bag4 was shown to strongly interact with three central components of the mRNA decapping complex (Taipale et al. 2014). Although interactions between Bag2, Bag4 and HSF1 were already detected with LUMIER assay (Taipale et al. 2014), this assay cannot distinguish between direct and indirect interactions. In this work, evidence of a direct interaction was shown.

4.2 Bag2 and Bag4 interact with HSF1 and Hsp70

In this study, the interaction between HSF1 and the two nucleotide exchange factors Bag2 and Bag4 was confirmed. Indeed, it was possible to detect both Bag2 and Bag4 when pulling on HSF1. Moreover, it appeared very clearly that Bag4 interacts with HSF1 through its N-terminal fragment, and with Hsc70/Hsp70 through its Bag domain. The N-terminal domain of Bag4 is composed of 67 Proline, 44 Glycine and 33 Tyrosine (out of a total of 378 amino-acids). Therefore it can be expected that it has little structure, and that it is relatively hydrophobic, even if these tyrosine are spread all over the protein. This could explain why the N-terminal fragment of Bag4 co-immunoprecipitated with Hsc70, as it could be considered as a good chaperone substrate. This lack of structure also marks the protein as being quite instable, thus explaining the difficulties encountered when purifying it from *E. coli*.

Immuno-precipitations using an anti-MYC antibody (so with Bag2 or Bag4 as target) revealed that HSF1 could be co-immunoprecipitated with the full length Bag4, its N-terminal domain, and its Bag domain to a lower extend. This last interaction is however unexpected. Pulling on Bag2 did not enrich HSF1, but this could be explained with the fact that Bag2, being a general non-substrate specific nucleotide exchange factor (Taipale et al. 2014), might interact with many different substrates of Hsc70 (or Hsp70), only a fraction of which being HSF1. The interactome of Bag4 in contrast was reported to be related to the mRNA decapping mechanism, and was found localized in P-bodies (Taipale et al. 2014). Thus, a much more substrate-specific nucleotide exchange factor could enrich HSF1 more efficiently than a general one, such as Bag2.

Bag2 appeared to interact with HSF1 through both its Bag domain and its N-terminal fragment. It was proposed that the Bag domain of Bag2 interacts with Hsp70s' substrate, and favors its binding to the SBD of the (Xu et al. 2008). In the present work, this interaction between Bag2_BD and HSF1 may have

been seen, in addition to an interaction through Bag2_NTD, but the model proposed by Xu and colleagues does not make much sense, as it is unlikely that Bag2 acts first as a J-domain protein, providing its substrate to the chaperone, and then as a NEF. In addition, only the full-length Bag2 seemed to bind Hsc70. This was surprising, as Xu and colleagues published the structure of the Bag domain of Bag2, dubbed Brand New Bag domain (BNB), as a dimer, and as a complex with the Nucleotide binding domain of Hsc70 (Xu et al. 2008). The complex showed some conformational changes proposed to lead to release of ADP. The conformational changes observed are similar but not as extensive as those induced by Bag1 and Hsp110. They also attested of the activity of their purified full length Bag2, but only of the activity of the Bag domain of the murine Bag2. No mention of the activity of human Bag2_BNB was made. In this study, the purified Bag domain of human Bag2 was not active in some ADP-release experiments, and seemed to be aggregated after one freeze/thaw cycle. In their model, Xu et al present the structure of a homodimer of Bag2, bound to two different Hsc70. It is possible that a dimer of Bag2 interacts with two neighboring Hsc70, which in turn interact with two different transactivation domains of a HSF1 trimer. This would lead to a simultaneous and hence more efficient nucleotide exchange from the chaperones interacting with HSF1.

The *in vitro* GST-pull-downs performed in this work confirmed the direct interaction of Bag2 and Bag4 with HSF1. Indeed, the absence of human Hsp70 or Hsc70 in *E. coli* renders the interaction of HSF1 with the GST-tagged Bag protein doubtlessly direct. It was however quite surprising that the two Bag domains were also capable of interacting with HSF1. In the case of Bag2_BD, this would confirm what was seen *in vivo*, but also the observations made by Xu et al. However, no *in vivo* interaction between the 70 kDa molecular chaperone and Bag4_BD was detected in the present work. It could be the case that Bag4_BD interacts with HSF1 in a similar manner than Bag2_BD, but this would be rather unlikely, as the two Bag domains have different structures, the Bag domain of Bag4 displaying a structure close to the canonical Bag domain, even if shorter (Briknarová et al. 2002). It could be possible that in absence of molecular chaperone of the Hsp70 family, the α-helical structure of Bag4_BD interacts in a non-physiological manner with HSF1, by forming coiled-coil structures for example.

The oligomeric nature of HSF1 in the interaction with Bag2 and Bag4 is still unanswered. The concentration used presently should not lead, at 4°C, to spontaneous concentration-dependent trimerization. However, the cell line from which these interactions were identified is most probably arrested in the attenuation phase, where HSF1 is supposed to be trimeric. The *in vitro* pull-downs performed here would have to be repeated, using this time trimeric HSF1.

4.3 Bag2 and Bag4 as in vitro nucleotide exchange factor

The *in vitro* activities of Bag2 and Bag4_BD were measured in this work. The stimulation of ADP release was measured for both Bag proteins, with Hsc70 and Hsp70, and Bag4_BD was shown to be much more efficient at stimulating ADP release than Bag2. Gässler and colleagues did a similar work with Bag1-M, one of the isoform of Bag1 in 2001. In her work, much higher concentration of nucleotide exchange factors could be tested, but it appeared that Bag1-M could stimulate ADP-release with an intermediate efficiency, when comparing with Bag2 and Bag4_BD (Gässler et al. 2001). Indeed, with Hsc70 as the chaperone, and for nucleotide exchange factor concentrations of 5 µM and 10 µM, Bag2 had k_{off} values of 1.75 s^{-1} and 3.4 s^{-1} respectively, Bag4_BD 37.5 s^{-1} and 50.5 $s^{-1}$and Bag1-M had, with the same chaperone, and the same concentrations of NEF, k_{off} values of approximately 15 $s^{-1}$and 18 s^{-1}.

For both active nucleotide exchange factors tested in this work, it appeared that the stimulation of ADP-release was more efficient on Hsc70 than on Hsp70. In Gässler et al, Hsp70 appeared to be slightly more sensitive than its cognate homolog to the actions of Bag1-M (Gässler et al. 2001). Differences between Hsp70 and Hsc70 are still not completely unraveled. Tutar and colleagues suggested that, in yeast, the main differences between the two chaperones reside in their ATPase domains, which have different roles (Tutar et al. 2006). They also bring evidence that Hsc70 fulfils roles in yeast growth that Hsp70 cannot take over. Altogether, the constitutive expression of Hsc70 hints its role in housekeeping mechanisms. However, Finka and Goloubinoff hinted that Hsp70 might also take charge of housekeeping roles, as it represents, in cancer cells and in the absence of stress, a copy number of about one third of all the proteins involved in the Hsp70 machineries (Finka & Goloubinoff 2013).

Moreover, Hsc70, the most abundant 70 kDa molecular chaperone was also shown to be able to interact with Hsp110 to resolubilize heat-aggregated substrates. Hsp70 was shown to be less efficient in that role (Rampelt et al. 2012; Nillegoda et al. 2015; Gao et al. 2015). One would however expect that the heat-inducible Hsp70 would be more effective at refolding misfolded proteins during heat shock, but the different roles of these two chaperones are still elusive. The higher sensitivity of Bag2 and Bag4 to Hsc70 could be linked to the abundance of the preferred Hsp70-like chaperone for which these nucleotide exchange factor are needed the most. Bag1 is known to regulate the degradation of some Hsp70 clients (Tsukahara & Maru 2010), and was linked to several proteasome subunits (Taipale et al. 2014). Its higher stimulation of Hsp70 might be then linked to the necessity of redirecting misfolded protein for degradation during cellular stress, when Hsp70 levels are increased.

Bag2 and Bag4_BD both showed similar effects on influencing the refolding by Hsc70 of heat-denaturated luciferase despite the difference observed in their stimulation of ADP-release. In contrast to the data obtained by Gässler and colleagues for Bag1-M, no inhibition of Bag proteins at the concentrations measured was seen. It is however not possible to compare the data generated in this work to the ones obtained by Gässler and colleagues. Indeed, the stimulation of luciferase refolding by Bag1-M was measured in the presence of reticulocyte lysate, and a positive effect was only seen in the presence of inorganic phosphate at low concentrations of Bag1-M (Gässler et al. 2001). Also, the buffer used in these measurements were different than the ones used to measure the stimulation of luciferase refolding by Bag2 and Bag4_BD. Extensive work on Bag proteins was performed by Rauch and colleagues, but Bag4, or fragments of it, were never tested, and the heat-induced Hsp70 and not Hsc70 was used as the chaperone protein (Rauch & Gestwicki 2014; Rauch et al. 2016). As it was shown in this work that the stimulation of ADP-release can be highly chaperone dependent, their results are hardly comparable to the ones presented in this work.

4.4 Bag2 and Bag4 tune up the heat shock response

In Figure 18, evidence is presented that the overexpression of two nucleotide exchange factors of Hsp70 can activate the heat shock response by ending the attenuation of the trimer, or eventually, by allowing a trimer of HSF1 to bind back to the promoter of heat shock genes. This effect might be specific to Bag2 and Bag4, as the Bag domain of Bag4, although active *in vitro* for stimulating the release of ADP by the nucleotide binding domain of Hsp70 and in increasing the refolding rates of heat-denaturated luciferase could not have this heat shock response activating effect in living cells. It was shown that both N-terminal domains of these two Bag proteins can interact with HSF1 *in vivo* and supposedly *in vitro* (Figure 9 and Figure 11 respectively). Despite these interactions, the N-terminal fragments of these nucleotide exchange factors were not able on their own, to lead to HSF1 trimer release from Hsp70/Hsc70. The full protein is therefore needed for such an effect.

The earlier start of the attenuation phase observed (Figure 18) in the case of the overexpression of the two full-length nucleotide exchange factor could be explained by the fact that a stronger heat shock response, due to the overexpression of Bag2 and Bag4, would lead to a higher concentration of Hsp70 in the cell. This would in turn lead to an earlier negative feed-back loop as less time would be needed to have enough chaperones to enter the attenuation phase. Similar effect was reported by Shi and colleagues, as an overexpression of Hsp70 was reported to hamper the capacity of HeLa cells to deploy a heat shock response (Shi et al. 1998a). In the present case, where Hsp70 is thought to be up-

regulated, but not over-expressed, the cells are still able to mount a further heat shock response when submitted to temperature stress. This heat shock response is just attenuated earlier than in control cells.

Recently, a similar effect of the *S. pombe* yeast orthologues Bag101 and Bag102 on the heat shock response was uncovered by Poulsen et al. They provide evidence that the overexpression of Bag101 and Bag102 in yeast leads to constitutive HSF1 activation and growth defects in yeast presumably by prompting the release of HSF1 from Hsp70 (Poulsen et al. 2017). Bag101 and Bag102 are the only proteins of the Bag family in *S. pombe*, and even if their sequences homology related them more with human Bag1, it is possible that they overtake the role of Bag2 and Bag4 when it comes to hamper the repression of the transcription activity of trimeric HSF1. They however did not report any direct interaction between these Bag proteins and HSF1.

Many co-chaperones of the Hsp70 machinery can bind to chaperone substrates. J-domains proteins are known to deliver substrate to Hsp70, and to stimulate Hsp70s ATP hydrolysis rate to ensure stronger affinity of the chaperone for its substrates. Hsp110s, also nucleotide exchange factors of Hsp70, were also shown to interact with misfolded proteins (Liu & Hendrickson 2007; Schuermann et al. 2010), even if this can be related to the intrinsic chaperone activity of Hsp110. It is however assumed that Hsp110s can interact with many misfolded proteins in a non-specific manner. In the case of co-factors of the Bag family, substrate specificity is unclear. Taipale and colleagues identified families of substrates for every Bag protein (beside Bag2 who appeared to interact with most of Hsc70's substrates), linking each of them to specific cellular pathways. Consistent to what was already suggested, the non-conserved sequences of the N-terminal domains of the Bag proteins allow to think that maybe substrate recognition is made through that part of the protein (Mayer & Bukau 2005).

Another role of the N-terminal domain of Bag proteins was proposed recently: a bi-dentate mechanism in which non-Bag domain parts of Bag1 and Bag3 interact with the substrate binding domain of Hsc70 to promote client release (Rauch et al. 2016). Rauch and colleagues also showed evidences that client-release was still possible without Bag domain, but not nucleotide release. Such an interaction could compete with the client protein binding to Hsc70s' substrate binding domain, and hence prevent rebinding. This could explain the effect described in Rauch et al. Gässler and colleagues did not compare the abilities of the full length Bag1, and of its Bag domain alone to promote substrate release (Gässler et al. 2001). A similar effect was shown in *E. coli*, where GrpE N-terminal domain interacts with the substrate binding domain of DnaK (Mally & Witt 2001; Chesnokova et al. 2003; Brehmer et al. 2004). Such a mechanism could exist for Bag2 and Bag4, even though the small size of the N-terminal fragment of Bag2 might render such an interaction not possible. If indeed Bag2 can just promote trimeric HSF1 release from Hsp70 through its Bag domain and not through interacting with the

substrate binding domain of Hsp70, it could explain the weaker up-regulation of the heat shock response by Bag2 (compared to Bag4) when it is overexpressed in cells (Figure 18). This could also be explained by its much weaker ADP-release stimulation (Figure 15).

Bag2 was shown to inhibit protein degradation, by interacting with the E3 ubiquitin ligase CHIP (Arndt et al. 1990). Longer association between Hsp70 and its substrate was shown to lead to its poly-ubiquitination and therefore its degradation (Stankiewicz et al. 2010). By inhibiting CHIP, Bag2 would delay HSF1's degradation by the proteasome system, hence leading to more stable HSF1 trimers. This effect could counter-act the weak ADP-release stimulation of Bag2.

The fact that two nucleotide exchange factors were found to interact directly with HSF1, and that they both seem to act as positive regulators of the heat shock response is puzzling. More work would have to be conducted to unravel the implication of two nucleotide exchange factors up-regulating the heat shock response. Bag2 is the most abundant Bag protein in the cell (Finka & Goloubinoff 2013), but also much less active than Bag4 at stimulating the ADP-release. Moreover, it has been shown that Bag2 does not show any client specificity, as the other Bag proteins do (Taipale et al. 2014). Therefore, there is a possibility that Bag4 is the canonical NEF acting as a positive regulator of the heat shock response, and that Bag2 is the non-specific NEF which can fulfil the same role, only less efficiently.

Most recent studies suggest the existence of an equilibrium between monomer and dimer of HSF1. Concentration or temperature increase (and hence proteotoxic damages) would lead to trimerization, and acquisition of DNA-binding capacity (Hentze et al. 2016). The fact that HSF1 has some roles in the absence of cellular stress leads to two possibilities: either HSF1 is activated through another unknown mechanism, or trimeric HSF1 is present in the absence of stress. According to the model described by Hentze and colleagues in 2016, HSF1 trimerization can happen continuously at low levels, with the help of Hsp90. This ensures the existence of a basal pool of transcriptionally active HSF1, even in the absence of stress. The Hsp70/Hsp40 complex would then be responsible of moderating that basal transcription level of HSF1 target genes. Upon stress, the formation of trimer would be favored, and molecular chaperones normally maintaining HSF1 inactive would be titrated away, allowing for a longer time in which HSF1 could drive the synthesis of heat shock proteins in large quantities. Therefore, the overexpression of Bag2 or Bag4 increased the fraction of active HSF1 before stress by releasing trimeric HSF1 from Hsp70. Very recently, a mathematical model in which the titration of Hsp70 away from HSF1 leads to activation of the heat shock response in yeast was proposed (Zheng et al. 2016). This model, combined with the evidences presented in this work gives to Hsp70s a much more central role in the heat shock response.

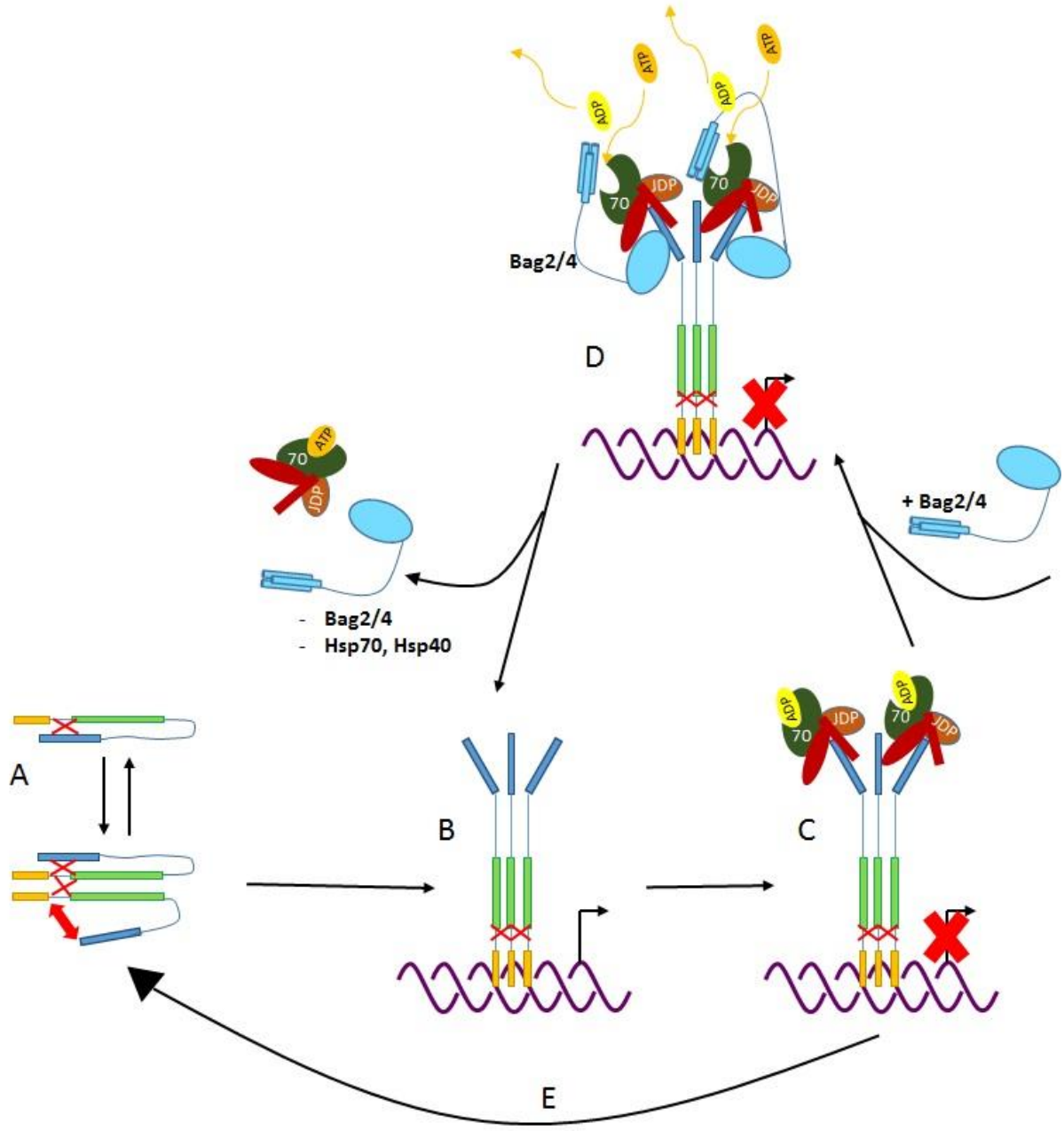

Figure 19: Revised cycle of the heat shock response. HSF1 exists in an equilibrium between monomer and dimer (A). Certain conditions such as local concentration increase lead to trimerization, acquisition of DNA-binding activity, and protein synthesis (B). Hsp70 (or Hsc70) in complex with a J-domain protein (JDP) represses HSF1 transcription capacity (C). In the absence of stress, HSF1 goes back to the monomer dimer equilibrium (or is degraded) (E). Upon stress, Hsp70 is titrated away, and Bag2 and Bag4 assist substrate release (D), leading to a longer "DNA-bound time" of the trimer, hence a stronger heat shock response (B). With time, the very high concentration of chaperones, combined with the eventual end of the cellular stress might outnumber Bag2 and Bag4, which expression is not heat shock dependent, and monomerization of HSF1 might happen.

Chapter 5. Material and Method

5.1 Materials

5.1.1 Bacterial strains and plasmids

5.1.1.1 E.coli K12 strains

Top 10	F$^-$ *mcr*A Δ(*mrr* $^-$ *hsd*RMS$^-$ *mcr*BC) Φ80lacZΔM15 Δ*lac*X74 *rec*A1 *ara*D139 Δ(*ara leu*) 7697 *gal*U *gal*K *rps*L (StrR) *end*A1 *nup*G
BL21(DE3) Rosetta™	F$^-$ *omp*T *gal dcm lon hsd*SB (r^-_B m^-_B) *λ*(DE3[*lac*I *lac*UV5-T7 gene 1 *ind*1 *sam*7 *nin*5]) pRARE(Cam^R)
MC 1061	*Δ(araA-leu)7697 [araD139]$_{B/r}$ Δ(codB-lacI)3 galK16 galE15*(GalS) *λ*$^-$ *e14- mcrA0 relA1 rpsL150*(strR) *spoT1 mcrB1 hsdR2*

5.1.1.2 Plasmids

Table 2: Plasmids used in this work

pCA528	T7 promoter, Kan^R	AG Mayer Lab collection
pCA528_HsBag2	T7 promoter, Kan^R	This work
pCA528_HsBag2_BD	T7 promoter, Kan^R	This work
pCA528_HsBag4	T7 promoter, Kan^R	This work
pCA528_HsBag4_BD	T7 promoter, Kan^R	This work
pIRES-GFP II-HA	CMV promoter, Kan^R	Courtesy of AG Melchior
pIRES-GFP II-CtermHA-HsHSF1	CMV promoter, Kan^R	This work
pIRES II-mCherry	CMV promoter, Kan^R	This work (S. Hennes)
pIRES-3xmyc_rhGFP	CMV promoter, Kan^R	This work (S. Hennes)
pcDNA4-TO	Tet-ON promoter, Amp^R	Courtesy of AG Stoecklin

pcDNA4-3xMYC-Bag4-IRES-rhGFP	CMV promoter, Amp^R	This work (S. Hennes)
pcDNA4-3xMYC-Bag4_BD-IRES-rhGFP	CMV promoter, Amp^R	This work (S. Hennes)
pcDNA4-3xMYC-Bag4_Nterm-IRES-rhGFP	CMV promoter, Amp^R	This work (S. Hennes)
pcDNA4-3xMYC-Bag2-IRES-rhGFP	CMV promoter, Amp^R	This work (S. Hennes)
pcDNA4-3xMYC-Bag2_BD-IRES-rhGFP	CMV promoter, Amp^R	This work (S. Hennes)
pcDNA4-3xMYC-Bag2_Nterm-IRES-rhGFP	CMV promoter, Amp^R	This work (S. Hennes)
pIRES II CMV-rLuci-mCherry_pHSE-fluci	CMV promoter, HSE promoter, Kan^R	This work (S. Hennes)
p273-GST-omega	Arabinose promoter, Amp^R	AG Mayer Lab collection
p273-GST-Bag2_BD	Arabinose promoter, Amp^R	This work
p273-GST-Bag2_NTD	Arabinose promoter, Amp^R	This work
p273-GST-Bag2	Arabinose promoter, Amp^R	This work
p273-GST-Bag4_BD	Arabinose promoter, Amp^R	This work
p273-GST-Bag4_NTD	Arabinose promoter, Amp^R	This work
p273-GST-Bag4	Arabinose promoter, Amp^R	This work

5.1.2 Mammalian cell lines

U2-OS	Courtesy of AG Stoecklin
U2-OS pIRES-GFP II-CtermHA-HsHSF1	This work
U2-OS pIRES-GFP II-HA	This work

5.1.3 Oligodesoxynucleotides

All Oligodesoxynucleotides were ordered at Sigma-Aldrich

Table 3: Oligodesoxynucleotides used in this work

hsHSF_EcoRI_5	5'-CGGAATTCACCATGGATCTGCCCGTGGGCCC-3'
hsHSF1_HA_stop_NotI_3	5'-AGTCGAGCGGCCGCTTAAGCGTAATCTGGAACATCGTATGGGTAGGAGACAGTGGGGTCCTTGGCTTTGGGAGG-3'
Bag2_BsmBI_5	5'-CCAGTGCGTCTCAGGTGGTATGGCTCAGGCGAAGATCAA-3'
Bag2_XhoI_3	5'-GATCCTCGAGCTAATTGAATCTGCTTTCAGCATTTTGTTG-3'

Bag2_BD_BsmBI_5	5'GATCCCGCGGCGTCTCAGGTGGTATGCAAGAATCCCTGAAGCATGCCAC-3'
Bag2_SacII_5	5'-GATCCCGCGGGGTCTCAGGTGGTATGGCTCAAGCGAAGATCAACGC-3'
Bag2_BD_SacII_5	5'-GATCCCGCGGGGTCTCAGGTGGTATGCAAGAATCCCTGAAGCA-3'
Bag2_NotI_3	5'-GATCGCGGCCGCTTAATTAAAACGGCTTTCAGCATTTT-3'
Bag2_Nterm_stop_NotI_3	5'-GATCGCGGCCGCTCATTCTTGCTGCTGGGGGTTACGA-3'
Bag4_BsmBI_5	5'-CCAGTGCGTCTCAGGTGGTATGTCGGCCCTGAGGCGCTC-3'
Bag4_BD_BsmBI_5	5'-CCAGTGCGTCTCAGGTGGTATGAGTACTCCTCCGAGTATTAA-3'
Bag4-HindIII_3	5'-CTCTAGAAGCTTCAGGCTTCCACTTTGTTCTAAATCC-3'
Bag4_SacII_5	5'-GATCCCGCGGGGTCTCAGGTGGTATGTCGGCCCTGAGGCGCTC-3'
Bag4_BD_SacII_5	5'-GATCCCGCGGGGTCTCAGGTGGTATGAGTACTCCTCCGAGTATTAA-3'
Bag4_NdeI_5	5'-GCAAAACATATGTCGGCCCTGAGGCGCTC-3'
Bag4_BD_NdeI_5	5'-GCAAAACATATGAGTACTCCTCCGAGTATTAA-3'
Bag4-SalI_3	5'-GCAAAAGTCGACTTCAGGCTTCCACTTTGTTCTAAATCC-3'
Bag4_Nterm_stop_SalI_3	5'-GCAAAAGTCGACTCATTCATCTGAAGGTACACATTCTTCA-3'

5.1.4 Chemicals, enzymes and kits

Table 4: Chemical used in this work

Acetic Acid (100%)	Neolab
Acetone	J.T. Baker
Acrylamide stock solution 30% (mixing ratio 37.5:1; Rotiphorese Gel 30)	Roth
Albumin Fraktion V	Roth
Aprotinin	AppliChem
8-[(4-Amino)butyl]-amino-ADP – MANT (MABA-ADP)	Jena-Bioscience
Adenosine-Tri-Phosphate (ATP)	Roth
Benzonase	Sigma-Aldrich
Bromophenol blue	Waldeck
Coomassie Brilliant Blue G-250	Roth
1,2 Diaminocyclohexane-N,N,N',N'	Sigma-Aldrich
Digitonin	Sigma-Aldrich
Dimethyl-sulfoxyde (DMSO)	VWR
Dithiothreitol	AppliChem
Ethylenediaminetetraacetic acid	AppliChem
Ethylene glycol-bis(β-aminoethyl ether tetraacetic acid	AppliChem
Ethanol p.a., 99.9 %	AppliChem
Ethidium bromide (1% w/v in H2O)	Roth
Geneticin	Gibco
Glycerol	Sigma-Aldrich
4-(2-hydroxyethyl)-1-piperazineethanesulfonic acid	Sigma-Aldrich

Hygromycin	Roth
Igepal (NP-40)	Sigma-Aldrich
Imidazole	ACS
Isopropyl-*β*-D-thiogalactopyranosid	Roth
Isopropanol	VWR
Kanamycin	Roth
Leupeptin	Applichem
Magnesium Chloride	AppliChem
2-Mercaptoethanol	Roth
Penicillin/Streptomycin	Sigma-Aldrich
Phenylmethylsulfonyl fluoride	AppliChem
Pepstatin	AppliChem
Polyethylenimine (PEI)	Polysciences, Inc
Potassium chloride	Sigma-Aldrich
Potassium Dihydrogen Phosphate	AppliChem
Protino© Ni-IDA	Macherey-Nagel
Protino© Glutathione agarose 4B	Macherey-Nagel
Rotiagarose NEEO Ultra	Roth
Saccharose	Roth
Sodium dodecyl sulfate	Roth
Sodium chloride	Sigma-Aldrich
Sodium Hydroxide	Sigma-Aldrich
Tris(hydroxymethyl)aminomethane	Sigma-Aldrich
Trichloroacetic acid	AppliChem
Trifluoroacetic acid	AppliChem
Triton X-100	AppliChem
Tween 20	Roth

Table 5: Commercial standards and kits

Page Ruler Prestained Protein Ladder	Fermentas
Mini-preps kit	MiniBio GmbH
Gel Extraction kit	MiniBio GmbH
Universal RNA purification kit	EurX
Gene Ruler™ 1kb DNA Ladder	Fermentas
Chemiluminescent Substrate West Pico	Thermo Scientific
Random Hexamer Primers	Thermo Scientific
Light Cycler 480 SYBR Green I Master	Roche
Passive Lysis Buffer	Promega
Roti-Fect Plus transfection kit	Roth

Table 6: Proteins and enzymes

Restriction enzymes	New England biolabs
T4 DNA Ligase	Fermentas
BSA	New England biolabs
M-MLV Reverse Transcriptase	Promega
RNAse inhibitor RNAsin	Promega
Firefly luciferase	Lab collection
Hsp70	Lab collection

Bag1	Lab collection
Hdj1	Lab collection
6xHis-Ulp1	Lab collection
HSF1	Lab collection

Table 7: Antibodies and antibodies-coupled beads

Antibody	*Dilution*	*Provider*
Anti HA.11	(1:1000 dilution)	Covance
Anti-myc	(1:1000 dilution)	Cell signaling
Anti-Hsf1	(1:1000 dilution)	Santa-Cruz biotechnologies
Anti-Hsp70	(1:2000 dilution)	Lab-stock
Anti-Gst-ram2	(1:2000 dilution)	Lab-stock
Anti-Hsc70/Hsp70	(1:5000 dilution)	Santa-Cruz biotechnologies
Anti-mouse ECL	(1:10000 dilution)	Dianova
Anti-rabbit ECL	(1:10000 dilution)	Dianova
Anti-HA beads (A2095)	-	Sigma-Aldrich
Anti-myc beads (A7470)	-	Sigma-Aldrich

Table 8: Media and Serum

Dubbeco‘s Modified Eagle Medium (DMEM)	Life Technologies
Fetal Calf Serum (FCS)	Life technologies
Luria-Bertani (LB) medium[2]	10 g/L tryptone 5 g/L yeast extract 5 g/L NaCl
2X YT medium	16 g/L tryptone 10 g/L yeast extract 5 g/L NaCl

Table 9: Equipment

ÄKTA HPLC	GE Healthcare
Ressource Q column (6mL)	GE Healthcare
Superdex 75	GE Healthcare
Superdex peptide	GE Healthcare
HiTrap Desalting column 5 mL	GE Healthcare
Fluorometer LS-35	Perkin-Elmer
CD spectropolarimeter	Jasco715
Centrifuges	Sorvall, Eppendorf, Heraeus
Microfluidizer EmulsiFlex-C5	Avestin
Stopped-Flow instrumentation SX-18MV	Applied Photophysics
SDS-PAGE gel chambers for minigels	Biorad
Trans Blot© Turbo™	Biorad
UV/VIS sprectrophotometer NanoDrop	PeqLab

[2] For Petri dishes, 15 g/L agar is added

Thermomixer	Eppendorf
Liquid chromatograph Ultimate 3000	Dionex
Mass spectrometer ORBITRAP ELITE	Thermo Scientific
Mass spectrometer Maxis	Bruker
Biolumat	Berthold
Luminescent Image Analyzer LAS 4000	FujiFilm
HeraCell 150i CO_2 incubator	Thermo Scientific
Luna™ *fl* cell counter	Logos

Table 10: Software

ApE	M.Wayne Davis
Prism 5.0	GraphPad software
Microsoft Office 2013	Microsoft
Mendeley Desktop	Mendeley Ltd.
ImageJ	Wayne Rasband

5.2 Common solutions and buffers

Agarose gel electrophoresis

Sample loading buffer (5X)
Bromophenol blue 0.1 % (w/v)
Xylencyanol blue 0.2 % (w/v)
Orange G 0.2 % (w/v)
Glycerol 50 % (v/v)
EDTA 50 mM
SDS 1 % (w/v)

TAE buffer
TRIS 40 mM
Acetic acid 20 mM
EDTA 1 mM

Coomassie Staining

Staining solution
Methanol 30 % (w/v)
Acetic acid 10 % (v/v)
Coomassie Brilliant Blue R-250 0.25 % (w/v)

De-staining solution
Methanol 30 % (v/v)
Acetic acid 10 % (v/v)

SDS-PAGE

5X Laemmli Buffer

TRIS (pH 6.8) 0,5M
4,4% SDS
20% glycerol
2-Mercaptoethanol 2%
Bromophenol-blue 0,6%

1X running-buffer pH 8.3

TRIS 25mM
Glycine 200mM
SDS 0.1%

Cell-culture

Phosphate buffered saline (PBS)

NaCl 137 mM
KCl 27 mM
Na_2HPO_4 8.1 mM
KH_2PO_4 1.5 mM

PBS- EDTA

NaCl 137 mM
KCl 27 mM
Na_2HPO_4 8.1 mM
KH_2PO_4 1.5 mM
EDTA 0.8 mM

5.3 Methods

5.3.1 Cell culture and transfection

5.1.1.1 Cultivation of cells

In this work, U2-OS cells were cultivated in DMEM, supplemented with 10% FCS and 1% Penicillin/ Streptomycin, in an atmosphere containing 5% CO_2 and, unless said otherwise, at a temperature of 37°C. When cultures became subconfluent, cells were passaged by resuspending them in PBS-EDTA, and diluting them in fresh growth-media.

If needed, cells were counted using the Luna™ *fl* cell counter. The cell suspension whose concentration was to be measured was diluted 1:1 with 0.1% Trypan Blue before measurement.

5.1.1.2 Transfection

Per default, transfection was performed using Polyethylenimine (PEI) as a transfection reagent. Cells were seeded so that they would reach 60% confluency on the next day. For a 10 cm cell culture dish to be transfected, 1.5 mL DMEM (without FCS, not antibiotics) were mixed with 30 µL of a PEI (stock solution at a concentration of 1 mg/mL), and with 12 µg of plasmid DNA. The mixture was gently

vortexed, and incubated for 10 min at room temperature. 4.5 mL of DMEM (supplemented with FCS and antibiotics) was added, and the mixture was added dropwise to the cells. The medium was changed 7 hours later. For transfection of 15 cm culture dishes, the quantities were increased accordingly. In case of a transient transfection, the cells were harvested after 48 hours as well.

In case of stable transfections, antibiotic selection was applied 48 hours after transfection, and successfully transfected cells were later enriched through Fluorescence Assisted Cell Sorting (FACS), using the presence of GFP or mCherry in the cytoplasm as a criteria of successfully transfected cells. Three to four sorts were performed for each cell line over 2 months.

In the case of dual transient transfections the Rotifect-Plus reagent was used, in order to increase transfection efficiency and according to manufacturer's instructions. 20 µg DNA from each plasmid to be transfected were used for a 15 cm diameter dish. The DNA/lipid complex was only incubated with the cells for 2 hours, so cell mortality could be reduced. Transfection efficiency was assayed with FACS 24 hours after transfection, and cells were harvested after 48 hours.

5.1.1.3 Cryo-conservation of cultivated cells

Subconfluent cells were resuspended in PBS-EDTA, centrifuged at 1000 rpm for 10 min at 4°C and resuspended in 1 mL medium containing 50% FCS and 10% DMSO. The cells were then frozen at -80°C for 24 h and kept in liquid nitrogen for long-term storage.

Cells cryo-tubes were thawed in 70% Ethanol, previously warmed-up at 37°C, and added to a 15 cm culture dish containing 25 mL DMEM (supplemented with 10%FCS and 1% Penicillin/Streptomycin), so that the DMSO is too diluted to harm growing cells.

5.3.2 Molecular biology techniques

5.3.2.1 Cloning techniques

Total RNA isolation

Total RNA was isolated with the Universal RNA purification kit according to the manufacturer's instructions. RNA concentration was determined by measuring its absorbance (230 – 400 nm) using a NanoDrop spectrometer.

Generation of cDNA

1 µg of total RNA was mixed with distilled water so that the total volume would be 14 µL. 1 µL Random Hexamer primer was added. This was incubated 5 minutes at 70°C, before being kept on ice for at least 5 minutes. 5 µL M-MLV RT 5X buffer, 2.5 mM DNTPs, 0.5 µL RNAsin, 0.5 µL M-MLV RT RNAse and 1.5 µL distilled water were them added. The whole mixture was then incubated for 1 h at 37°C. Concentration was then assayed with the NanoDrop.

Polymerase chain reaction

Unless the gene of interest was already cloned, 1 µg of total cDNA was used as a template for PCR. If already cloned, 100 ng of template DNA would be used.

Standard PCR protocol:

Template DNA	100 ng
dNTPs (10 mM)	1 µL
Each primer (10 pmol/µL)	0.5 µL
10 X buffer	5 µL
OptiTaq polymerase (2.5 U/µL)	1 µL
Distilled H_2O	up to V final = 50 µL

Standard PCR program:

Step 1	Melting 9°C 2 min
Repeat step 2-4 30X	
Step 2	melting 96°C 1min
Step 3	annealing 50-60°C (primers-dependent) 30s
Step 4	elongation 68°C 5min
Step 5	pause 4°C

Amplified DNA was then purified either through Agarose Gel, followed by MiniBio GmbH Gel extraction kit, or using the PCR purification kit from MiniBio GmbH.

Restriction digestion of DNA

Restriction enzymes (type II endonuclease) from New England Biolabs were used to digest the 3' and 5' ends of the PCR products, as well as to open the wished vector, hence forming compatible ends

between each other's. Buffer used, temperature and incubation time were chosen according to the manufacturer's instructions.
Digested PCR fragments and digested vectors were then loaded on an agarose gel, bands were cut, and DNA was purified using the Gel Extraction kit from MiniBio GmbH.

Ligation of DNA fragments

The T4 DNA ligase was later used to form phosphodiester bonds between compatible ends of PCR fragments and linearized vector. Reactions were conducted for 30 minutes at 30°C. Molar ratios of vector to insert were 1:3.

Preparation of competent *E. coli* cells and transformation

Transformation were made in chemically competent *E. coli* cells. These cells were first grown to OD_{600} of 0.4-0.5 in about 30mL of LB medium. After centrifugation, cells were washed twice and then resuspended in ice-cold 60mM $CaCl_2$ + 15% glycerol. This solution was previously sterilized. This cell suspension was incubated on ice for 1 hour. The cells were then aliquoted (100 µL) and snap-frozen in liquid nitrogen. Storage was done at -80°C.
Competent *E. coli* were thawed on ice, and 2-5 µL of ligation mixture were added. An incubation of 5 minutes on ice followed. The mixture was subsequently heat-shocked for 1 minute at 42°C, before being put back on ice for 5 minutes. 1 mL of LB medium was then added, and the cells were allowed to recover for 1 hour at 37°C. Centrifugation for 1 minute at 6000 rpm followed. After removing most of the supernatant by decanting, the pellets were resuspended in the remaining medium, and spread onto LB-agar Petri dishes, containing the appropriate antibiotic. The dishes were then incubated overnight at 37°C.

5.3.2.2 Quantitative real-time polymerase chain reaction

cDNA were synthetized as described previsouly. Samples were analyzed in triplicate on a 384-wells plate using the Light Cycler© 480 II from Roche. The cDNA obtained were first diluted five times, and the PCR primers were diluted to 10 pmol/ µL. For each replicate, 2.5 µL of cDNA dilution, 5 µL of 2X SYBR Green Master Mix, 0.4 µL of each primer dilution and 1.7 µL of distilled water were mixed. HPRT1 was used for internal normalization. The PCR program used was the following:

Step 1:	95°C	5 min
Repeat step 2-4 40X		
Step 2	95°C	10 s
Step 3	55°C	20 s
Step 4	72°C	10 s

The qPCR primers used are the following:

qPCR_HSPA1A_5	5'-ACCTTCGACGTGTCCATCCTGAC-3'
qPCR_HSPA1A_3	5'-TGGTTCACCAGCCTGGTTGTCAAA-3'
qPCR_HSPA8_5_c	5'-CAGAAGATTCTGGACAAGTG-3'
qPCR_HSPA8_3_c	5'-GTTGCAAACTTTCTCCCAGCT-3'
HPRT1_housekeeping_5	5'- TGACACTGGCAAAACAATGCA-3'
HPRT1_housekeeping_3	5'- GGTCCTTTTCACCAGCAAGCT-3

5.3.3 Immunoprecipitation and Western Blot

Modified Wade Harper Buffer (MWHB)

TRIS-HCl (pH 7.5) 50 mM
NaCl 150 mM
0.5% NP-40
EDTA 5mM
EGTA 5mM
DTT 1 mM
PMSF 1mM
8 µg/mL Pepstadin
10 µg/mL Aprotinin
5 µg/mL Leupeptin

IP elution buffer

1X TB buffer
NaCl 100 mM
HA peptide 0.2 mg/mL
0.2% Digitonin

Glutathione elution buffer

TRIS-HCl (pH 7.5) 50 mM
Glutathione 10mM
DTT 5 mM
Glycerol 10 %

TB buffer (10X)

HEPES (pH 7.3) 200mM
$K(CH_3COO)$ 1.1 M
$Mg(CH_3COO)_2$ 20 mM
EGTA 10 mM

Lysis buffer (TNS)

TRIS-HCl (pH 7.5) 50 mM
NaCl 300 mM
Saccharose 10%
2-Mercaptoethanol 3mM
PMSF 1mM
8 µg/mL Pepstadin
10 µg/mL Aprotinin
5 µg/mL Leupeptin

5.3.3.1 Immunoprecipitation

Adherent cells were scraped from the dish in Modified Wade Harper Buffer (MWHB). 1 µL Benzonase were added, and the lysates were incubated for 15 minutes et 4°C. This step is meant to degrade genomic DNA in the cells. The lysates were thereafter clarified by centrifugation at 18.000 rpm for 30 minutes, at 4°C. The clarified lysates were then incubated with anti-HA, or anti-myc beads, for 2.5 hours (in the case of immunoprecipitation followed by mass-spectrometry analysis), or 30 minutes (in case of immunoprecipitation followed by a Western-Blot). The beads were later washed several times with 1 mL MWHB, for 10 minutes each, at 4°C.

Interacting proteins were eluted differently differently whether mass-spectrometry or immunoblotting was performed afterwards. In both cases any residual liquid would be removed carefully from the beads with the micropipette. If the immunoprecipitation was followed by Western-blotting, the beads were resuspended in 2X Laemmli buffer, and cooked for 5 minutes at 96°C. If the immunoprecipitation was followed by mass-spectrometry analysis, the beads were resuspended in 200 µL IP elution buffer, and incubated 10 minutes at 30°C, with shaking, to prevent sedimentation of the beads. This step was repeated two more times.

The 600 µL eluate were then concentrated by TCA precipitation: Trichloacetic Acid (TCA) was added to the eluate so that its final concentration was 12%, and incubated on ice for 1 h. Centrifugation at 20,000 g/ 4°C for 30 minutes followed: The supernatant was carefully removed using the micropipet. The pellet was washed with acetone, and a second centrifugation, as previously described, followed. The acetone was then removed with the micropipette, and the pellets were air-dried for 30 minutes. The pellets were finally resuspended in 50 µL 2X Laemmli Buffer, and cooked 5 minutes at 96°C.

In the case of in vitro pull-downs, GST fusion of the Bag constructs were expressed in MC 1061 strain, overnight at 20°C. Cells pellets were resuspended in Lysis buffer (TNS), and lysed through sonication (output 5 / 3 times 10 pulses). Cell extracts were then clarified by centrifugation at 13000 rpm for 15 minutes, at 4°C. Clarified lysates were subsequently incubated with 20 µL Protino-Glutathione agarose for 30 minutes at 4°C, and with or without 2 µM of purified HSF1. Agarose beads were then washed once with lysis buffer, and later the GST-fusion protein were eluted in 40 µL Glutathione elution buffer for 30 minutes at 4°C.

5.3.3.2 SDS-PAGE and immunoblotting

In this work, 12% and 16% acrylamide separation gels were prepared and used.

Table 11: Gel preparation scheme for SDS-PAGE

Substance	*Separation gel 12%*	*Separation gel 16%*	*Stacking gel 6%*
Acrylamide	12% [v/v]	16% [v/v]	6% [v/v]
Tris-Hcl, pH 6,8	-	-	125 mM
Tris-Hcl, pH 8,8	375 mM	375 mM	-
SDS 10%	0.1% [w/v]	0.1% [w/v]	0.1% [w/v]
Ammonium persulfate (APS) 10%	0.6% [w/v]	0.6% [w/v]	0.05% [w/v]
TEMED	0.06% [v/v]	0.06% [w/v]	0.01% [v/v]

Whole protein cell lysates, or purified proteins were mixed with 5X Laemmli buffer, so that the final concentration of Laemmli buffer would be 1X. After 5 minutes heating at 96°C, samples, and molecular ladder would be loaded into the wells of the gels, and separated with 120 V for 20 minutes, followed by 45 minutes to 2 hours with 180 V in running buffer. When no Western Blot was needed, the gels were stained with coomassie staining for 1 hour, and de-stained with de-staining solution.

For immunoblotting, the separated proteins were transferred on a PVDF membrane using the Trans Blot© Turbo™, and according to the manufacturer's default procedure. After blocking of unspecific binding using 3% Milk/PBS-Tween (0.1%) for 30 minutes, cells were incubated with the appropriate antibody at the appropriate dilution, in blocking solution, overnight, at 4°C. Next day, the membranes were washed 7-8 times with PBS-Tween (0.1%) for 5 minutes, before being incubated for 2 hours at room temperature with the appropriate secondary antibody coupled with the Horseradish Peroxidase, diluted in blocking solution. Membranes were once again washed 7-8 times with PBS-Tween (0.1%) for 5 minutes. All incubations were performed on a roller shaker in a 50 mL tube. Protein bands were detected using the Chemiluminescent Substrate West Pico reagent, and the LAS 4000 instrumentation.

5.3.4 Analysis by Shotgun Proteomics

Eluates from immunoprecipitations were processed and analyzed by the Core Facility for mass spectrometry and proteomics of the ZMBH (Zentrum für Molekularebiologie Heidelberg). The Proteome of U2-OS pIRES-GFP II-CtermHA-HsHSF1 cells was hence compared to the proteome of U2-

OS pIRES-GFP II-HA cells using the Dimethyl labelling method. Control cell eluates were labelled after trypsin digest with light dimethyl ($H_2CO/NaBH_3CN$) and HA-HSF1 cell eluates with medium ($D_2CO/NaBH_3CN$) dimethyl (+4 Da).

The eluates were run separately on SDS-PAGE, and fractions on the gels were cut. Samples were reduced with DTT, alkylated with iodoacetamide, before being digested with trypsin, whereas digested peptides were then extracted from the gel pieces with 50% acetonitrile/0.1% trifluoroacetic acid (TFA), concentrated with a SpeedVac vacuum centrifuge, and diluted in 0.1% TFA, so that the total volume reaches 30 µL. 10 µL of it were analyzed with a nano HPLC (Dionex Ultimate 3000), coupled to an Orbitrap Elite mass spectrometer (Thermo Scientific). Sample was loaded onto a C18 Acclaim PepMap100 trap-column (Thermo Fisher Scientific) with a flow rate of 30ul/min 0.1% TFA. Peptides were eluted and separated on an C18 Acclaim PepMap RSLC analytical column (75um x 250mm) with a flow rate of 300nl/min in a 90 min gradient of 3% buffer A (0.1% formic acid) to 40% buffer B (0.1% formic acid, acetonitrile. A full peptide scan was followed by up to 15 MS/MS scans. The peptides found were compared to the UniProt database, taking into account the carbamidomethylation of the cysteines, and the eventual oxidation of Methionine and acetylation of protein N-termini. Data were analyzed with MaxQuant 1.5.2.8 and later with MaxQuant 1.5.3.30 and standard settings.

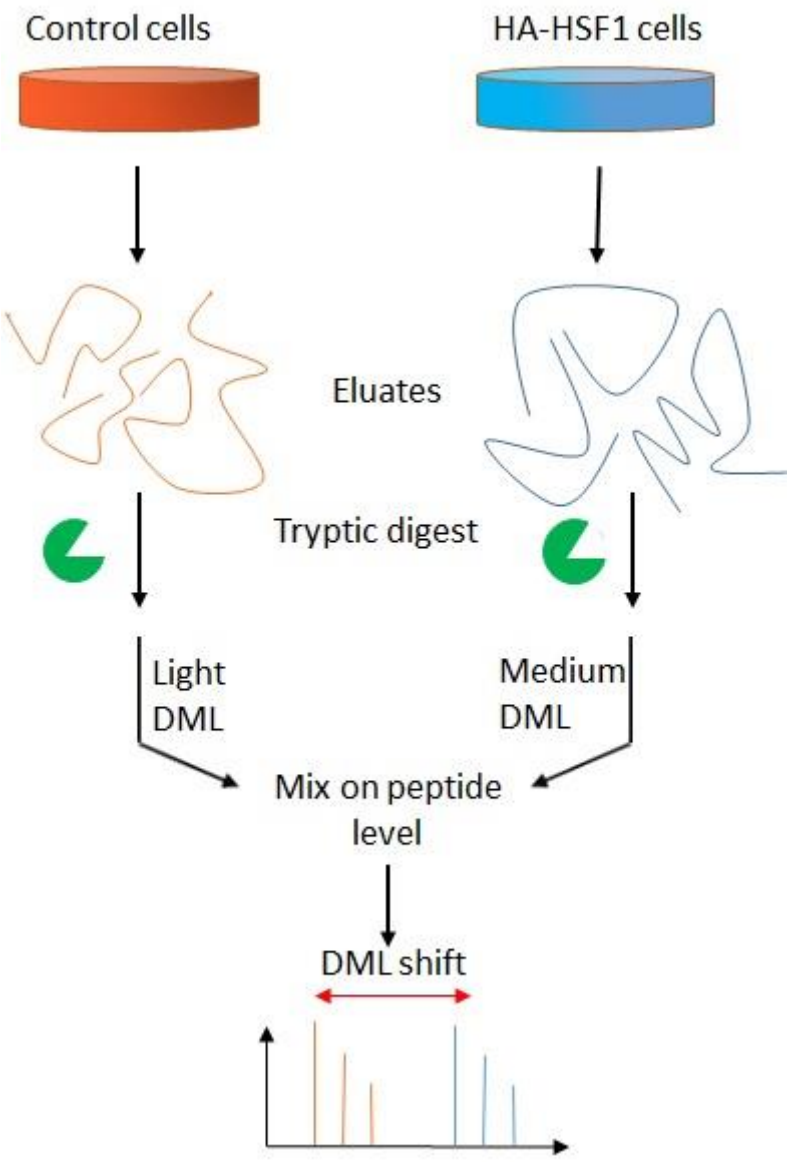

Figure 20: Dimethyl labeling workflow.

5.3.5 Protein expression and purification

Lysis buffer (TNS)

TRIS (pH 7.5) 50mM
NaCl 300mM
Saccharose 10%
2-Mercaptoethanol 3mM
PMSF 1mM
8 µg/mL Pepstadin
10 µg/mL Aprotinin
5 µg/mL Leupeptin

High salt buffer

TRIS (pH 7.5) 50mM
NaCl 1M
Saccharose 10%
2-Mercaptoethanol 3mM
PMSF 1mM
8 µg/mL Pepstadin
10 µg/mL Aprotinin
5 µg/mL Leupeptin

Elution buffer

TRIS (pH 7.5) 50mM
NaCl 300mM
Saccharose 10%
2-Mercaptoethanol 3mM
PMSF 1mM
8 µg/mL Pepstadin
10 µg/mL Aprotinin
5 µg/mL Leupeptin
Imidazole 300mM

HKM-buffer

HEPES (pH 7.6) 25mM
KCl 150mM
$MgCl_2$ 5mM

ATP-buffer

HEPES (pH 7.6) 25mM
KCl 150mM
$MgCl_2$ 5mM
5 mM ATP

Buffer A

HEPES (pH 7.6) 25mM
KCl 10mM
$MgCl_2$ 5mM

Buffer B

HEPES (pH 7.6) 25mM
KCl 1M
$MgCl_2$ 5mM

Buffer C

Sodium-Phosphate buffer (pH 7.2) 50mM
NaCl 300mM
Glycerol 10 %
2-Mercaptoethanol 3mM
PMSF 1mM
8 µg/mL Pepstadin
10 µg/mL Aprotinin
5 µg/mL Leupeptin

All protein purified were expressed as 6xHis-SUMO fusion in BL21(DE3) Rosetta™. The cultures were grown at 37°C in 2xYT medium containing kanamycin. Once the optical density at 600 nm reached 0.7 – 0.9, the cultures were induced with either 1 mM IPTG or 0.2% L(+)-arabinose. Expression proceed differently according to the protein purified: Bag2 full length was expressed for 5 h at 25°C. The Bag

domain of Bag2 (Bag2_BD) overnight at 20°C, and the Bag Domain of Bag4, for 4 h at 30°C. Hsc70 was expressed overnight at 25°C.

At the end of expression, the cells were harvested by centrifugation at 5000 rpm for 15 minutes, and pellets were frozen dry, if the expression was not overnight. On the day of the purification, the pellets were resuspended in Lysis buffer (30 mL buffer / 1 L of culture) and lysed with a Micro fluidizer. The lysates were then clarified by centrifugation at 18000 rpm for 30 minutes. The supernatant was incubated with 0.5 g – 1 g of Protino resin (Ni-IDA, Macherey-Nagel) for 15-20 minutes at 4°C. The mixture was thereafter poured onto a polypropylene column where the resin with loaded material would sediment, and the flow-through hence be separated. The column with loaded material would then be washed with 20 column volumes of lysis buffer, followed by 20 column volumes of High-salt buffer. In the case of Hsc70 purification, all purification buffers were HKM based, and a wash with 10 column volumes of ATP-buffer was performed before the high-salt wash, in order to remove bound substrates from Hsc70. Proteins were eluted with 5 mL of elution buffer, and fractions of 0,5 mL were collected. Fractions containing the protein were pooled. From this point, each purification differs.

5.3.5.1 Purification of Bag4 Bag Domain

The pooled fraction after elution were pooled together, and dialyzed overnight at 4°C against HKM buffer, with subsequent Ulp1 digestion of the SUMO tag. On the next day, the dialyzed protein were incubated with 0.5 g of Protino resin, in order to remove Ulp1, free SUMO, and any protein that would bound to the protein in an unspecific manner. The flow-through would contain the protein. Purity was checked by SDS-PAGE.

5.3.5.2 Purification of Bag2 full length

After Nickel affinity purification, the fractions collected were pooled, and the buffer was changed into HKM buffer on a HiTrap desalting column. This step was meant to remove Imidazole from the protein solution. For the next step, fresh Protino beads were saturated with Ulp1: 0.1g Protino were incubated with 2g Ulp1 in 10 mL HKM buffer for 15min at 4°C. The mixture was then centrifuged for 2 minutes at 1000 rpm, and the supernatant was removed. The beads were washed twice in 10 mL HKM buffer.

The Imidazole-free Bag2 solution was then mixed with the beads, and incubated for 2 hours at 4°C. This step was necessary to ensure that Bag2 would not interact with the Protino resin in a His tag independent fashion, which appeared to be the case.

Next, a gel filtration with a Superdex 75 column was performed, and purity was checked by SDS-PAGE.

5.3.5.3 Purification of Bag2_BD

In the case of the Bag Domain of Bag2, the Lysis buffer used was Buffer C, and high salt (with 1M NaCl) and elution (with 300 mM Imidazole) version of it were used. After Nickel affinity purification, the protein was dialyzed overnight against HKM buffer, with subsequent Ulp1 digest. Next day, a gel filtration on Superdex Peptide 10/300 GL was performed.

5.3.5.4 Purification of Hsc70

After Nickel affinity purification, buffer exchange was performed on a HiTrap desalting column, and overnight incubation with Ulp1 followed. On the next day, a second incubation with Protino was made, to remove uncut protein, alongside with Ulp1 and free SUMO. A new buffer exchange were performed, in order to put the protein in Buffer A. Ion-exchange chromatography on a Resource Q column followed. The column was pre-equilibrated in buffer A. Hsc70 was eluted from the column by a linear gradient from 0 to 100 % of Buffer B within 15 column volumes. Purity was checked by SDS-PAGE.

5.3.5.5 Determination of the protein concentration

The protein concentrations were determined with the Bradford assay (Biorad). In this assay, absorption at 595 nm of a dilution of the protein into Bradford reagent is measured on a spectrophotometer. A calibration curve was prepared using BSA as a standard.

5.3.6 Biochemical assays

5.3.6.1 Luciferase refolding assay

<u>Refolding buffer</u>
HEPES (pH 7.5) 25mM
Potassium-Acetate 50mM
Magnesium-Acetate 10mM
ATP 2mM
DTT 5mM

<u>Firefly Assay buffer A</u>
Glycylglycine (ph 7.4) 25mM
K_2PO_4 100mM
KH_2PO_4 100mM
ATP 5mM
Potassium-Acetate 100mM
Magnesium-Acetate 15mM

Firefly luciferase (25 nM) was mixed with Hsc70 (2 µM) and Hdj1 (1 µM) in refolding buffer, and denaturated by heat treatment at 42°C for 10 minutes. After Heat-Shock, Bag2 or Bag4 was added to the desired concentration, and incubated at 30°C. At a given time-point, 2 µL of the reaction mixture were taken, and mixed with 123 µL of Firefly assay buffer A, and subsequently mixed with 125 µL of luciferin (160 µM) in a Biolumat. The measurement started directly after adding of luciferin, and lasted for 5 seconds.

5.3.6.2 Luciferase assay on cell lysates

Renilla Assay buffer
NaCl 1,1 mM
Na_2EDTA 2,2 mM
K-Phosphate buffer (pH 5.1) 0.22 mM
BSA 0.44 mg/mL
NaN_3 1.3 mM
Coelenterazine 1.43 µM

Firefly Assay buffer
Glycylglycine (pH 7.4) 25 mM
K-Phosphate buffer (pH 8.0) 15 mM
Potassium-Acetate 100mM
Magnesium-Acetate 15 mM
ATP 2 mM
DTT 1 mM
Luciferin 75 µM

Luciferase Lysis buffer (5X)
Tris-HCl (pH 7.8) 125 mM
1,2 Diaminocyclohexane-N,N,N',N' 10 mM
Glycerol 50 %
Triton X-100 5 %
DTT 2mM

Cells were scraped from the dish in Luciferase Lysis buffer (1X), vortexed, and centrifuged 2 minutes at 4°C at 12,000 g. Cell extracts were then flash-frozen in liquid nitrogen, and stored at -80°C. Before measurement, cells were thawed on ice, and 10 µL of the lysate was mixed with 115 µL of Firefly assay buffer A, and subsequently mixed with 125 µL of luciferin (160 µM) in a Biolumat. Measurement started directly after adding of luciferin, and lasted for 20 seconds.

In case of dual luciferase assay, the cell were lysed with Passive Lysis Buffer (Promega), according to manufacturer's instructions, to ensure fast and complete lysis. 20 µL of lysate were used, and first mixed with 125 µL of Firefly assay buffer. Measurement started directly, and lasted for 10 seconds. 125 µL of Renilla assay buffer was then added. This buffer would deactivate firefly luciferase (Dyer et al. 2000), and allow that only the activity of Renilla luciferase is measured. Measurement started directly after injection, and lasted for 10 seconds as well.

5.3.6.3 Kinetics of ADP-release

0.5 µM of Hsc70 or Hsp70 were mixed with 0.5 µM MABA-ADP, and incubated 30 minutes at 30°C, and subsequently rapidly mixed with a solution containing 1 mM ATP and Bag2, Bag2_BD or Bag4_BD, at the desired concentration. Mixing was performed at 30°C in a stopped-flow device SX.18MV. The samples were excited at 360 nm and the decrease in fluorescence was measured using a 420 nm cut-off filter. A single-exponential function was fitted to the obtained traces, and the rate constants of ADP-release were hence obtained.

5.3.7 Circular Dichroism

Circular Dichroism (CD) consist in the interaction of polarized light with optically active chiral molecules. Ultra violet CD is used to investigate the secondary structure of proteins. In this case, the chirality of the peptide bond strongly contribute to the CD spectrum of the protein. In a CD spectrum, two minima at 222 and 208 nm and a maximum peak at 195 nm are characteristic of a α-helical structure. On the contrary, a maximum at 195 nm, and a broad single minimum around 215 are seen in the CD spectra of a polypeptide rich in β-sheets.

In this work, the proteins to be analyzed were dialyzed overnight in 10 mM Sodium-Phosphate buffer at pH 7.6. At least 140 µL of protein dilution were placed in a 1.0 cm x 0.1 cm quartz cuvette, and the CD spectrum was obtain with a Jasco 715 CD spectropolarimeter. A temperature gradient of 10-90°C was applied to the sample, in order to obtain a denaturation curve.

Bibliography

Abravaya, K., Phillips, B. & Morimoto, R.I., 1991a. Attenuation of the heat shock response in HeLa cells is mediated by the release of bound heat shock transcription factor and ! s modulated by changes in growth and m heat shock temperatures. *Genes & Development*, 5, pp.2117–2127.

Abravaya, K., Phillips, B. & Morimoto, R.I., 1991b. Heat Shock-Induced Interactions of Heat Shock Transcription Factor and the Human hsp70 Promoter Examined by In Vivo Footprinting INLiL. *Molecular and cellular biology*, 11(1), pp.586–592.

Åkerfelt, M. et al., 2010. Heat Shock Transcription Factor 1 Localizes to Sex Chromatin during Meiotic Repression * □. *Journal of Biological Chemistry*, 285(45), pp.34469–34476.

Åkerfelt, M., Trouillet, D. & Erie, V.A.L., 2007. Heat Shock Factors at a Crossroad. *Annals of the New York Academy of Sciences*, 27, pp.15–27.

Ali, A. et al., 1998. HSP90 Interacts with and Regulates the Activity of Heat Shock Factor 1 in Xenopus Oocytes. *Molecular and cellular biology*, 18(9), pp.4949–4960.

Amin, J., Ananthan, J. & Voellmy, R., 1988. Key Features of Heat Shock Regulatory Elements. *Molecular and cellular biology*, 8(9), pp.3761–3769.

Anckar, J. et al., 2006. Inhibition of DNA Binding by Differential Sumoylation of Heat Shock Factors. , 26(3), pp.955–964.

Anckar, J. & Sistonen, L., 2011. Regulation of HSF1 function in the heat stress response: implications in aging and disease. *Annual review of biochemistry*, 80, pp.1089–115. Available at: http://www.ncbi.nlm.nih.gov/pubmed/21417720 [Accessed November 11, 2013].

Andrulis, E.D. et al., 2000. High-resolution localization of Drosophila Spt5 and Spt6 at heat shock genes in vivo : roles in promoter proximal pausing and transcription elongation. *Genes & Development*, pp.2635–2649.

Anfinsen, C.B., 1973. Principles that Govern the Folding of Protein Chains. *Science*, 181(4096), pp.223–230.

Arakawa, A. et al., 2010. The C-Terminal BAG Domain of BAG5 Induces Conformational Changes of the Hsp70 Nucleotide- Binding Domain for ADP-ATP Exchange. *Structure*, 18(3), pp.309–319. Available at: http://dx.doi.org/10.1016/j.str.2010.01.004.

Arndt, V. et al., 1990. BAG-2 Acts as an Inhibitorof the Chaperone-associated Ubiquitin Ligase CHIP. *Genetics*, 125(2), pp.351–369.

Ashburner, M. & Bonnert, J.J., 1979. The Induction of Gene Activity Drosophila by Heat Shock in Review. *Cell*, 17(June), pp.241–254.

Auluck, P.K. et al., 2002. Chaperone Suppression of alpha-Synuclein Toxicity in a Drosophila Model for Parkinson ' s Disease. *Science*, 295(February), pp.865–869.

Baler, R., Welch, W.J. & Voellmy, R., 1992. Heat Shock Gene Regulation by Nascent Polypeptides and Denatured Proteins: hsp70 as a Potential Autoregulatory Factor. *Journal of Cell Biology*, 117(6), pp.1151–1159.

Ben-zvi, A.P. & Goloubinoff, P., 2001. Review : Mechanisms of Disaggregation and Refolding of Stable Protein Aggregates by Molecular Chaperones. *Journal of Structural Biology*, 93, pp.84–93.

Bharadwaj, S., Ali, A. & Ovsenek, N., 1999. Multiple Components of the HSP90 Chaperone Complex

Function in Regulation of Heat Shock Factor 1 In Vivo. *Molecular and cellular biology*, 19(12), pp.8033–8041.

Bonini, N.M., 2002. Chaperoning brain degeneration. *Proceedings of the National Academy of Sciences of the United States of America*, 99, pp.16407–16411.

Bracher, A. & Verghese, J., 2015. The nucleotide exchange factors of Hsp70 molecular chaperones. *Frontiers in Molecular Biosciences*, 2(April), pp.1–9.

Brehmer, D. et al., 2004. Influence of GrpE on DnaK-substrate interactions. *Journal of Biological Chemistry*, 279(27), pp.27957–27964.

Brehmer, D. et al., 2001. Tuning of chaperone activity of Hsp70 proteins by modulation of nucleotide exchange. *Nature structural biology*, 8(5), pp.427–432.

Briknarová, K. et al., 2002. BAG4/SODD protein contains a short BAG domain. *Journal of Biological Chemistry*, 277(34), pp.31172–31178.

Brockmann, C. et al., 2004. The solution structure of the SODD BAG domain reveals additional electrostatic interactions in the HSP70 complexes of SODD subfamily BAG domains. *FEBS Letters*, 558(1–3), pp.101–106.

Brown, I.R. & Rush, S.J., 1999. Cellular localization of the heat shock transcription factors HSF1 and HSF2 in the rat brain during postnatal development and following hyperthermia. *Brain Research*, 821, pp.333–340.

Brown, S.A. et al., 1998. Transcriptional activation domains stimulate initiation and elongation at different times and via different residues. *EMBO Journal*, 17(11), pp.3146–3154.

Brown, S.A., Imbalzano, A.N. & Kingston, R.N., 1996. Activator-dependent regulation of transcriptional pausibg on nucleosomal templates. *Genes & Development*, pp.1479–1490.

Chesnokova, L.S. et al., 2003. Deletion of DnaK ' s Lid Strengthens Binding to the Nucleotide Exchange Factor , GrpE : A Kinetic and Thermodynamic Analysis †. *Biochemistry*, 42, pp.9028–9040.

Chiti, F. & Dobson, C.M., 2006. Protein Misfolding , Functional Amyloid , and Human Disease. *Annual review of biochemistry*, 75, pp.333–366.

Choi, Y., 2000. Divergent hTAFII31-binding Motifs Hidden in Activation Domains. *Journal of Biological Chemistry*, 275(21), pp.15912–15916. Available at: http://www.jbc.org/cgi/doi/10.1074/jbc.275.21.15912 [Accessed December 13, 2013].

Christians, E. et al., 2000. Maternal effect of Hsf1 on reproductive success. *Nature*, 407(October), pp.693–694.

Cicero, M.P. et al., 2001. The wing in yeast heat shock transcription factor (HSF) DNA-binding domain is required for full activity. *Nucleic acids research*, 29(8), pp.1715–1723.

Clark, D.A. et al., 2007. Temporal Activity Patterns in Thermosensory Neurons of Freely Moving Caenorhabditis elegans Encode Spatial Thermal Gradients. *The Journal of Neuroscience*, 27(23), pp.6083–6090.

Cohen, E. et al., 2006. Opposing Activities Protect Against Age-Onset Proteotoxicity. *Science*, (September), pp.1604–1611.

Connell, P. et al., 2001. The co-chaperone CHIP regulates protein triage decisions mediated by heat-shock proteins. *Nature Cell Biology*, 3(January), pp.93–96.

Corey, L.L. et al., 2003. Localized recruitment of a chromatin-remodeling activity by an activator in vivo drives transcriptional elongation. *Genes & Development*, 17, pp.1392–1401.

Dai, C. et al., 2007. Heat Shock Factor 1 Is a Powerful Multifaceted Modifier of Carcinogenesis. *Cell*, 130, pp.1005–1018.

Dai, Q. et al., 2003. CHIP activates HSF1 and confers protection against apoptosis and cellular stress. *The EMBO journal*, 22(20), pp.5446–5458.

Dai, Q. et al., 2005. Regulation of the Cytoplasmic Quality Control Protein Degradation Pathway by BAG2 *. , 280(46), pp.38673–38681.

Deuerling, E. et al., 1999. Trigger factor and DnaK cooperate in folding of newly synthesized proteins. *Nature*, 133(1998), pp.693–696.

Diamant, S. et al., 2001. Chemical Chaperones Regulate Molecular Chaperones in Vitro and in Cells under Combined Salt and Heat Stresses *. *Journal of Biological Chemistry*, 276(43), pp.39586–39591.

Dragovic, Z. et al., 2006. Molecular chaperones of the Hsp110 family act as nucleotide exchange factors of Hsp70s. *The EMBO journal*, 25(11), pp.2519–2528.

Dyer, B.W. et al., 2000. A Noncommercial Dual Luciferase Enzyme Assay System for Reporter Gene Analysis 1. , 161(1991), pp.158–161.

Farkas, T., Kutskova, Y. a & Zimarino, V., 1998. Intramolecular repression of mouse heat shock factor 1. *Molecular and cellular biology*, 18(2), pp.906–918.

Finka, A. & Goloubinoff, P., 2013. Proteomic data from human cell cultures refine mechanisms of chaperone-mediated protein homeostasis. *Cell stress & chaperones*, 18(5), pp.591–605. Available at: http://www.ncbi.nlm.nih.gov/pubmed/23430704 [Accessed February 7, 2014].

Franceschelli, S. et al., 2008. Bag3 Gene Expression Is Regulated By Heat Shock Factor 1. *Journal of Cellular Physiology*, 215(3), pp.575–577.

Frydman, J., 2001. Folding of newly translated proteins in vivo: The Role of Molecular Chaperones. *Annual review of biochemistry*, 70, pp.603–647.

Fujimoto, M. et al., 2004. HSF4 is required for normal cell growth and differentiation during mouse lens development. *The EMBO journal*, 23(21), pp.4297–4306.

Fujimoto, M. et al., 2012. RPA assists HSF1 access to nucleosomal DNA by recruiting histone chaperone FACT. *Molecular cell*, 48(2), pp.182–94. Available at: http://www.ncbi.nlm.nih.gov/pubmed/22940245 [Accessed November 20, 2013].

Gamer, J. et al., 1996. A cycle of binding and release of the DnaK , DnaJ and GrpE chaperones regulates activity of the Escherichia coli heat shock transcription factor & 2. *The EMBO journal*, 15(3), pp.607–617.

Gao, X. et al., 2015. Human Hsp70 Disaggregase Reverses Parkinson's-Linked α-Synuclein Amyloid Fibrils. *Molecular Cell*, 59(5), pp.781–793. Available at: http://dx.doi.org/10.1016/j.molcel.2015.07.012.

Gässler, C.S. et al., 2001. Bag-1M Accelerates Nucleotide Release for Human Hsc70 and Hsp70 and Can Act Concentration-dependent as Positive and Negative Cofactor *. , 276(35), pp.32538–32544.

Geiss-friedlander, R. & Melchior, F., 2007. Concepts in sumoylation: a decade on. *Nature reviews. Molecular cell biology*, 8(december), pp.947–956.

Genevaux, P., Georgopoulos, C. & Kelley, W.L., 2002. Scanning Mutagenesis Identifies Amino Acid Residues Essential for the in Vivo Activity of the Escherichia coli DnaJ (Hsp40) J-Domain.

Genetics, 1053(November), pp.1045–1053.

Gilmour, D.S. et al., 1988. Topoisomerase I Interacts with Transcribed Regions in Drosophila Cells. *Cell*, 44, pp.401–407.

Glover, J.R. & Lindquist, S., 1998. Hsp104 , Hsp70 , and Hsp40 : A Novel Chaperone System that Rescues Previously Aggregated Proteins. *Cell*, 94, pp.73–82.

Goloubinoff, P. et al., 1999. Sequential mechanism of solubilization and refolding of stable protein aggregates by a bichaperone network.

Gómez, A. V et al., 2008. Article CoREST Represses the Heat Shock Response Mediated by HSF1. *Molecular cell*, 31, pp.222–231.

Goodson, M.L. & Sarge, K.D., 1995. Heat-inducible DNA binding of Purified Heat Shock Transcription Factor 1. *Journal of Biological Chemistry*, 270(February 10), pp.2447–2450.

Guettouche, T. et al., 2005. Analysis of phosphorylation of human heat shock factor 1 in cells experiencing a stress. *BMC Biochemistry*, 14, pp.1–14.

Guo, Y. et al., 2001. Evidence for a Mechanism of Repression of Heat Shock Factor 1 Transcriptional Activity by a Multichaperone Complex *. *Journal of Biological Chemistry*, 276(49), pp.45791–45799.

Haslbeck, M. et al., 2005. Some like it hot : the structure and function of small heat-shock proteins. *Nature Structural & Molecular Biology*, 12(10), pp.842–846.

Heikkila, J.J., Schultz, G.A. & Tnn, A., 1982. Expression of a Set of Fish Genes Following Heat or Metal Ion Exposure*. *Journal of Biological Chemistry*, 257(20), pp.12000–12005.

Hentze, N. et al., 2016. Molecular mechanism of thermosensory function of human heat shock transcription factor Hsf1. *eLife*, (1), pp.1–24.

Hietakangas, V. et al., 2006. PDSM, a motif for phosphorylation-dependent SUMO modification. *Proceedings of the National Academy of Sciences of the United States of America*, 103(1), pp.45–50. Available at: http://www.pubmedcentral.nih.gov/articlerender.fcgi?artid=1324973&tool=pmcentrez&rendertype=abstract.

Hietakangas, V. et al., 2003. Phosphorylation of Serine 303 Is a Prerequisite for the Stress-Inducible SUMO Modification of Heat Shock Factor 1 Phosphorylation of Serine 303 Is a Prerequisite for the Stress-Inducible SUMO Modification of Heat Shock Factor 1.

Hightower, L.E., 1980. Cultured Animal Cells Exposed to Amino Acid Analogues or Puromycin Rapidly Synthesize Several Polypeptides. *Cell*, 427, pp.407–427.

Höhfeld, J., Cyr, D.M. & Patterson, C., 2001. From the cradle to the grave : molecular chaperones that may choose between folding and degradation. *EMBO reports*, 2(10), pp.885–890.

Hohfeld, J. & Jentsch, S., 1998. GrpE-like regulation of the Hsc70 chaperone by the anti- apoptotic protein BAG-1. *Embo Journal.*, 17(3), p.847.

Holmberg, C.I. et al., 2001. Phosphorylation of serine 230 promotes inducible transcriptional activity of heat shock factor 1. *the EMBO*, 20(14), pp.3800–3810.

Hsu, A., Murphy, C.T. & Kenyon, C., 2003. Regulation of Aging and Age-Related Disease by DAF-16 and Heat-Shock Factor. *Science*, 936(June), pp.1142–1145.

Inouye, S. et al., 2004. Impaired IgG Production in Mice Deficient for Heat Shock Transcription Factor 1 *. *Journal of Biological Chemistry*, 279(37), pp.38701–38709.

Jaeger, A.M. et al., 2016. Structures of HSF2 reveal mechanisms for differential regulation of human heat-shock factors. *Nature Structural & Molecular Biology*, (August 2015). Available at: http://www.nature.com/doifinder/10.1038/nsmb.3150.

Jin, Y., Ahn, S. & Kim, S., 2015. BAG3 affects the nucleocytoplasmic shuttling of HSF1 upon heat stress. *Biochemical and Biophysical Research Communications*, 464(2), pp.561–567. Available at: http://dx.doi.org/10.1016/j.bbrc.2015.07.006.

Kabani, M., McLellan, C., et al., 2002. HspBP1, a homologue of the yeast Fes1 and Sls1 proteins, is an Hsc70 nucleotide exchange factor. *FEBS Letters*, 531(2), pp.339–342.

Kabani, M., Beckerich, J.-M. & Brodsky, J.L., 2002. Nucleotide exchange factor for the yeast Hsp70 molecular chaperone Ssa1p. *Molecular and cellular biology*, 22(13), pp.4677–89. Available at: http://www.pubmedcentral.nih.gov/articlerender.fcgi?artid=133915&tool=pmcentrez&rendertype=abstract.

Kampinga, H.H. & Craig, E.A., 2010. The HSP70 chaperone machinery : J proteins as drivers of functional specificity. *Nature reviews. Molecular cell biology*, 11(August), pp.579–592. Available at: http://dx.doi.org/10.1038/nrm2941.

Karzai, A.W. & Mcmacken, R., 1996. A Bipartite Signaling Mechanism Involved in DnaJ-mediated Activation of the Escherichia coli DnaK Protein. *Journal of Biological Chemistry*, 271(19), pp.11236–11246.

Kelley, W.L., 1998. The J-domain family and the recruitment of chaperone power. *Trends in Biochemical sciences*, 40(98), pp.222–227.

Kilpatrick, K. et al., 2013. Chemical Induction of Hsp70 Reduces α-Synuclein Aggregation in Neuroglioma Cells. *ACS chemical biology*. Available at: http://www.ncbi.nlm.nih.gov/pubmed/23594135.

Kline, M.P. & Morimoto, R.I., 1997. Repression of the Heat Shock Factor 1 Transcriptional Activation Domain Is Modulated by Constitutive Phosphorylation. *Molecular and cellular biology*, 17(4), pp.2107–2115.

Klucken, J. et al., 2004. Hsp70 Reduces alpha-Synuclein Aggregation and Toxicity *. *Journal of Biological Chemistry*, 279(24), pp.25497–25502.

Kugel, J. & Goodrich, J., 2006. Beating the Heat : A Translation Factor and an RNA Mobilize the Heat Shock Transcription Factor HSF1. *Molecular Biology of the Cell*, 22(April 21), pp.153–154.

Lee, J.-H. et al., 2013. Heat shock protein 90 (HSP90) inhibitors activate the heat shock factor 1 (HSF1) stress response pathway and improve glucose regulation in diabetic mice. *Biochemical and biophysical research communications*, 430(3), pp.1109–13. Available at: http://www.ncbi.nlm.nih.gov/pubmed/23261432 [Accessed November 20, 2013].

Li, J., Soroka, J. & Buchner, J., 2012. Biochimica et Biophysica Acta The Hsp90 chaperone machinery : Conformational dynamics and regulation by. *BBA - Molecular Cell Research*, 1823(3), pp.624–635. Available at: http://dx.doi.org/10.1016/j.bbamcr.2011.09.003.

Li, X. & Green, M.R., 1998. The HIV-1 Tat cellular coactivator Tat – SF1 is a general transcription elongation factor. *Genes & Development*, (508), pp.2992–2996.

Liberek, K. et al., 1991. The Escherichia coli DnaK chaperone, the 70-kDa heat shock protein eukaryotic equivalent, changes conformation upon ATP hydrolysis, thus triggering its dissociation from a bound target protein. *Journal of Biological Chemistry*, 266(22), pp.14491–14496.

Liberek, K., Agnieszka, L. & Zietkiewicz, S., 2008. Focus Quality Control Chaperones in control of protein disaggregation. *The EMBO journal*, 27(2), pp.328–335.

Lis, J.T. et al., 2000. P-TEFb kinase recruitment and function at heat shock loci. *Genes & Development*, 14, pp.792–803.

Littlefield, O. & Nelson, H.C.M., 1999. A new use for the " wing " of the " winged " helix-turn-helix motif in the HSF – DNA cocrystal. *Nature Structural & Molecular Biology*, 6(5).

Liu, Q. & Hendrickson, W.A., 2007. Insights into Hsp70 Chaperone Activity from a Crystal Structure of the yeast Hsp110 Sse1. *Cell*, 454(1), pp.42–54.

Lorès, P. et al., 2010. The SWI / SNF protein BAF60b is ubiquitinated through a signalling process involving Rac GTPase and the RING finger protein Unkempt. *The FEBS Journal*, 277, pp.1453–1464.

Mally, A. & Witt, S.N., 2001. GrpE accelerates peptide binding and release from the high affinity state of DnaK. *Nature structural biology*, 8(3), pp.254–257.

Martin, J., Horwich, A.L. & Hartl, F.U., 1992. Prevention of Protein Denaturation Under Heat Stress by the Chaperonin Hsp60. *Science*, 258(13), pp.995–998.

Masson, F. Le et al., 2011. Identification of Heat Shock Factor 1 Molecular and Cellular Targets during Embryonic and Adult Female Meiosis †. *Molecular and cellular biology*, 31(16), pp.3410–3423.

Mayer, M.P., Schröder, H., et al., 2000. Multistep mechanism of substrate binding determines chaperone activity of Hsp70. *Nature Structural & Molecular Biology*, 7(7), pp.586–593.

Mayer, M.P. & Bukau, B., 2005. Cellular and Molecular Life Sciences Hsp70 chaperones : Cellular functions and molecular mechanism. *Cellular and Molecular Life Sciences*, 62, pp.670–684.

Mayer, M.P., Rüdiger, S. & Bukau, B., 2000. Molecular Basis for Interactions of the DnaK Chaperone with Substrates. *Biological Chemistry*, 381(October), pp.877–885.

Mckeon, A.M. et al., 2016. and Colorectal Cancer Cells. *Molecules*, 1(i), pp.1–10.

Mcmillan, D.R. et al., 1998. Targeted Disruption of Heat Shock Transcription Factor 1 Abolishes Thermotolerance and Protection against Heat-inducible Apoptosis *. *Journal of Biological Chemistry*, 273(13), pp.7523–7528.

Meacham, G.C. et al., 2001. The Hsc70 co-chaperone CHIP targets immature CFTR for proteasomal degradation. *Nature Cell Biology*, 3(January), pp.100–105.

Mercier, P.A., Winegarden, N.A. & Westwood, J.T., 1999. Human heat shock factor 1 is predominantly a nuclear protein before and after heat stress. *Journal of Cell Science*, 112, pp.2765–2774.

Morimoto, R.I., 1998. Regulation of the heat shock transcriptional response: cross talk between a family of heat shock factors, molecular chaperones, and negative regulators. *Genes & Development*, 12(24), pp.3788–3796. Available at: http://www.genesdev.org/cgi/doi/10.1101/gad.12.24.3788 [Accessed November 13, 2013].

Morley, J.F. & Morimoto, R.I., 2004. Regulation of Longevity in Caenorhabditis elegans by Heat Shock Factor and Molecular Chaperones. *Molecular Biology of the Cell*, 15(February), pp.657–664.

Mosser, D.D. et al., 1990. In vitro activation of heat shock transcription factor DNA-binding by calcium and biochemical conditions that affect protein conformation. *Proceedings of the National Academy of Sciences of the United States of America*, 87(May), pp.3748–3752.

Mosser, D.D., Theodorakis, N.G. & Morimoto, R.I., 1988. Coordinate Changes in Heat Shock Element-

Binding Activity and HSP70 Gene Transcription Rates in Human Cells. *Molecular and cellular biology*, 8(11), pp.4736–4744.

Nakai, A., Suzuki, M. & Tanabe, M., 2000. Arrest of spermatogenesis in mice expressing an active heat shock transcription factor 1. *The EMBO journal*, 19(7), pp.1545–1554.

Neef, D.W. et al., 2014. A Direct Regulatory Interaction between Chaperonin A Direct Regulatory Interaction between Chaperonin TRiC and Stress-Responsive Transcription Factor HSF1. *CellReports*, 9(3), pp.955–966. Available at: http://dx.doi.org/10.1016/j.celrep.2014.09.056.

Neudegger, T. et al., 2016. Structure of human heat-shock transcription factor 1 in complex with DNA. *Nature Structural & Molecular Biology*, 1(November 2015). Available at: http://www.nature.com/doifinder/10.1038/nsmb.3149.

Neupert, W. & Brunner, M., 2002. THE PROTEIN IMPORT MOTOR OF MITOCHONDRIA. *Nature reviews. Molecular cell biology*, 3(August), pp.555–565.

Newton, E.M. et al., 1996. The Regulatory Domain of Human Heat Shock Factor 1 Is Sufficient To Sense Heat Stress. *Molecular and cellular biology*, 16(3), pp.839–846.

Nillegoda, N.B. et al., 2015. Crucial HSP70 co-chaperone complex unlocks metazoan protein disaggregation. *Nature*, 524(7564), pp.247–251. Available at: http://www.sciencedirect.com/science/article/pii/S002228361500100X%5Cnhttp://www.nature.com/doifinder/10.1038/nature14884.

Nylandsted, J. et al., 2000. Selective depletion of heat shock protein 70 (Hsp70) activates a tumor-specific death program that is independent of caspases and bypasses Bcl-2. *Proceedings of the National Academy of Sciences of the United States of America*, 97(14), pp.7871–7876.

Östling, P. et al., 2007. Heat Shock Factor 2 (HSF2) Contributes to Inducible Expression of hsp Genes through Interplay with HSF1 *. *Journal of Biological Chemistry*, 282(10), pp.7077–7086.

Pagliuca, M.G. et al., 2003. Regulation by heavy metals and temperature of the human BAG-3 gene, a modulator of Hsp70 activity. *FEBS Letters*, 541(1–3), pp.11–15.

Pellecchia, M. et al., 2000. Structural insights into substrate binding by the molecular chaperone DnaK. *Nature structural biology*, 7(4), pp.298–303. Available at: http://www.ncbi.nlm.nih.gov/pubmed/10742174.

Peteranderl, R. & Nelson, H.C.M., 1992. Trimerization of the Heat Shock Transcription Factor by a Triple-Stranded a-Helical Coiled-Coil ? *Biochemistry*, 96, pp.12272–12276.

Pierpaoli, E. V et al., 1997. The Power Stroke of the DnaK / DnaJ / GrpE Molecular Chaperone System. *Journal of Molecular Biology*, 269, pp.757–768.

Pinto, M., Morange, M. & Bensaude, O., 1991. Denaturation of Proteins during Heat Shock. *Journal of Biological Chemistry*, 266, pp.13941–13946.

Polier, S. et al., 2008. Structural Basis for the Cooperation of Hsp70 and Hsp110 Chaperones in Protein Folding. *Cell*, 133(6), pp.1068–1079.

Poulsen, E.G. et al., 2017. UBL/BAG-domain co-chaperones cause cellular stress upon overexpression through constitutive activation of Hsf1. *Cell Stress and Chaperones*, 22(1), pp.143–154. Available at: http://link.springer.com/10.1007/s12192-016-0751-z.

Prahlad, V., Cornelius, T. & Morimoto, R.I., 2008. Regulation of the cellular heat shock response in Caenorhabditis elegans by thermosensory neurons. *Science*, 320, pp.811–814.

Prahlad, V. & Morimoto, R.I., 2009. Integrating the stress response : lessons for neurodegenerative

diseases from C . elegans. *Trends in Cell Biology*, 19(December), pp.52–61.

Rabindran, S.K. et al., 1994. Interaction between Heat Shock Factor and hsp7O Is Insufficient To Suppress Induction of DNA-Binding Activity In Vivo. *Molecular and cellular biology*, 14(10), pp.6552–6560.

Rabindran, S.K. et al., 1993. Regulation of Heat Shock Factor Trimer Formation: Role of a conserved leucine zipper. *Science*, 259(14), pp.230–234.

Rampelt, H. et al., 2012. Metazoan Hsp70 machines use Hsp110 to power protein disaggregation. *The EMBO Journal*, 31(21), pp.4221–4235. Available at: http://emboj.embopress.org/cgi/doi/10.1038/emboj.2012.264%5Cnhttp://dx.doi.org/10.1038/emboj.2012.264.

Rasmussen, E.B. & Lis, J.T., 1993. In vivo transcriptional pausing and cap formation on three Drosophila heat shock genes. *Proceedings of the National Academy of Sciences of the United States of America*, 90(September), pp.7923–7927.

Rauch, J.N. & Gestwicki, J.E., 2014. Binding of Human Nucleotide Exchange Factors to Heat Shock Protein 70 (Hsp70) Generates Functionally Distinct Complexes in Vitro * □. *Journal of Biological Chemistry*, 289(3), pp.1402–1414.

Rauch, J.N., Zuiderweg, E.R.P. & Gestwicki, J.E., 2016. Non-canonical Interactions between Heat Shock Cognate Protein 70 (Hsc70) and Bcl2-associated Anthanogene (BAG) Co-Chaperones Are Important for Client Release * □. , 291(38), pp.19848–19857.

Raviol, H. et al., 2006. Chaperone network in the yeast cytosol: Hsp110 is revealed as an Hsp70 nucleotide exchange factor. *The EMBO journal*, 25(11), pp.2510–8. Available at: http://www.pubmedcentral.nih.gov/articlerender.fcgi?artid=1478168&tool=pmcentrez&rendertype=abstract.

Raychaudhuri, S. et al., 2014. Interplay of acetyltransferase EP300 and the proteasome system in regulating heat shock transcription factor 1. *Cell*, 156(5), pp.975–85. Available at: http://www.ncbi.nlm.nih.gov/pubmed/24581496 [Accessed January 4, 2015].

Richter, K., Haslbeck, M. & Buchner, J., 2010. Review The Heat Shock Response : Life on the Verge of Death. *Molecular Cell*, 40(2), pp.253–266. Available at: http://dx.doi.org/10.1016/j.molcel.2010.10.006.

Ritossa, F., 1962. A new puffing pattern induced by temperature shock and DNP in drosophila. *Experientia*, 18(12), pp.571–573.

Rosati, A. et al., 2009. BAG3 protein regulates caspase-3 activation in HIV-1-infected human primary microglial cells. *Journal of Cellular Physiology*, 218(2), pp.264–267.

Rougvie, A.E. & Lis, J.T., 1988. The RNA Polymerase II Molecule at the 5 â€™ End of the Uninduced hspTO Gene of D . melanogaster Is Transcriptionally Engaged. *Cell*, 54(September 9), pp.795–804.

Salmand, P.A. et al., 2008. Mouse Heat-Shock Factor 1 (HSF1) Is Involved in Testicular Response to Genotoxic Stress Induced by Doxorubicin 1. *Biology of Reproduction*, 1101(August), pp.1092–1101.

Sandqvist, A. et al., 2009. Heterotrimerization of Heat-Shock Factors 1 and 2 Provides a Transcriptional Switch in Response to Distinct Stimuli. *Molecular Biology of the Cell*, 20, pp.1340–1347.

Santoro, N., Johansson, N. & Thiele, D.J., 1998. Heat Shock Element Architecture Is an Important

Determinant in the Temperature and Transactivation Domain Requirements for Heat Shock Transcription Factor. *Molecular and cellular biology*, 18(11), pp.6340–6352.

Sarge, K.D., Murphy, S.P. & Morimoto, R.I., 1993. Activation of heat shock gene transcription by heat shock factor 1 involves oligomerization, acquisition of DNA-binding activity, and nuclear localization and can occur in the absence of stress. *Molecular and cellular biology*, 13(3), pp.1392–407. Available at: http://www.pubmedcentral.nih.gov/articlerender.fcgi?artid=359449&tool=pmcentrez&rendertype=abstract.

Schmid, D. et al., 1994. Kinetics of Molecular Chaperone Action. *Science*, 263(5149), pp.971–973.

Schuermann, J.P. et al., 2010. Structure of the Hsp110:Hsc70 Nucleotide Exchange Machine. *Molecular Cell*, 31(2), pp.232–243.

Shamovsky, I. et al., 2006. RNA-mediated response to heat shock in mammalian cells. *Nature*, 440(March), pp.4–8.

Shamovsky, I. & Nudler, E., 2008. Visions & Reflections (Minireview) New insights into the mechanism of heat shock response activation. *Cellular and Molecular Life Sciences*, 65, pp.855–861.

Shi, Y., Mosser, D.D. & Morimoto, R.I., 1998a. Molecular chaperones as HSF1-specific transcriptional repressors. *Genes and Development*, 12, pp.654–666.

Shi, Y., Mosser, D.D. & Morimoto, R.I., 1998b. Molecular chaperones as HSF1-specific transcriptional repressors. *Gen Dev*, pp.654–666.

Shin, B.K. et al., 2003. Global Profiling of the Cell Surface Proteome of Cancer Cells Uncovers an Abundance of Proteins with Chaperone Function *. *Journal of Biological Chemistry*, 278(9), pp.7607–7616.

Shinka, T. et al., 2004. Molecular Characterization of Heat Shock-Like Factor Encoded on the Human Y Chromosome , and Implications for Male Infertility 1. *Biology of Reproduction*, 306(March), pp.297–306.

Shomura, Y. et al., 2005. Regulation of Hsp70 function by HspBP1: Structural analysis reveals an alternate mechanism for Hsp70 nucleotide exchange. *Molecular Cell*, 17(3), pp.367–379.

Shopland, L.S. et al., 1995. HSF access to heat shock elements in critically on promoter architecture defined by GAGA factor, TFIID, and RNA polymerase II binding sites. *Genes & Development*, pp.2756–2769.

Sivéry, A., Courtade, E. & Thommen, Q., 2016. A minimal titration model of the mammalian dynamical heat shock response. *Physical Biology*, 13(6), pp.1–13. Available at: http://dx.doi.org/10.1088/1478-3975/13/6/066008.

Slepenkov, S. V & Witt, S.N., 2002. The unfolding story of the Escherichia coli Hsp70 DnaK : is DnaK a holdase or an unfoldase ? *Molecular Microbiology*, 45, pp.1197–1206.

Sondermann, H., Scheufler, C. & Schneider, C., 2001. Structure of a Bag / Hsc70 Complex : Convergent Functional Evolution of Hsp70 Nucleotide Exchange Factors. *Science*, 291(2001), pp.1553–1558.

Sorger, P.K. & Pelham, H., 1987. Purification and characterization of a heat-shock element binding protein from yeast. *EMBO*, 6(10), pp.3035–3041.

Sousa, R., 2014. Structural mechanisms of chaperone mediated protein disaggregation. *Frontiers in Molecular Biosciences*, 1(September), pp.1–18.

Stacchiotti, A. et al., 1999. Cell-specific expression of heat shock transcription factors 1 and 2 in unstressed rat spinal cord. *Neuroscience Letters*, 268, pp.73–76.

Stankiewicz, M. et al., 2010. CHIP participates in protein triage decisions by preferentially ubiquitinating Hsp70-bound substrates. *The FEBS Journal*, 277, pp.3353–3367.

Steel, G.J. et al., 2004. Coordinated activation of Hsp70 chaperones. *Science*, 303(5654), pp.98–101. Available at: http://www.ncbi.nlm.nih.gov/pubmed/14704430.

Straus, D., Walter, W. & Gross, C.A., 1990. DnaK , DnaJ and GrpE heat shock proteins negatively regulate heat shock gene expression by controlling the synthesis and stability of σ32. *Genes & Development*, pp.2202–2209.

Sullivan, E.K. et al., 2001. Transcriptional Activation Domains of Human Heat Shock Factor 1 Recruit Human SWI / SNF. *Molecular and cellular biology*, 21(17), pp.5826–5837.

Taipale, M. et al., 2014. Resource A Quantitative Chaperone Interaction Network Reveals the Architecture of Cellular Protein Homeostasis Pathways. *Cell*.

Tatum, M.C. et al., 2015. Article Neuronal Serotonin Release Triggers the Heat Shock Response in C . elegans in the Absence of Temperature Increase. *Current Biology*, 25(2), pp.163–174. Available at: http://dx.doi.org/10.1016/j.cub.2014.11.040.

Teter, S.A. et al., 1999. Polypeptide Flux through Bacterial Hsp70 : DnaK Cooperates with Trigger Factor in Chaperoning Nascent Chains. *Cell*, 97, pp.755–765.

Theyssen, H. et al., 1996. The Second Step of ATP Binding to DnaK Induces Peptide Release. *Journal of Molecular Biology*, 263(5), pp.657–670. Available at: http://linkinghub.elsevier.com/retrieve/pii/S0022283696906063.

Tsukahara, F. & Maru, Y., 2010. Bag1 directly routes immature BCR-ABL for proteasomal degradation. *Blood*, 116(18), pp.3582–3592.

Tutar, Y., Song, Y. & Masison, D.C., 2006. Primate chaperones Hsc70 (constitutive) and Hsp70 (induced) differ functionally in supporting growth and prion propagation in Saccharomyces cerevisiae. *Genetics*, 172(2), pp.851–861.

Vuister, G.W. et al., 1994. Solution structure of the DNA-binding domain of Drosophila heat shock transcription factor. *Structural Biology*, 1(9), pp.605–614.

Vujanac, M., Fenaroli, A. & Zimarino, V., 2005. Constitutive nuclear import and stress-regulated nucleocytoplasmic shuttling of mammalian heat-shock factor 1. *Traffic (Copenhagen, Denmark)*, 6(3), pp.214–29. Available at: http://www.ncbi.nlm.nih.gov/pubmed/15702990 [Accessed January 13, 2015].

Wall, D., Zyliczll, M. & Georgopoulosss, C., 1994. The NH2-terminal 108 Amino Acids of the Escherichia coli DnaJ Protein Stimulate the ATPase Activity od DnaK and sufficient for lambda replication. *Journal of Biological Chemistry*, 269(7), pp.5446–5451.

Weibezahn, J. et al., 2004. Thermotolercance Requires Refolding of Aggregated Proteins by Substrate Translocation through the Central Pore of ClpB. *Cell*, 119, pp.653–665. Available at: http://linkinghub.elsevier.com/retrieve/pii/S0968000405000435.

Westerheide, S.D. et al., 2009. Stress-Inducible Regulation of Heat Shock Factor 1 by the Deacetylase SIRT1. *Science*, 323(5917), pp.1063–1066.

Westwoodt, J.T. & Wu, C., 1993. conformational change associated with a Activation of Drosophila Heat Shock Factor : Conformational Change Associated with a Monomer-to-Trimer Transition. *Molecular and cellular biology*, 13(6).

Whitesell, L. & Lindquist, S., 2009. Inhibiting the transcription factor HSF1 as an anticancer strategy. *Expert Opinion on Therapeutic Targets*, pp.469–478.

Wiedemann, N., Frazier, A.E. & Pfanner, N., 2004. The protein import machinery of Mitochondria. *Journal of Biological Chemistry*, pp.14473–14477.

Wu, C., 1995. HEAT SHOCK TRANSCRIPTION FACTORS : Structure and Regulation translocation , higher order assembly , and protein degradation (Gething &. *Annu. Rev. Cell Dev. Biol.*

Xiao, H.U.A. & Lis, J.T., 1987. Germline Transformation Used to Define Key Features of Heat-Shock Response Elements. *Science*, 1053(1986).

Xiao, X. et al., 1999. HSF1 is required for extra-embryonic development , postnatal growth and protection during inflammatory responses in mice. *The EMBO journal*, 18(21), pp.5943–5952.

Xing, H. et al., 2005. Mechanism of hsp70i Gene Bookmarking. *Science*, 307, pp.421–423.

Xu, Z. et al., 2008. Structural basis of nucleotide exchange and client binding by the Hsp70 cochaperone Bag2. *Nature Structural & Molecular Biology*, 15(12), pp.1309–1317.

Young, J.C. et al., 2004. PATHWAYS OF CHAPERONE-MEDIATED PROTEIN FOLDING IN THE CYTOSOL. *Nature reviews. Molecular cell biology*, 5(October).

Zheng, X. et al., 2016. Dynamic control of Hsf1 during heat shock by a chaperone switch and phosphorylation. *eLife*, 90, pp.1–26.

Zou, J. et al., 1998. Repression of Heat Shock Transcription Factor HSF1 Activation by HSP90 (HSP90 Complex) that Forms a Stress-Sensitive Complex with HSF1. *Cell*, 94, pp.471–480.

Zuo, J. et al., 1994. Activation of the DNA-Binding Ability of Human Heat Shock Transcription Factor 1 May Involve the Transition from an Intramolecular to an Intermolecular Triple-Stranded Coiled-Coil Structure. *Molecular and cellular biology*, 14(11), pp.7557–7568.

List of Figures

List of Tables

List of abbreviations

E. coli	Escherichia coli
APS	Ammonium persulfate
ATP	Adenosine-5'-triphosphate
BSA	Bovine serum albumin
COREST	REST corepressor 1
(k)Da	(kilo)Dalton
DBD	DNA-binding domain
DNA	Deoxyribonucleic acid
dNTP	2'-deoxy-nucleoside-5'-triphosphate
DTT	Dithiothreitol
EDTA	Ethylenediaminetetraacetic acid
EGTA	Ethylen glycol-bis(β-aminoethyl ether) tetraacetic acid
HEPES	4-(2-Hydroxyethyl)-1-piperazineethansulfonic acid
HR	Heptad repeat
HS	Heat shock
HSE	Heat shock elements
HSF1	Heat Shock transcription Factor 1
Hsp	Heat shock protein
IPTG	Isopropyl-β-D-1-thiogalactopyranoside
JDP	J-domain protein
M	Molar
MS	Mass spectrometry
NBD	Nucleotide binding domain
NEF	Nucleotide exchange factor
OD	Optical density
PAGE	Polyacrylamide gel electrophoresis
PCR	Polymerase chain reaction
PMSF	Phenylmethylsolphonyl fluoride
rpm	revolutions per minutes
SBD	Substrate binding domain
SUMO	Small ubiquitin-like modifier
SDS	Sodium dodecyl sulfate
TAD	Transactivation domain
TEMED	N,N,N',N'-tetramethylethylendiamine
TRIS	Tris(hydroxymethyl)aminomethane
Ulp1	Ubiquitin-like specific protease 1
UV	Ultraviolet
v/v	volume per volume
w/v	Weight per volume
WT	Wild type

Acknowledgment

This work was conducted in the Zentrum for Molekularbiologie der Universität Heidelberg (ZMBH) under the supervision of Professor Matthias Mayer.

I would first like to thank Prof. Mayer for offering me the opportunity to do my doctoral thesis in his laboratory. His constant availability, his kindness and his excellent supervision of my work highly contributed to the completion of this project. In addition, his open-mindedness and broad culture outside of biochemistry allowed me to consider him not only as a PhD supervisor, but also as a mentor.

I would also like to thank Prof. Georg Stoecklin and Prof. Frauke Melchior for the helpful suggestions during the four years that were needed to finalize this work. Their help and cell lines gifts were particularly appreciated as no cell culture was performed in our laboratory prior to the beginning of my work. I am also thankful to both of them for sitting in my Thesis Advisory Committee, and for being among my PhD examiners.

In addition, I thank Dr. Sebastian Schuck for being member of my PhD examination committee.

I would like to address my thanks to my fellow PhD students and colleagues in the Mayer group – Roman Kityk, Laura Le Breton, Nikolai Hentze, Minh Nguyen, Soumya Daturpalli, Jan Wiesner, Marta Boysen, Robert Knieß. Special thanks goes to the “Buddies Lunch” group: these weekly lunches were well-spent time that allowed me to release some pressure, even when nothing would go my way at the bench. The laboratory technicians Elsbeth Schwarz and Anette Müller also deserve my thanks. I would like to thank separately Stefan Hennes for the many DNA-preparation he made for me, hence allowing to save precious time towards the end of my project.

I also wish to address my warm thanks to my parents, my sisters, and my family in general. Their support throughout all my life is one of the major contributions to this work. It was the education they provided me that nurtured my interest in natural sciences, and in biology in particular.

Finally, I would like to thank my better half, Lisa Monshausen, for her patience, her moral support, and for dealing with me on a daily basis. I am not sure this thesis would have come to fruition without her.